PERFORMANCE OF FLY ASH PELLETS IN COLD CLIMATES

by

Özlem Adalı

B.S., Civil Engineering, Yıldız Technical University, 2017

Submitted to the Institute for Graduate Studies in
Science and Engineering in partial fulfillment of
the requirements for the degree of
Master of Science

Graduate Program in Civil Engineering

Boğaziçi University

2019

ACKNOWLEDGEMENTS

I would like to express my sincere gratitude to Professor Gökhan Baykal for submission of the subject, for his suggestions, advises and ideas in the development of this study and for his invaluable guidance and help during the preparation of the thesis. I am grateful to him for being my thesis supervisor.

I would also like to express my gratitude to members of my thesis committee, Prof. Dr. Ayşe Edinçliler and Assoc. Prof. Dr. Murat Tonaroğlu who devoted their valuable time for the presentation and for their precious suggestions for the final edition of this thesis.

Thanks to our technicians Belgin Özgül and Kadir Gündoğdu for providing valuable technical assistance during the laboratory work.

Finally, I must express my gratitude to my parents and beloved friend Aykut Onursal for continuous support and encouragement during the study and through the experiments of this thesis. This accomplishment would not have been possible without them. Thank you.

ABSTRACT

PERFORMANCE OF FLY ASH PELLETS IN COLD CLIMATES

The construction season is very short due to difficulties of water handling in cold regions. The harsh climate of cold areas causes soil to be frozen from September to May. The main scope of this study is to investigate whether the engineering properties of lightweight pellets produced from fly ash by cold bonding process are durable enough for use in geotechnical engineering applications in cold regions. Potential use of pellets without compaction with water is investigated. Therefore, the pellets were covered with snow to represent frozen soil and subjected to the freeze-thawing cycles. A cycle in this experiment is intended to correspond to one year duration in the cold regions.

Cold bonding pelletization technique was used to produce fly ash pellets of sand and gravel size. Pellets have been exposed to ten freeze-thaw cycles. The pellets were observed with the thermal imager during freeze-thaw. Then, freeze-thaw procedure was evaluated by thermal imaging during freeze-thaw cycles. California Bearing Ratio (CBR), direct shear, cyclic simple shear and crushing value tests were conducted. An optical microscope was used for the observation of the surface of pellets. Thin section analysis was performed on pellets to observe the microfabric of the inner section of the pellets. Then, ESEM analysis was performed to examine the microfabric of pellets. Based on test results, although pellets lose strength after freeze-thaw, they still preserve their form. Usage of proper paving, may lead to successful applications of fly ash pellets in cold climates. Limited construction season of cold regions may be extended with the use of fly ash pellets. Better understanding of the cold weather performance of fly ash pellets will lead to enhanced utilization in cold climates.

ÖZET

UÇUCU KÜL PELETLERİNİN SOĞUK İKLİMLERDEKİ PERFORMANSI

Soğuk bölgelerin sert iklim şartları zeminin eylül-mayıs ayları arasında donmasına sebep olur. Bu çalışmanın temel amacı uçucu külden soğuk bağ yöntemiyle üretilen hafif peletlerin mühendislik özelliklerinin soğuk ülkelerdeki geoteknik uygulamalarında kullanımı için yeterince dayanıklı olup olmadığını araştırmaktır. Uçucu kül peletlerinin sıkıştırılmadan ve ideal su muhtevası sağlanmadan çeşitli geoteknik uygulamalarında ve hatta aşırı soğuk iklimlere maruz kalan bölgeler için bakım onarım amacıyla kullanılıp kullanılamayacağı üzerinde çalışılmıştır. Bu bağlamda, uçucu kül peletler, donmuş zemini temsil etmek için kar ile kaplandı ve donma-çözülme testine tabi tutuldu. Bu deneydeki bir devrin soğuk bölgelerde bir yıla karşılık gelmesi amaçlanmıştır.

Uçucu kül peletleri üretmek için soğuk bağ tekniği kullanıldı. Peletler, donma-çözülme döngüsüne maruz bırakılmıştır. Peletler donma çözülme sırasında termal kamera ile gözlenmiştir. Kullanılan donma-çözünme metodu termal fotoğraflama yöntemi ile değerlendirilmiştir. Kaliforniya taşıma oranı, direk kesme, çevrimsel basit kesme ve kırma testleri yapılmıştır. Peletlerin yüzeyinin gözlenmesi için optik mikroskop kullanılmıştır. Optik mikroskopun sonuçlarını desteklemek için ince kesit analizi yapılmıştır. Peletlerin mikro yapısını incelemek için ESEM analizi yapılmıştır. Test sonuçlarına dayanarak, donma-çözünme sonucunda uçucu kül peletler, dayanımını bir miktar kaybetse dahi, formlarını korudukları görülmüştür. Uygun bir kaplamanın kullanımı, başarılı pelet uygulamalarının yolunu açabilir. Soğuk ülkelerdeki kısa inşaat sezonu peletlerin kullanımı ile uzatılabilir. Uçucu kül peletlerin soğuk hava performansının daha iyi anlaşılması, peletlerin soğuk iklimlerdeki kullanımının önünü açacaktır.

TABLE OF CONTENTS

LIST OF FIGURES

LIST OF TABLES

LIST OF SYMBOLS

c	Cohesion
D	Diameter of Disc Pelletizer
D_{5_0}	Mean grain size
h	Height of liquid column
β	Central angle of the meniscus
δ	Angle of contact
μm	Micrometer
ρ	Density
σ	Normal stress
τ	Shear stress
ϕ	Internal friction angle

LIST OF ACRONYMS/ABBREVIATIONS

AASHTO	American Association of State Highway and Transportation
ASTM	American Society for Testing and Materials
Btu	British Thermal Units
CBR	California Bearing Ratio
CFA	Coal fly ash
CLSM	Controlled Low Strength Material
CSA	Canadian Standards Association
EN	European Union
EPS	Electrostatic Precipitators
EU	European Norm
FBC	Fluidized Bed Combustion
FHWA	The Federal Highway Administration
kWh	Kilo watt hour
MW	Mega watt
LOI	Loss on ignition
PCC	Portland cement concrete
PSB	Portland stabilized base
PSM	Portland stabilized mixture
RCRA	The Resource Conservation And Recovery Act
RPM	Revolution per minute
TSE	Turkish Standards Institute
UK	United Kingdom
UKQAA	UK Quality Ash Association
US	United States
USGS	United States Geological Survey

1. INTRODUCTION

All year round, cold regions go through frozen periods. The construction is more challenging than other regions in the cold areas when the ground is frozen. This also includes situations that need to be solved relatively quickly, such as maintenance and repair of embankments.

One of the construction limitation during below zero degrees is to compact clayey and silty soils. These soils in frozen condition are problematic to work with. Moreover, thawing can badly affect these soils and they will lose strength. Soils which contains sand and gravel mixtures are not as difficult to compact compared to compacting clayey and silty soils [8]. When available, pellets made from fly ash may be the solution.

Cold weather affects embankment construction when temperatures dip below freezing. Soil are affected by cold weather because it contains water. Cold weather regions are defined as those that typically experience subfreezing temperatures for periods of several weeks to several months each year.

Some soils are susceptible to frost heave during prolonged periods of subfreezing temperatures. Frost heave may occur if there is a continual supply of moisture being drawn up by capillary action from the groundwater table. The forces created from the continued growth of ice lenses in the soil can be large enough to give damage to the pavement. This can lead to differential movements if the heave is not uniform and it can develop cracks in the pavement. Additional damage may occur when the ice lenses begin to thaw. The soil typically thaws from the ground surface down. As the ice in the soil melts, the water can not drain into the underlying ground that is still frozen. The soil may then settle owing to the increase in the water content and the loss of support of the now non-existing ice lenses. This settlement typically is non-uniform and leads to differential settlements and damage the structure [1].

Soils consisting primarily of silt-sized particles are the most susceptible to frost action. It is actually the size of the pore spaces in the soil that controls the susceptibility to frost heave. Soil deposits that consist of up to 25% clay particles can exhibit a strong susceptibility to frost action if their porosity, and thus permeability, are relatively high. Although clay soils can exhibit high capillary rises, their permeability is relatively low and, therefore, they do not allow water to move fast enough to create significant ice lenses during a single freezing event. Conversely, silty soils can generate relatively high capillary rises in a relatively short time. This combination can lead to the formation of large ice lenses [1].

Due to the problems of cold regions, construction season is only limited to approximately three months. The construction season normally refers to the period of high building activity during the year; this excludes the winter. In Sweden this season lasts from four months in the north to six months in the south. In southern Canada it lasts from seven months on the prairies to more than nine months on the lower British Columbia mainland. In the upper fringe of the United States the duration is comparable to that of southern Canada. Thus, the construction season is relatively short. Use of fly ash pellets may extend the construction season [9].

In this study, difficulties of cold regions were tried to be solved. Fly ash pellets which may be used without compaction water in case of any repair, maintenance or urgent situations which needs immediate intervention mainly in highways in cold periods. Moreover, this study aims to increase the utilization of fly ash and to achieve a higher performance and environment friendly construction material especially for cold regions. In this way, the use of fly ash which is not used as much as needed and generally stocked in landfills, can be increased.

Fly ash is an industrial waste product which is produced by coal burning thermal power plants in vast amounts annually. It is successfully used as subbase, structural fill and embankment material for construction projects at the present time across the world.

On the other hand, when it comes to work with fly ash; control, handling and disposal of this waste material is a serious problem. If the annual production of fly ash is considered, it becomes a problem to be handled. As a result of the 1 kWh energy production of the coal burning thermal power plant, an average of 110 g of ash is produced as a waste material. Therefore, approximately 650 000 tons of ash is produced in a year from a 1 000 MW power plant. In order to store ash production at this level, there is a constant need for a land of 60.000 m^2 per year and a land of 1 800 000 m^2 within a period of 30 years which can be considered as the service life of the plant. The removal and storage of these industrial wastes causes environmental pollution, financial and technical problems in the fields of operation [10].

Suitable usage of fly ash decreases the need for large landfill areas by means of both economic and environmental reasons. It also presents a fairly cheap alternative resource for construction applications which requires mass quantity of construction material [10].

In present time, the need for economic and convenient materials is increasing. One of the reasons for increasing the requisition is the rapid increase in population. This situation becomes a more important issue specifically in the cold regions where the construction season is very limited but, maintenance demand for construction is constant.

Despite the fact that the use of fly ash as a recycled construction material is practical and economical, the environmental impact of using fly ash should also be considered. Fly ash is a coal based waste material and as a result of its origin, there may be dangerous and undesirable effects on environment such as trace metal leaching and gamma radiation in the long run [11].

The differences in physical and chemical properties of fly ash clearly affect the engineering performance of fly ash. The properties of fly ash considerably changes with the origin of the coal which is burned in thermal power plants. Properties and composition of coal also affect the mineralogical and chemical configuration of fly ash.

This proves the importance of the origin of the coal which determines the chemical composition and the class of fly ash. The diameter of coal due to feeding procedures, design and types of boiler units have considerable impact on the physical properties of the end product. In addition, storage and transporting methods are the important factors which can influence the characteristics of fly ash. Considering all these variables, it is certain that the characteristics of the fly ashes will change notably, even at the same plant [12].

2. LITERATURE REVIEW

2.1. Cold Regions

Approximately 48 percent of the Northern Hemisphere's land is categorized as cold regions. There, the southern limit of the cold regions extends to the 40 th parallel. In general sense, it includes areas with seasonal frost and permanent frozen ground which is also known as permafrost. However, definition of cold regions requires both climatological and geographical description. Climatologists use the isotherm based upon the average temperature for the warmest month of the year being above 0°C but not above 10°C to define the southern boundary of the cold areas. 150 and 300 mm frost penetration are identification factors for the southern boundaries of cold regions in the USA. Continuous, discontinuous and sporadic permafrost limits are demonstrated in Figure 2.1. Continuous permafrost refers to an environment where more than 80% of the ground surface is underlain by permafrost. The southern limit of continuous permafrost corresponds closely to a mean annual isotherm of –8°C. Discontinuous permafrost refers to an environment where 30%–80% of the ground surface is underlain by permafrost. The southern limit of discontinuous permafrost corresponds closely to a mean annual isotherm of –1°C. Sporadic permafrost refers to an environment where less than 30% of the ground surface is underlain by permafrost. There is no commonly acknowledged thermal criteria for the southern boundary of sporadic permafrost. The presence of sporadic permafrost is often dependent on the presence of organic soils that help preserve the permafrost under temperate climates. Operation requirements for industrial and social economy determines practical definition of cold areas [9], [13].

Degree and presence of frost are strongly connected with climate and attitude. Vertical temperature in mountain slopes changes for dry air from 3°C per 100 m. and for saturated air it changes 1.6°C per 100 m. Climatologists use 1.8°C per 100 m to transfer temperature information from lower parts of a mountain to the higher elevations. Due to the high elevation, some of the mountain regions of North America and southeast Eurasia are located in cold areas too [13].

In polar regions, sun rays arrives at oblique angle over a large area and they travel longer in the Earth's atmosphere which they can be absorbed, scattered or reflected the sun's energy back into the space. For normal zones, this causes winters to be colder than other seasons through the rest of the year [13].

Seasonally and perennially frozen ground is one of the engineering considerations of cold regions especially for geotechnical engineering. The transferred load to ground changes with seasonal and permafrost areas. In areas with seasonal frost, the loads transferred below the active zone and special soils, have been used to minimize heave and lateral thrust. In permafrost areas structure loads are often transferred to frozen ground with special care taken to maintain the frozen state. It is essential that the engineer have an understanding of the freezing process, thawing, and permafrost. In permafrost regions, knowledge of polygons, wedges and lakes gives an understanding of the ground features which may be encountered. The cold environment may create special problems such as buildup of successive ice layers adjacent to a small stream, which requires consideration when it occurs near roads or buildings The thickness of the active layer varies from year to year, depending on such factors as the ambient air temperature, vegetation, drainage, soil or rock type and water content, snow cover, and degree and orientation of slope. In case of permanent frozen ground, while frozen state is preserved, the load is transferred to frozen ground [14].

2.1.1. Seasonally and Permanent Frozen Ground

2.1.1.1. Permanent Frozen Ground. If any kind of ground stays in temperatures below zero degrees for a long period of time such as one or two years, it is defined as permafrost. Frozen soil without any kind of ice in it can be tracked as normal soil in temperate regions. However, many frozen grounds are also inter-bedded with large ice masses whose melting could bring about subsidence, erosion, and structural distress. Figure 2.1 shows the visible ice content in the upper 10-20 m of the ground. Generally, permafrost is present around poles as seen in the Figure 2.1, and has thick layer which it may range from less than 1 m to more than 1000 m.

According to Figure 2.1, continuous permafrost zones have the highest over burden cover which covers more than 20% of the ground. At the upper part of the permafrost there is a thin layer of seasonally melting soil. The thickness of permafrost changes with respect to lower altitudes and makes it thinner as seen Figure 2.3. However, on the mountain peaks there may be permafrost even near the equator but permafrost south of the bush country of Alaska,Canada, and Siberia is rare. On the other hand, even Scandinavia, despite its high latitude, has permafrost only in isolated areas of high altitude [14].

The continuous layer of frozen subsoil extends far southward in continental parts of Canada and Siberia. Trees can and do grow over frozen soils, but the tree line marks fairly well the southern boundary of the continuous layer of permafrost. It is not far wrong to say that the treeless tundra overlies continuous permafrost and that the forested taiga covers the frayed margins of the permafrost blanket. In the interior of Alaska, in the taiga of the Yukon, Kuskokwim, and Copper River valleys, for instance, the permafrost is marginal. Almost at the melting point, permafrost exists or not in these areas depending on such apparently minor influences as whether the land slopes to the north or to the south, whether the forest cover has remained intact in recent years, or whether the land is swampy. If climate allows conditions for permafrost such as being cold for a long period, then, there will be permafrost [9], [14].

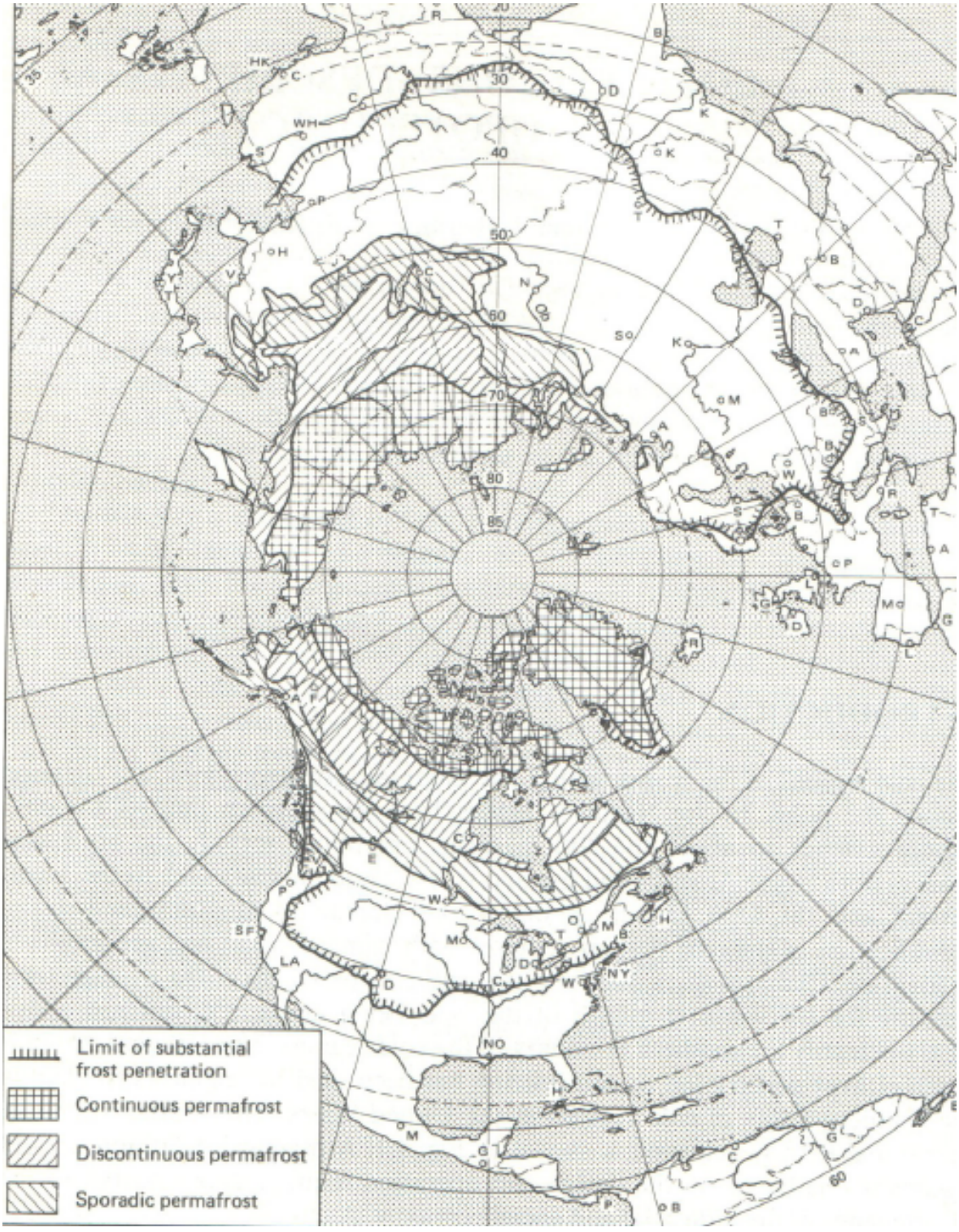

Figure 2.1. Cold areas of the northern hemisphere [1]

2.1.1.2. Seasonally Frozen Ground. Cold regions are typically classified on whether the ground is seasonally frozen, permafrost occurs in everywhere or whether permafrost is active in some areas. Seasonally frozen ground covers large areas of North America, Europe and Asia. The seasonal frost layer may be described as the top layer of the ground in which the temperature fluctuates above and below zero degrees during the year. It corresponds to the active layer above perennially frozen ground (permafrost). In the far north the active layer is as shallow as 150 mm. Farther south, near the discontinuous permafrost zone, the active layer or frost penetration can be as much as 3 m thick [2].

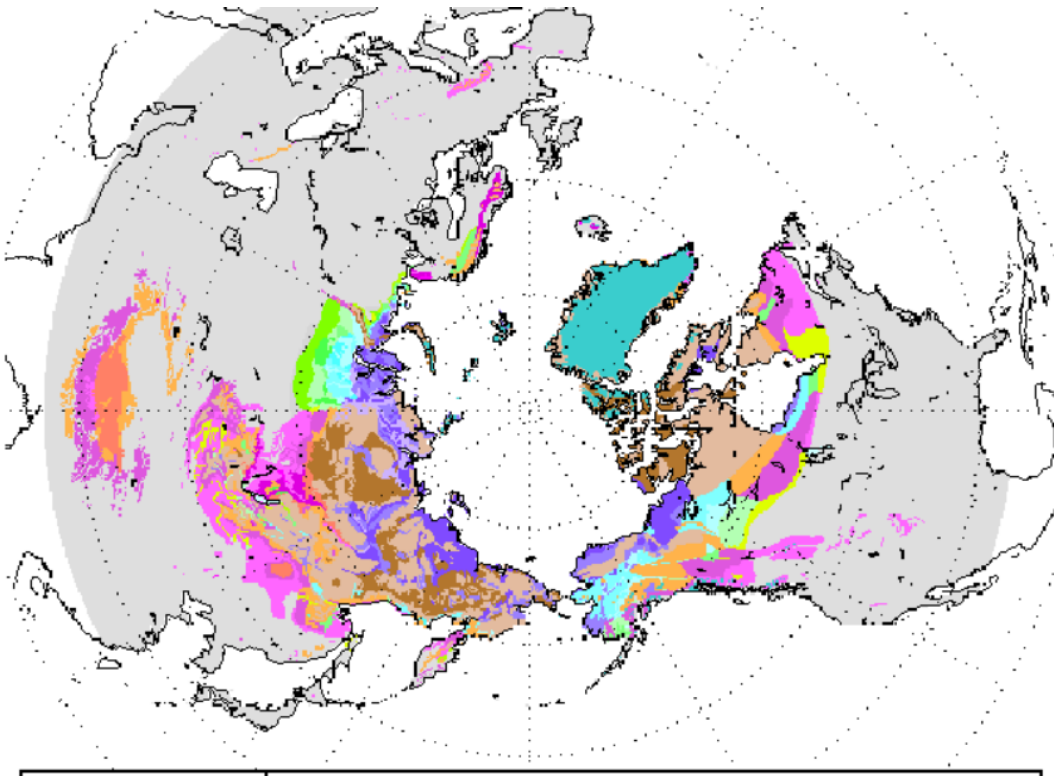

Figure 2.2. Arctic map of permafrost and ground ice conditions [2]

Where ice in lakes, rivers, and harbors interferes with navigation, where frost heaving affects roadways and the possible snow load on structures must be considered in design, the engineer is dealing with a cold region environment. Snow and ice control in the United States costs more than 100 million dollars each winter. Regions where frost penetrates the ground to a depth of about 0.3 m. or more at least once in 10 years are part of the cold regions of the world. Because the depth of frost penetration is not regularly reported or easy to measure, the annual freezing index is used as a measure of potential frost penetration. The freezing index is the area above the curve of mean daily temperatures and below the 0°C line, that is the accumulated negative degree-days during a single freezing season. If the mean freezing index is 50 degree-days or more, the criterion for about 0.3 m. of frost penetration is considered to be met. This makes the assessment of the boundary of cold regions independent of the complexities of other factors, such as the variation of thermal diffusivity among differing soils, the variations of freezing temperature among soils, the water contents, the surface cover, and so forth [1].

2.1.2. Properties of Frozen Ground and Construction Difficulties in Cold Regions

Where in many cases frozen soil may be advantageous over normal soil however, an engineer have to deal with problems such as freezing and thawing causing damage by frost heave, collapse upon thawing, and loss of durability [15].

The effects of frozen ground on engineering considerations can be grouped into various categories according to cause or end results. In moderate climates foundations and water-mains are protected against the effects of frost by placing them deep enough to avoid frost heave or freezing. Problems of permafrost involves thawing of ice-rich permafrost and subsequent subsidence of the surface under unheated roads and airfields; subsidences under heated structures, frost action, generally intensified by poor drainage caused by permafrost, and those involved only with the temperature of permafrost, causing buried sewer, water and soil lines to freeze.

When people from the outside began to enter the arctic and subarctic regions to harvest their natural resources or occupy their strategic locations, they were immediately engaged in reproducing the buildings, communication routes and utilities that had become necessities in their civilization. At this time the properties of frozen ground became an engineering consideration [16].

It is logical to divide problems into ones related with freezing, thawing process and the steady-state frozen soil condition [17].

2.1.2.1. The Freezing Process. While many of the geotechnical engineering problems of cold regions are mainly associated with the arctic and subarctic, the occurrence of most difficulties caused by the freezing of soil depends only upon sufficient degree-days, below 0°C to freeze approximately the top meter of the soil. This condition, occurs over a large portion of the temperate zone.

In cold regions where ground temperature falls below zero degrees, freeze-thaw cycles should not be negligible. Slope failures frequently occur during snow-melt season and differential settlement results from frost heaving. The most problematic side of soil freezing is the frost heaving [17].

2.1.2.2. Frost Heave. Cold weather can affect embankment construction when temperatures are below freezing. Soil is affected by cold weather because it contains water. Cold weather regions are defined as those that typically experience subfreezing temperatures for periods of several weeks to several months each year. When damp ground of silty texture freezes, there is a migration of moisture to the freezing surface. Masses of ice begin to form along the freezing front, supplied with water by vapor transfer and by liquid migration. If water is available from a lower layer and if the soil has capillarity, ice layers of considerable thickness (1 to 100 mm are common) may develop, displacing the soil to make room for the ice. The accumulation of ice under such circumstances has been known to double the volume of the frozen soil. More commonly, the total amount of heave amounts to anything from 0 to about 150 mm in a season [1].

Frost heave occurs if continuous supply of moisture being drawn because of the capillary action from the groundwater table. This causes differential movements if the heave is not uniform and if it develops cracks in the pavement. In addition, if ice lenses present in the soil begin to thaw, water can not be drained from underlying layer of soil because of the reason that it is still frozen. The soil generally thaws from the ground surface and additional damage may occur when the ice lenses begin to thaw. Then, soil may settle due to the increase in the water content and the loss of support of the now non-existing ice lenses. These settlements are non-uniform and causes differential settlements and as a result damaging the pavement. Conditions for frost heave are [15]:

- a cold surface to propagate freezing;
- the physical composition of the soil must promote the migration of the moisture to the freezing front;
- a source of water to feed the ice growth.

While frost heave is usually thought of as vertical movement, it can produce displacement in any direction. A vertical face exposed to the freezing temperatures by the retaining wall creates a horizontal thermal gradient, resulting in the lateral bulge and a forward rotation of the wall. Non-frost-susceptible soils are usually placed behind retaining walls to avoid this problem. Structures with exposed foundations are also subject to frost heaving. The differential effects are particularly severe where part of the foundation is heated and part is not. Normally footings are placed below the level of frost penetration. Insulation can be used to prevent this frost heave. Figure 2.3 shows the ranking of the susceptibility of different soils to frost heave [18].

Frost Heave Susceptibility	**Soil Type**
None	Gravel and Sand
Moderate	"Fine" Clay (>40% Clay)
Strong	Silt and "Coarse" (clay content—15-25%)

Figure 2.3. Frost heave susceptibility of various soil types [1]

Pile jacking is another frost-heave phenomenon. When piles are installed in frost-susceptible soil, a bond is developed between the pile and frozen earth at the ground surface, transferring uplift forces to the pole [18].

Another problem produced by the freezing of soil is a result of shrinkage caused by thermal contraction and desiccation. The polygonal cracking of the ground is reflected through surface pavements and creates additional maintenance difficulties. The movement of water through these cracks tends to increase the rate of stripping in asphalt pavements and can result in the formation of an ice lens below the crack which produces an upward litting of both edges. In some cases localized thawing of the base occurs when deicing solution enters the cracks [9].

2.1.2.3. Thawing. For convenience, the engineering considerations pertaining to the thawing of soil can be divided into those relating to seasonal frost, or the active layer, and those relating to permafrost. In the active layer, when the previously described ice lenses that caused the heaving melt and the resulting water escapes, voids are left in the soil. When loads are applied to pavements, which depend on support from the soil, the pavements sag into the depressions and begin to crack and fail. Even when there is no significant ice segregation, pavement distress may develop. As the 0°C thawing isotherm progresses downward below the plowed roadway surface, the meltwater produced cannot penetrate the frozen soil and often it cannot dissipate laterally as snow berms keep the sides of the roadway from thawing quickly. The trapped water induces a high moisture content directly under the pavement reducing the bearing capacity. Until a drainage path is restored, loads must be restricted to prevent disintegration of the road surface. When seasonal ice melts under piles, or spread footings, it is rare for the member to settle back to its original elevation. Instead, the surrounding soil may tend to fill the space formerly occupied by ice; this, combined with skin friction, will restrict downward movement. This cycle of heaving and blocked restoration can be repeated yearly until failure results. When ice is well distributed and its volume is less than the pore volume of the soil, the consolidation and resultant settlement are negligible. As the ice content increases, so does the potential for settlement [1], [9].

Buildings which introduce a concentrated heat source, like a dwelling are particularly vulnerable to settlement. Thermal equilibrium can be changed by changing the existing ground cover. Unless the new construction provides a heat balance that matches that of the original surface, the permafrost level will change. In high-arctic roadway embankments, gravel 1 to 2 m. thick will approximate the natural cover. In the subarctic, where the permafrost temperature approaches below zero, the height of fill required to maintain equilibrium becomes prohibitive. Roadway settlements can be expected when normal fills are placed over ice-rich permafrost. Vigorous maintenance can keep a gravel surface serviceable while a new thermal equilibrium is reached [9].

In addition to settlement, the general stability of soil can be lowered by thawing. Not only is the binding force of the ice removed, but the released moisture may act both as a "lubricant" and under some conditions as a transport agent in promoting soil flow. Slope stability should be investigated whenever an engineering project changes the thermal regime of a permafrost region. Thawing permafrost can have effects on drainage patterns which must be considered. Water which cannot penetrate the frozen ground will follow porous paths thawed in the permafrost. Buried pipes transporting warm liquids can create new drainage channels below ground, and vehicle traffic can thaw out surface channels. That these changes can direct water to new locations must be recognized. In addition to allowing the passage of water, thawing also permits the movement of the soil particles, and the combination of these two conditions may produce serious erosion with its resultant problems [9].

2.1.3. Properties of Snow

Ice is the frozen state of water, it has crystals and all the physical properties of a mineral. Ice has several important attributes and uses that helps make the living earth what it is today. The different types of ice such as glaciers, ice caps, and snowflakes have a definite affect on the climate of all the geographic regions around the world. Some of them are huge masses that cover the ground for many miles and others are small chunks that fall from the sky. Naturally, the more natural ice there is in a given region, the colder it will be.

With the current technology ice is also very important in climates that are relatively warm all year round or at least part of the year. Ice is considered a mineral because it is a natural, inorganic, homogeneous solid with definite chemical composition and crystalline structure. It has a white color but can appear blue or colorless. It is a part of the hexagonal crystal system. It can occur as a dihexagonal dipyramidal. Ice has a hardness of about 1.5, a specific gravity of 0.9, and a density of 0.99 grams per cubic centimeter [19], [20].

Ice is defined as any of the solid states of pure water. Water also exists in solid forms that are not usually referred to as ice. In natural snowflakes, adhesion is affected partly by interlocking of the crystals and by sintering of the ice at the points of contact, although deposition of water vapour and the freezing of collected supercooled droplets may act as a cement [19], [20].

2.1.4. Aggregation of Ice Crystals to Form Snowflakes

When two ice particles come into contact, adhesion occurs as the bridge between them grows in order to minimize the surface free energy of the system. When two ice spheres were pushed together to touch at a point, the area of contact grew with time, even when the original force of contact was removed. By measuring the growth rate of the neck between the two spheres, the material was transferred from the convex surfaces of the spheres into the concave neck by surface diffusion. With pure ice, the growth rate of the neck was quite slow; typically it took some hours for the radius of the neck to grow to one quarter of the radius of the sphere. Under these conditions, there was no evidence for a liquid-like layer on the ice surfaces, but if the ice contained dissolved salts, or if the surfaces of the spheres became otherwise contaminated, the neck grew much more rapidly by the flow into it of a film of contaminated liquid. In a layer cloud releasing persistent snow, only the first kilometre or so above the 0°C level may be appreciably supersaturated and contain supercooled droplets, and this may explain why aggregation of snow crystals to form large flakes occurs most readily at temperatures just below 0°C. Accordingly, it would appear that vapour deposition and riming are more effective than sintering in causing the adhesion of crystals [19], [20], [1].

2.2. Fly Ash

2.2.1. General Description

Fly ash, also called as flue ash is a residue product of coal combustion process. Fly ash is basically consist of fine particles which remains after burning process of a coal. These fine particles driven out of boilers together with the flue gases. In general, standard coal has two main phase called as volatile matter and ash. When the process of coal combustion occurred, inorganic and incombustible matter present in that coal has been fused into fly ash. 85 percent of the ash content of coal turn into fly ash. Remaining part of the ashes that collected from the bottom of the same boiler is called bottom ash. After that, ashes are collected by mechanical and electrostatic methods and stored generally in the vicinity of the power plant or in other suitable places. Ashes accumulate over time and become a problem for central management [21].

Fly ash is hardened while suspended in the flue gases. Since the particles hardened while suspended in the flue gases, fly ash particles are generally spherical in shape and range in size from 0.5 μm to 100 μm [22]. Most fly ash is pozzolanic, which means it's a siliceous or siliceous-and-aluminous material and reacts with calcium hydroxide to form a cement [23]. Cement has the same major compounds found in fly ash. However, proportion of each compound differs significantly comparing fly ash. Major chemical composition of fly ash consist of Silica Oxide (SiO), Aluminium Oxide (Al_2O_3), Iron Oxide (Fe_2O_3) and Calcium oxide (CaO). In addition, fly ash contains some heavy metals [23].

Coal is one of the major sources of energy in many countries. In 2018, a total of 113.3 tera watt hour electricity was generated from coal-based power plants and its share in total electricity generation was 37.3% in Turkey. 3,2 percent of the total world reserves of lignite/sub-bituminous coal are in Turkey. In Turkey, only one of the thermal plants anthracite is used. In the rest of the plants lignite is used [3].

The mineralogical properties of fly ash obtained from different power plants can be similar, the physical and chemical properties may vary depending on the operational conditions. Fly ash has to meet ASTM C618 standard, which is the standard specification for coal fly ash and raw or calcined natural pozzolan for use in concrete. Afsin, Kangal, Soma and Tunçbilek fly ash can be defined as Type C fly ash according to ASTM C 618. However, Yenikoy fly ash can not defined as Type C fly ash by ASTM standards because of the low $SiO_2 + Fe_2O_3 + Al_2O_3$ value. Yeniköy fly ash has 27,85 % of $SiO_2 + Fe_2O_3 + Al_2O_3$ value, however, it should be at least 50 percent in Type C fly ashes. On the other hand, the $S0_3$ contents of Yenikoy and Kangal and Afsin fly ash are higher than 6 percent as the limits specified for Type C fly ash. The most suitable fly ash for use in construction industry is Soma and Tuncbilek fly ash that possesses cementitious property without necessity of desulphurization treatment [3].

2.2.2. Composition of Coal

Origin of coal comes from the heterogeneous mixture called peat. Peat is a decomposed organic material which is formed in water-rich environment and the absence of oxygen. Peat may develop even in cold regions such as Siberia, Canada, and Scandinavia. If geological processes gradually apply pressure on peat with time, different types of coal occurs. This process called coalification [24]. Coal sample analysis is mostly used to determine the quality of coal along with its unique characteristics and composition.The properties of coal are classified as physical and chemical properties in an overall sense. Physical properties can be determined by different analyses such as heating value and proximate analysis. On the other hand, chemical properties can be determined by ultimate analysis. In general, coal analysis and testing methods can be described as below:

- Proximate analysis is the most common and simplest coal analysis method. It gives the approximate results compared to ultimate analysis. Proximate analysis determines moisture content, ash content, volatile matter and fixed carbon of the coal sample [1].
- Ultimate analysis determines composition of elements of the coal such as carbon, hydrogen,nitrogen, sulfur and oxygen. The remaining mineral matter is shown as ash [1].

Typical composition of coal consist of 75 to 90 percent fixed carbon, 4.5 to 5.5 percent hydrogen, 1 to 1.5 percent nitrogen, 1 to 2 percent sulfur, 5 to 20 percent oxygen, 2 to 10 percent ash and 1 to 10 percent moisture, roughly [25], [1].

Besides the volatile matter, carbon and moisture found in the coal, there is also a inorganic material part. Mineral matter enters the coal deposit at various times of its formation history. One of the many different resources of the inorganic matter found in coal is the weathering and erosion of minerals from the surrounding area. It stored together with organic matter during the flood or stream-flow throughout the coal formation process [26].

Another source of the inorganic components comes from the volcanic explosions. Volcanic eruption caused ash deposition to occur with the parent vegetation of inorganic component simultaneously. A wide scope of minerals can be found in coal. Only about 33 minerals are present in most coal samples. Among these 33 different minerals, just 8 of these are generally plenty enough to be considered as major constituents according to U.S. Geological Survey (2016). The most common elements are quartz, kaolinite, illite, montmorillonite, chlorite, pyrite, calcite, and siderite. These minerals can be found in coal with different concentrations changing with the depositional environments. Since it determines the chemical structure of fly ash, the composition of these minerals in coal are crucial. Non-combustible part of the coal consists of fly ash. That is the reason why, after the parent coal combustion process, inorganic minerals define the chemistry of ash [26]

2.2.3. Classification of Fly Ash

The composition and characteristics of the fly ash changes broadly based on time and place due to various reasons, many developed countries have required standards that will enable the use of ash in different areas. There are several fly ash classification systems. Some of them are changing with country. In this dissertation, ASTM classification for US, EN classification for EU and TSE classification for Turkey has been given.

2.2.3.1. ASTM Classification of Fly ash. : According to ASTM C618, there are two types of fly ash. These are defined as the Class F and Class C based on its chemical composition. The major difference between these classes is the amount of calcium, silica, alumina, and iron content in the ash. The reason behind the different chemical composition of fly ash is the parent coal source.

Class C ashes are generally derived from sub-bituminous coals or younger lignites and consist primarily of calcium alumino-sulfate glass, as well as quartz, tricalcium aluminate, and free lime (CaO). In type C fly ashes, the total $SiO_2 + Al_2O_3 + Fe_2O_3$ content is greater than 50 percent. Class C type of fly ash is also concerned as high calcium fly ash because it typically contains more than 20 percent CaO [27]. Class C fly ash is both pozzolanic, hydraulic and has self-cementing properties which is it forms cementitious hydrates in presence of water. It does not require an external activator. It also has pozzolanic properties.

On the other hand, Class F type of fly ash is pozzolanic and it does demand external activator or cementing agent such as Portland cement, quicklime, or hydrated lime to form cementitious compounds. In Class F type fly ashes, the total $SiO_2 + Al_2O_3 + Fe_2O_3$ percentage is greater than 70 percent. Class F type fly ash typically is a product of burned bituminous coal and harder, older anthracite.

2.2.3.2. EN Classification. : Fly ash is classified as Class V and Class W according to European Standard EN 197-1. Class V fly ash is fundamentally composed of reactive silica dioxide SiO_2 and aluminum oxide (Al_2O_3); the rest are ashes containing iron oxide and other components. For type V fly ash, the reactive lime (CaO) ratio should be less than 10 percent and the reactive silica amount should be more than 25 percent. Type W ashes, mainly composed of reactive lime (CaO), reactive SiO_2 and Al_2O_3; the rest are ashes containing iron oxide (Fe2O3) and other components. In these ashes, reactive lime (CaO) ratio should be more than 10 percent and reactive silica amount should be more than 25 percent. Chemical criteria of class W and V type of fly ash according to EN 197-1 standard are given in Figure 2.4.

Chemical Properties (%)	W Class	V Class
Max. $S0_3$	-	-
Max. MgO	-	-
SiO_2	-	-
Al_20_3	-	-
Fe_2O_3	-	-
Minimum S+A+F	-	-
Reactive CaO (%)	<5	>5
Reactive SiO_2 (%)	>25	>25
Heating Loss (%)	<5	<5

Figure 2.4. Chemical criteria of class W and V type of fly ash

2.2.3.3. TSE Classification. Fly ash intended for use in cement production had been classified as stated in TS EN 197-1. This standard mainly adopted from EU laws, regulations and EN 197-1 standards. The standard, which has been in use since 2002, was updated in 2012.

A classification in the manner of the amount of CaO in fly ash may be made. This classification is made according to the activity of the fly ash and it is defined by the CaO content. According to the activity of fly ashes, ashes with very low activity consist less than 3.5 percent calcium oxide (CaO) while low activity ashes have CaO content in between 3.5 percent to 7 percent. Finally, very active ashes consist more than 14 percent CaO content [28].

2.2.4. Physical and Morphological Characteristics of Fly Ash

Fly ash is a very fine grained material. Fly ash particles are predominantly spherical in shape and range in size from 0.5 μm to 100 μm. The specific gravity of fly ash usually ranges from 2.2 to 2.7, while its specific surface area can range from 1800 to 5000 cm^2/gr. However, most of it in range between 2800 to 3800 cm^2/gr [29].

Particle morphology and grain size of fly ash depends on several factors such as the origin and uniformity of coal, the pulverization state of the coal, the conditions of combustion, the uniformity of combustion and type of dust collection system [30]. The fineness of the fly ash depends primarily on the degree of grinding of the coal supplied to the boiler, the second factor affecting the fineness is that the ashes are kept from being prevented from escaping from the chimney as much as possible. If the quantity escaped from the chimney decreases, the fineness of fly ash increases.

2.2.5. Chemical Characteristics of Fly Ash

The chemical properties of fly ash are broadly influenced by combustion of coals and the techniques used in transport and storage.There are roughly four ranks of coal. Each of which has unique and different characteristics in terms of ash component, heating value, geological history and its chemical structure. Different coal types have varying amounts of carbon and it calculated by the loss on ignition (LOI).

The loss on ignition (LOI), measured by the amount of unburnt carbon remaining in the fly ash [27]. LOI is one of the most significant chemical properties of fly ash. Loss on ignition (LOI) value used especially as an indicator of suitability for use as a cement replacement in concrete.

As seen in Figure 2.5, ashes produced by lignite coal has the most CaO and MgO percentage among bituminous and sub-bituminous based ashes. From the table it is certain that ashes came from lignite and sub-bituminous coals have a higher calcium oxide content and lower loss on ignition than fly ashes from bituminous coals.

Component	Bituminous	Sub-bituminous	Lignite
SiO_2	20-60	40-60	15-45
Al_2O_3	5-35	20-30	10-25
Fe_2O_3	10-40	4-10	4-15
CaO	1-12	5-30	15-40
MgO	0-5	1-6	3-10
SO_3	0-4	0-2	0-10
Na_2O	0-4	0-2	0-6
K_2O	0-3	0-4	0-4
LOI	0-15	0-3	0-5

Figure 2.5. Compositional ranges of the ashes of various coal types (% weight) [1]

2.2.6. Mineralogic Characteristics of Fly Ash

Fly ash is a non-homogeneous mixture of particles which has different in shape, size, and chemical structure. More than 85 percent of most fly ash involves glassy and crystalline components formed as a result of the thermal process of minerals [31], [32].

The chemical and mineralogical composition of fly ash depends upon the characteristics and chemical structure of the coal burned in the thermal power plant. Depending on the speed of cooling, fly ash consist 50 % to 90 % of mineral substance in the form of glassy particles and tiny amount of crystals occurs. Infrared, Mössbauer Spectroscopy, X-Ray diffractometry etc. techniques may be used to display the crystalline stages in fly ash as stated by several studies. [32], [33], [34], [35].

2.2.7. Utilization Areas of Fly Ash

Nowadays, as a result of economic developments and developments in the industry, the demand for electricity generation has increased. Thus, the number of power plants has increased. Coal based thermal power plants generate enormous amount of fly ash and waste related problems have been a major problem of coal burning power plants. As environmental awareness increases, the proper use of power plant wastes has become even more important.

The problems caused by these wastes and the increase of these problems in parallel with the production of energy have led to the exploration of the possibility of their evaluation in various fields. The evaluation of thermal power plant wastes has eliminated environmental problems as well as eliminating the problem of storage. As a result, fly ash and slag formed in the coal burning power plant found a wide range of applications.

2.2.7.1. Embankment and Fill Material. Coal fly ash has been used for various purposes in geotechnical engineering including fill material or embankments for highway constructions throughout the world. If coal fly ash compared with natural soils which are used in embankment construction, it has unique properties. When dry, fly ash is cohesionless and considered by many people as a problematic material. When saturated, fly ash becomes an unmanageable material. However, as with most fine grained soils, coal fly ash can be easily controlled and compacted with presence of moisture, and does display cohesion [36].

Fly ash can be mainly used for stabilization in geotechnical applications like stabilization of bases and/or sub-grades, backfills, enhancing slope stability and decrease the lateral earth pressures, because it improves the compressive and shearing strength of soils. The compressive strength of soils altered with fly ash depends on compaction moisture content, additive ratio and in-place soil properties. Class C and Class F with lime mix used to stabilizing agent in embankments, to manage expansive soil features like shrink and swell and used as a drying substance for better compaction [37].

Fly ash alters the volumetric expansion of plastic soils using unique cementing property. Fly ash manages shrink-swell properties of expansive soils by cementing the soil particles together.By connecting the soil particles each other, soil particle movements are limited [38].

In Europe, fly ash has been used for several years as an embankment or structural fill material. There has been relatively limited use of fly ash as an embankment material in many other countries, although its use in embankment application is becoming more widely accepted [39].

As an embankment or fill material, fly ash is used as a additive for natural soils. In this situation, fly ash must be stockpiled and conditioned to its optimum moisture content to ensure that the material is not too dry and dusty or too wet and unmanageable. When fly ash is near its optimum moisture content, it can be compacted to its maximum density and will perform in an equivalent manner to well-compacted soil [27].

The fortification of road bases with fly ash has a very wide use in highway constructions. This practice called as pozzolanic-stabilized mixture and it uses different variety of substances and their combinations to from stabilized bases. It consist of fly ash, aggregate, lime and/or cement with changing percentages. Also, Class C fly ash can solely used in constructions. When appropriately placed and well compacted, base courses fortified with fly ash are good alternative for standard base-courses. Also, they are convenient for flexible and rigid pavements [27]. Pozzolanic-stabilized base pavements have a successful history in terms of engineering. In general, these mixtures are certainly the most economical alternative of base materials. Use of pozzolanic-stabilized mixture is also important to recycle coal burning power plant wastes, to contribute environmental sustainability and reduce the use of natural resources [27].

2.2.8. Pelletization Process

The pelletization process is the process of forming fly ash pellets by using a rotating drum or disc. The purpose of pelletization operation is to agglomerate fine materials with water and turn into a fresh pellets. If higher strength pellets are desired, mixture of fly ash and binder substances can be added in addition to the water. The crushing strengths of the formed fresh pellets as a result of the process should be durable enough for conditions such as stockpiling and hauling.

One advantage of pelletization process is that desired number of pellets can be easily obtained. In addition, the demanded granulometric distribution of pellets may be obtained using pelletization process. These can be used as aggregates in construction projects or can be solely used in highway projects for various purposes including maintenance [1].

The pelletization process can be done in three different methods based on the procedure during production. These methods are listed below [3];

- sintering process,
- hydrothermal processing,
- cold bonding.

Sintering process may be basically explained as a heating process of materials to achieve high density and strength. Heat treatment is carried out at the temperature below the melting point of substances. These materials can be heated in the production in rotary kiln, or carried to a sintering oven just after production [40].

In hydrothermal processing and cold bonding process, either cement or lime is added to the material pelletized to strengthen the agglomerates with chemical reactions. In hydrothermal processing, the pellets are cured in the autoclave with pressurized steam, whereas in cold bonding, the pellets are cured under humid atmospheric conditions [40].

Cold-bonded fly ash can be hardened by water curing and steam curing. Among all these procedures, water curing is most efficient process to increase the strength of the pellets [40].

The origin of concept of the pelletization process was found by a swedish researcher A. G. Anderson in 1912. Only a year after that, C. A. Brackelsberg invented similar rounding process in Germany. The fine material used in the pelletization process were blast furnace flue dusts, and ores.

The studies of the pelletization process in the USA dates back to the 1920s. However, the commercial use of pellets began after the World War II. As a result of the researches conducted to develop and use the large amount of taconite resources around the Great Lakes, a new method invented for processing taconite consist of iron ore in 1943. The obtained ore is in the form of fine particles of 0.1 mm or less which are not suitable for sintering. This problem solved with the use of pelletizing [41].

2.2.8.1. Pelletization Theory. If a fine grained substance is moisturized, a thin liquid film is established on the surface of the particle as seen in the a section of the Figure 2.6. If the particles are rotated in a disc, spherical shaped structures are formed with fortified bonding forces are between particles as seen in the b section of the Figure 2.6 [42].

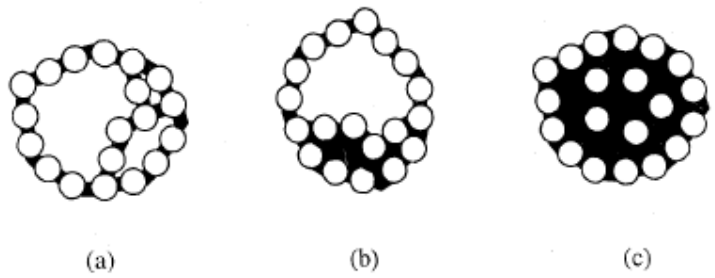

Figure 2.6. Mechanism of pellet formation

The first structure creates the core of the pellet. As the particles get moisturized, they move towards each other and become connected with a water bridge. If moisturised grains sticks to the core, pellets expand in size. Circular shape of pelletizer disc make the process easier for coating. Also, when pellets strike each other because of the shape of the disc and to the walls of pelletizer, it makes the pellets stronger and compact. As the voids of pellets decreased, particles become more compacted and more concentrated. In addition to the mechanical forces, the centrifugal and gravity forces affect the pellets during the production stage. All these forces diminish the voids in pellets and make more space for grains and moisture [43], [42].

The amount of water used during the formation of fresh pellet is an important issue. Pellets are very sensitive to water. However, if the amount of the water is less than the ideal moisture content during the pellet formation, it causes air voids inside the pellet. On the other hand, if the amount of water is higher than the ideal moisture content during the pellet formation, the pellets become too wet to form a nucleus by using surface tension of water. In this stage, there is only surface tension to hold particles together and capillary force is vanished. As a result, the formation is weaker than the capillary bonding state. The granulometric distribution of pellets can not be controlled during the pelletization process in this state. In addition, final pellets are random sized and they can easily be crushed by mechanical forces in the balling drum or disc. That is why, this is a undesirable situation compared to the production with moisture content below optimum [43]

In the second example of moisture content states, the size and engineering performance of the pellets may fluctuate in great variety. Homogeneity in the engineering performance of pellets is not ensured. It is a fact that keeping moisture content equal to or below than the ideal content during formation process affects results in a better way [43].

Water content and mechanism of ball formation are important subjects for pelletization process. However, there are other significant topics such as the angle of pelletization drum or disc's plane to the normal and the revolution speed [43], [42].

There are two forces affecting the pellet formation, centrifugal and gravitational force. If one of these forces becomes dominant on the movement, the pellet formation stops or the formed pellets have a loose structure. For low revolution speed the movement of pellets is governed by gravitational force, and for high speeds the movement is governed by the centrifugal force. In stage where centrifugal force is predominant, the pellet production is ceased and the grains will stick the walls of pelletizer disc with the help of moisture. In order to achieve successful pellet production, neither centrifugal nor gravitational force should be dominant [3].

Production and the structure of pellets are totally rely on the quantity of moisture used during the pellet manufacturing process other than the mechanical forces. Moisture content has a direct effect on the diameter of the fresh pellets and there is a linear relationship between them. In addition, moisture content effects the residence time of pellets in the balling drum or disc. It also effects the rate of production other than the sizes of pellets [3].

2.2.9. Previous Studies on Fly Ash and Fly Ash Pellets

Previous studies conducted by the researchers related to fly ash and fly ash pellets are presented in this section.

Döven and Baykal give the idea of the pelletization process and the tests performed on pellets to specify the properties of the produced pellets [3]. Döven investigated the engineering performance of the moist cured fly ash pellets including the effect of % 8 lime and %8 cement additions by weight. The minimum pellet diameter was 2 mm and the diameter range of pellets was varying between 22.6 mm and 2 mm. Döven performed specific gravity, water absorption, crushing strength, maximum and minimum index density, California Bearing Ratio and direct shear tests on fly ash pellets. The apparent specific gravity, saturated–surface dry specific gravity, bulk specific gravity and water absorption values are given for different sieve size ranges. The sizes of the fly ash pellets may be described as coarse to fine gravel. The materials were selected as uniformly graded so that the changing properties of the material with changing sizes can be discussed [3].

Döven found that as the size of the pellet decreases, the specific gravity increases and relatively the water absorption decreases. The addition of lime and cement, as an average, increases the specific gravity by 3% and 4%, and decreases the water absorption by 4 % and 9 % respectively relative to the corresponding grain sizes of fly ash only pellets as seen in Figure 2.7 and Figure 2.8 [3].

Table 2.1. Previous studies on fly ash and fly ash pellets, part 1

Year	Author(s)	Title	Performed Tests	Significant Findings	References
1998	Ata Gürhan Döven	*Lightweight Fly Ash Aggregate Production Using Cold Bonding Agglomeration Process*	-Unit Weight -Specific Gravity and Water Absorption -Maximum and Minimum Index Density -California Bearing Ratio -Crushing Strength Tests -Direct Shear Tests -Soundness of Aggregate by Using Sodium Sulphate	-The cement (FC8) and lime added (FL8) fly ash pellet aggregates are suitable for all types of civil engineering applications such as construction of fills and embankments, backfills, pavement base and subbase courses concerning the results obtained from performance tests. -The use of cement and lime will significantly increase both short and long-term strength of the pellets. -The angle of internal friction of fly ash group pellets is 29.4°. The angle of internal friction values for FC8 and FL8 group pellets are 45.4° and 44.4° respectively, which is in the range of natural aggregates. -Fly ash group aggregates are suitable for use in subbase courses with 58 % CBR value.	1
2003	Hardar Arslan	*The Effect of Grain Crushing on the Behavior of Granular Materials*	-Specific Gravity and Water Absorption -Crushing Strength Tests -Particle Size Analysis -Direct Shear Tests	-Fly ash pellets have very low unit weight and the properties such as water absorption and crushing strength are convenient for lightweight concrete applications. -The direct shear tests showed that it is possible to increase the shear strength parameters of the fly ash pellets by additives. -The internal friction angles of the pellets used in this study are between 30° and 42° which is in the range of natural soils. -The material may provide high stability in many geotechnical applications like landfills and embankments.	2

Table 2.2. Previous studies on fly ash and fly ash pellets, part 2

Year	Author(s)	Title	Performed Tests	Significant Findings	References
2007	Egemen Danyıldız	*The Interface Behavior between Granular and Concrete*	-Specific Gravity and Water Absorption -Direct Shear Tests -Interface Tests -Surface Topography -Crushing Strength Tests	-The results of interface tests showed that the interface performance is highly related with crushing strength, shape and surface characteristics of granular materials and the surface roughness of concrete blocks. -Surface roughness and angularity of pellets increase the contact efficiency. FA group aggregates had rougher surfaces and angular shapes; the contact efficiency between granular and concrete was higher than other groups. -The effects of grain crushing, particle shape and the surface roughness of both aggregates and concrete play an important role in the interface behavior between granular soils and concrete.	3
2008	Altuğ Saygılı	*Highway Embankment Construction Using Fly Ash and Snow in Cold Regions*	-Unconfined Compression Testing -Splitting Tensile Strength Testing -X-Ray Diffraction Analysis -ESEM Analysis -Thermal Conductivity Analysis -Leachate Analysis -Length Change Determination -pH Measurements	-The study demonstrates that snow may be successfully used to introduce extra water during the compaction of fly ash without causing any workability problem. -The snow addition caused 30 % increase in void ratio; 12 % decrease in unit weight and 70 % increase in shear strength. -By snow addition, voids uniformly dispersed in the matrix provided a reservoir for water to expand. This appears to be the most effective and economical method to improve the freeze-thaw property of the compacted fly ash specimens. -The observed increase in tensile strength for snow-added fly ash is beneficial for potential use as base and sub base material for highway construction. -30% increase in void ratio means extra savings from transportation costs of fly ash, which will allow construction more economically. -With the developed technique embankment construction activity will be continued even during wintertime.	4

Table 2.3. Previous studies on fly ash and fly ash pellets, part 3

Year	Author(s)	Title	Performed Tests	Significant Findings	References
2011	Murat Cenk Erdurak	*Artificial Sand Production for Laboratory Uses*	-Specific Gravity and Water Absorption -Roundness and Sphericity -Direct Shear Tests -Cyclic Triaxial -Constrained Modulus	- The pellets behave more ductile than natural aggregates. As the normal load is applied in the direct shear test, the sphere–shaped pellets become rectangular prisms. - For all type of sands, the change from the dense state to the loose state in relative density ends up with a decrease in internal friction angle and smaller θ and α angles. - The internal friction angles of the pellets produced from both fly ash and cement are showing similar or greater values in comparison with natural and crushed sand. Especially, the internal friction angle values for the pellets produced with cement are occurred greater than all other samples.	5
2013	Utku Takmaz	*Behavior of Crushable Sand Under Cyclic Loading*	- Crushing Strength Tests - The Shape Factor Analysis -Cyclic Direct Simple Shear Tests - Monotonic Triaxial Test	- For the monotonic behavior, it is found that fly ash pellets have slightly smaller strength values. - As compacting sand samples result up to 5% of damping ratio change, for fly ash pellets it differs less than 2%. This means they dissipate well the energy even in the loose condition and it has satisfactory damping characteristics even without any compaction. - Stiffness and damping ratio are found dependent on CSR. For both fly ash pellets and sand samples, damping ratio decreases as the CSR increasing. That means fly ash pellets dissipate less energy, for the large cyclic stresses. But still, their damping properties stay at higher values than those of sand.	6

Group	Sieve Size (mm)	Apparent G_s	G_s (SSD)	Bulk G_s	Water Absorption (%)
FA	22.6+	2.00	1.60	1.19	33.85
	16-22.6	2.02	1.62	1.22	32.38
	8-16	2.09	1.66	1.26	31.84
	4-8	2.11	1.66	1.26	31.77
	2-4	2.17	1.70	1.29	31.38
FC8	22.6+	2.17	1.71	1.33	29.31
	16-22.6	2.03	1.65	1.28	28.65
	8-16	2.09	1.68	1.31	28.66
	4-8	2.18	1.72	1.34	28.83
	2-4	2.35	1.81	1.40	28.77
FL8	16-22.6	2.10	1.66	1.26	31.61
	8-16	2.08	1.65	1.25	31.73
	4-8	2.11	1.67	1.27	31.53
	2-4	2.28	1.75	1.33	31.42

Figure 2.7. Specific gravity and water absorption test results of groups with respect to grain sizes [3].

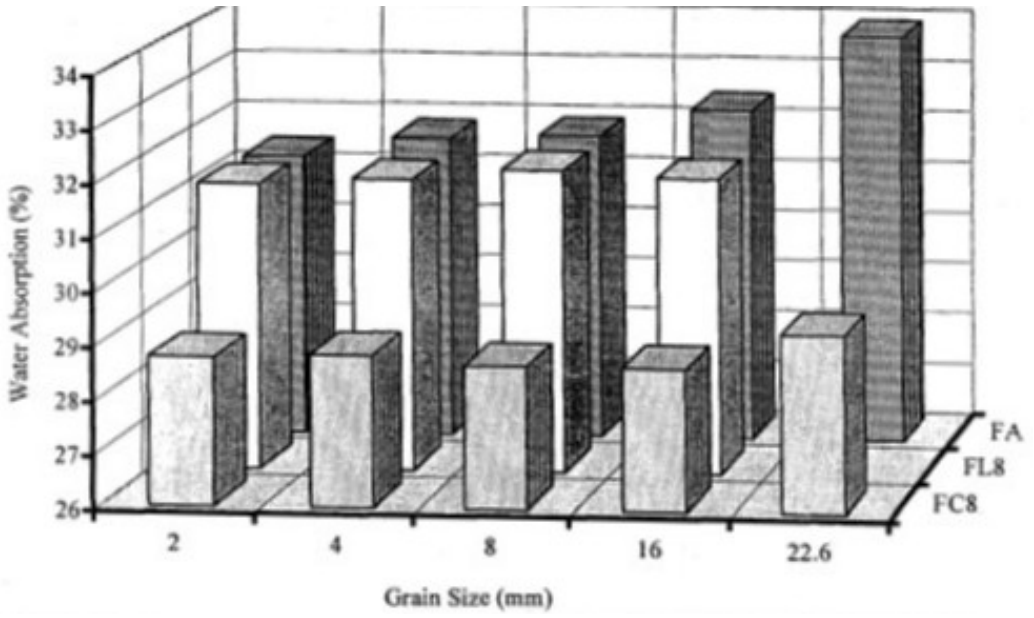

Figure 2.8. Water absorption percentages of pellets with respect to grain size [3].

The crushing strength tests are conducted on uniformly graded samples. The grain sizes of the pellets are given in the Figure 2.9. Pellets with different curing period and different grain sizes are compared. The crushing value of pellets increases as the particle diameter increases, however crushing strength decreases. While 8 mm fly ash pellets show 51 N crushing strength; for 4.75 mm, it was decreased to 23.5 N. Fly ash pellets with 8% lime addition by weight have the maximum crushing strength among three groups. Pellets with 28 days curing period have the maximum strength compared to 7 and 14 days for FA, FC8 and FL8 group of pellets. [3].

	Curing Period	7 Days	14 Days	28 Days
Group	Sieve Size (mm)	Crushing Strength (N)	Crushing Strength (N)	Crushing Strength (N)
FA	19	173.6	197.2	211.9
	16	147.2	160.9	170.7
	12.5	93.2	120.7	141.3
	10	71.6	74.6	85.3
	8	45.1	51.0	51.0
	6.3	29.4	35.3	38.3
	4.75	17.7	21.6	23.5
FC8	19	387.5	585.7	660.2
	16	353.2	516.0	570.0
	12.5	247.2	306.1	366.9
	10	155.0	193.3	246.2
	8	108.9	142.2	151.1
	6.3	84.4	93.2	105.9
	4.75	52.0	71.6	74.6
FL8	19	299.2	540.5	740.7
	16	253.1	411.0	687.7
	12.5	145.2	290.4	476.8
	10	113.8	187.4	312.0
	8	65.7	120.7	215.8
	6.3	33.4	79.5	141.3
	4.75	20.6	51.0	91.2

Figure 2.9. The crushing strength test results of groups with respect to grain size and curing periods [3].

For the CBR test, Döven were compacted pellets at 34 % water content with standard proctor compaction energy. The amount of water necessary to compact the pellets, other than the absorbed amount, was 4 % to 4.5%. For the FA group, CBR value was 58% as seen in the Figure 2.10. Lime and cement additions increased the CBR value from 58 % to 82 % as seen in Figure 2.5. According to Döven, FA group pellets are most suitable for subbases and may be used as a base material as well. The FC8 and FL8 group pellets, that have equivalent CBR values to that of gravel, crushed gravel and crushed rock, may be used in base layers [3].

Group	Opt. Water Content (%)	Dry Unit Weight (kN/m^3)	CBR (%)
FA	34.4	12.0	58
FC8	34.0	12.6	82
FL8	34.5	12.2	82

Figure 2.10. The optimum water content, dry unit weight and CBR values of groups with respect to grain size distribution used in the performance tests [3].

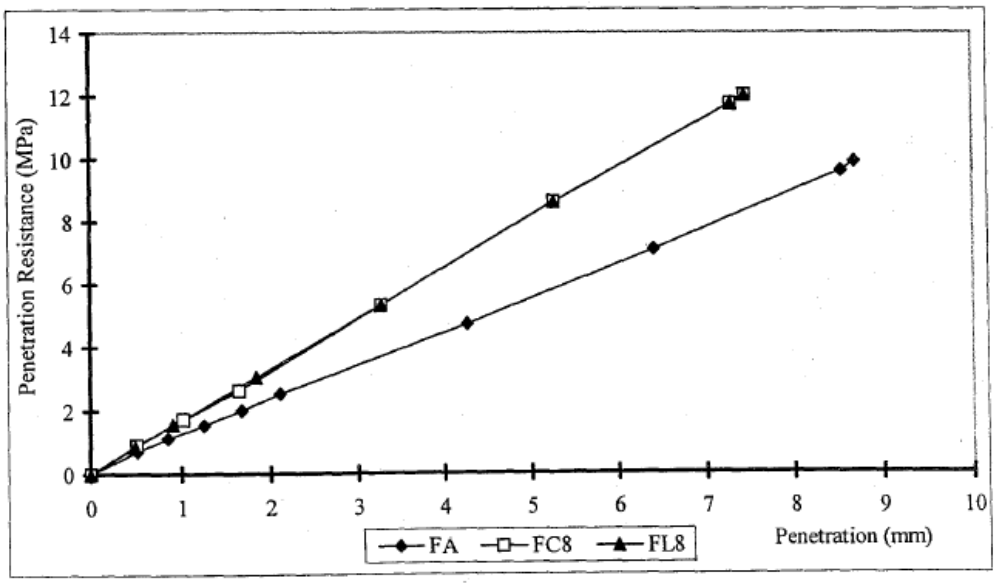

Figure 2.11. The CBR test results for all pellet groups for the chosen grain size distribution [3].

As seen in Figure 2.12, the angle of internal friction changes between 29 and 45 degrees for fly ash only (FA) group and both for FC and FL groups respectively. FC8 and FL8 groups have the same internal friction angle. The angle of internal friction of FA group pellets was 29.4°. The angle of internal friction values for FC8 and FL8 group pellets were 45.4° and 44.4°, respectively. The results show similarity with CBR test results as well [3], [44].

	Angle of Internal Friction (degrees)	
Group	Ultimate	Residual
FA	29.4	22.4
FC8	45.4	37.7
FL8	44.4	38.0

Figure 2.12. The shear strength parameters of the groups, - angle of internal friction [3].

Döven performed sieve analysis after direct shear tests, similar to Arslan. Grain size analysis results are given in Figure 2.13. Based on the results, the degradation under loading was greater for FA group pellets than FC8 and FL8 group pellets. The degradation occurs mostly at sizes greater than 2 mm for FA group pellets and at sizes greater than 8 mm for FL8 and FC8 group pellets, similar to crushing value test results [3]. Results of experiments showed that the fly ash pellets may be substituted for natural aggregates in many engineering applications [3], [44].

Sieve Size (mm)	FA Group		FL8 Group		FC8 Group	
	Before	After	Before	After	Before	After
31.5	–	–	–	–	100	100
16	–	–	100	100	65	69.4
8	100	100	65	68.0	42	43.8
4	66	72.2	40	41.4	30	31.7
2	44	45.0	27	27.3	18	18.2
1	30	31.9	17	17.4	11	11.1
0.25	7	8.3	5	5.4	3	3.1
0.075	N/A	2.0	N/A	0.3	N/A	0.3

Figure 2.13. Grain size analysis results of FA, FL8, and FC8 group aggregates before and after direct shear tests [3].

In further review of literature, Arslan analyzed the crushing of granular materials under shear loading by using manufactured granular materials (MGM) instead of natural soils to observe the influences of crushing sole on the behavior of granular materials. The main objective was to simulate the crushing of particles under shear loading. Arslan produced two different groups of pellets that have virtually the same particle sizes but different crushing strengths. After production of fly ash, fly ash with 10% cement, fly ash with 20% cement and fly ash with 30 % cement, the sand-sized particles are sheared in direct shear equipment and the internal friction angles are determined. There was no significant change in sieve analysis results after shearing under 50 and 100 kPa normal stresses. However, some crushing behaviour was seen under the normal stress of 200 kPa as can be seen in Figure 2.14. FA group pellets that are produced from only fly ash, and FC30 group pellets produced from 70 % fly-ash and 30 % cement mixtures to obtain the different crushing strength for the two different groups of pellets. Then, Arslan performed six single particle crushing tests for each class to obtain the crushing strength of single grains. Crushing strength test is performed by many researchers that have worked on fly ash pellets 2.14 [4].

Class	Load kN	d_1	d_2	d_3	$d_{average}$ (cm)	Crushing Stress (kPa)	Crushing Stress (MPa)
FA	0.392	0.51	0.49	0.55	0.52	184.676	0.185
FA	0.42	0.52	0.5	0.54	0.52	197.867	0.198
FA	0.408	0.48	0.45	0.51	0.48	225.584	0.226
FA	0.52	0.52	0.5	0.55	0.52	244.978	0.245
FA	0.44	0.55	0.45	0.52	0.51	215.498	0.215
FA	0.48	0.55	0.45	0.52	0.51	235.088	0.235
FC30	2.822	0.52	0.51	0.51	0.53	1279.781	1.280
FC30	2.905	0.55	0.5	0.51	0.52	1368.579	1.369
FC30	2.905	0.53	0.49	0.52	0.51	1422.775	1.423
FC30	2.8635	0.54	0.5	0.51	0.52	1349.028	1.349
FC30	3.1125	0.5	0.53	0.55	0.55	1310.733	1.311
FC30	3.071	0.51	0.52	0.55	0.55	1293.257	1.293

Figure 2.14. Crushing strength analysis of FA and FC30 group [4].

The stress-deformation behavior and the shear strength parameters of fly ash pellets were determined by direct shear tests. Direct shear tests were performed under 100, 200 and 400 kPa normal stresses. Results are given in Figure 2.15. The internal friction angles of the four groups of pellets are 30° for FA; 35° for FC10, 40° for FC20 and 42° for FC30 group pellets. Sieve analysis which are performed both before and after direct shear tests show that the pellets crushed greater under 400 kPa then, respectively, 200, and 100 kPa as can be seen in Figure 2.16.

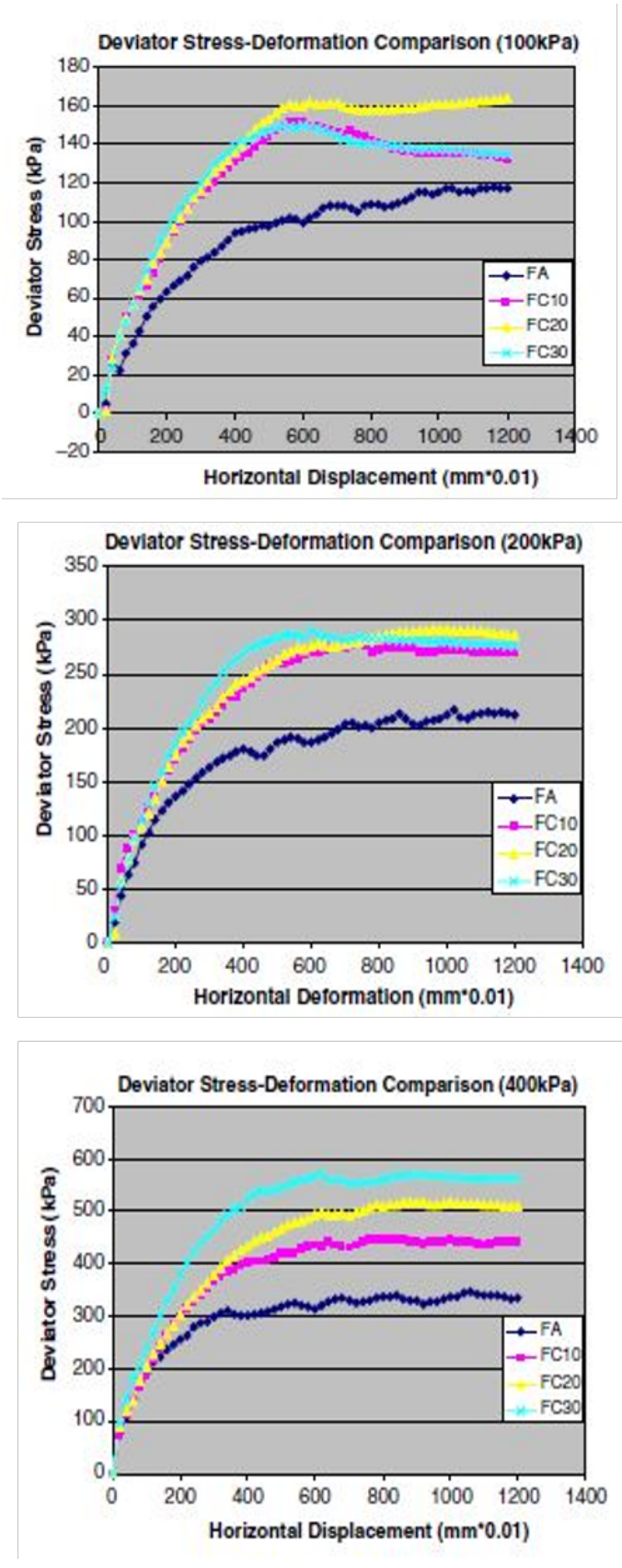

Figure 2.15. Comparison of deviator stress–deformation behavior of manufactured granular materials under 100,200 and 400 kPa normal pressure [4].

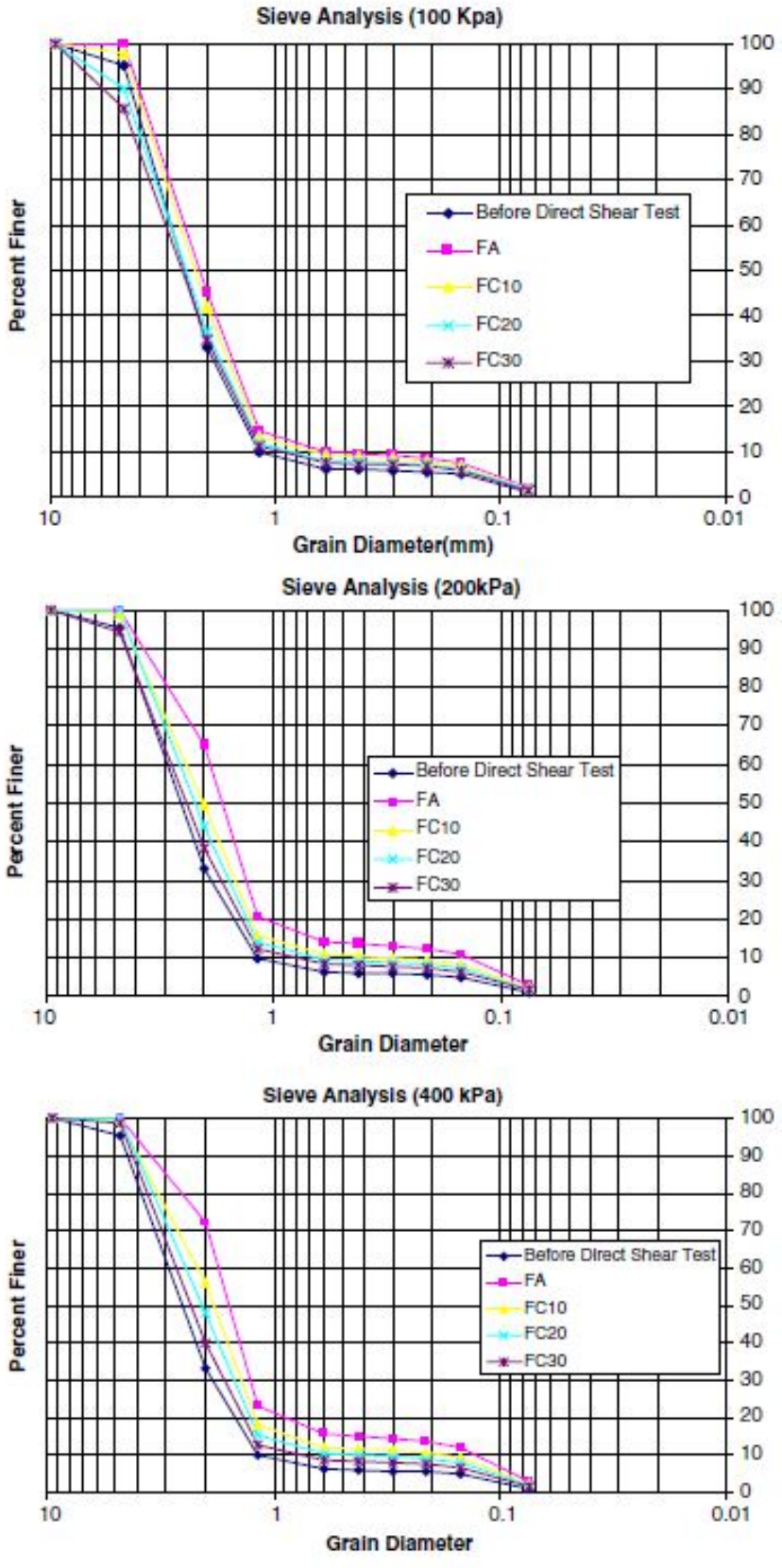

Figure 2.16. Sieve analysis of FA group before and after direct shear tests [4].

Danyıldız investigated the interface behavior between pellets and concrete in order to understand the influence of physical and mechanical properties of granular soils on the interface behavior. Danyıldız performed specific gravity, water absorption, crushing strength, direct shear and interface tests as seen in Figure 2.17 to Figure 2.22. Grain size analysis was performed before and after the direct shear tests. Danyıldız also investigated the effects of grain crushing, particle shape and roughness of interface surface. Danyıldız performed tests on three groups of pellets; FA, FAC10 and FAC20. FAC10 and FAC20 represent fly ash pellets with 10 % and 20% cement addition. For the crushing strength tests, the sizes of the pellets varied between 9.5 to 14 mm [5].

	Day	$F_{average}$ (N)	$d_{average}$ (cm)	$\sigma_{average}$ (N/cm^2)
FA	7	15.18	1.27	11.83
	14	65.55	1.29	49.88
	28	246.10	1.24	201.62
FAC10	7	63.11	1.23	52.81
	14	150.51	1.22	126.72
	28	320.53	1.21	278.15
FAC20	7	123.37	1.21	107.40
	14	269.19	1.16	254.20
	28	393.85	1.21	341.29

Figure 2.17. Crushing strength tests results of FA, FAC10 and FAC20 groups pellets [5].

Results show that pellets which were cured for 28 days have the maximum crushing strength, similar to Döven. Cement addition increased the crushing strength of fly ash pellets as seen in the Figure 2.17. Highest strength obtained with FAC20 group [5].

Specific gravity and water absorption values of three groups are given in Figure 2.18. Results show similarity with studies of Döven. The results indicate that the addition of cement to the mixture increased both oven dried and saturated surface dry bulk specific gravities while resulting in a decrease in the capacity of water absorption [5].

	A (gr)	B (gr)	C (gr)	OD	SSD	ARD	WA (%)
FA	106,5	144,6	55,1	1,19	1,67	2,07	35,74
FAC10	126,5	164,1	68,4	1,32	1,71	2,18	29,78
FAC20	119,5	145,5	68,3	1,55	1,88	2,33	21,81

Figure 2.18. Specific gravity and water absorption values of FA, FAC10 and FAC20 group pellets [5]

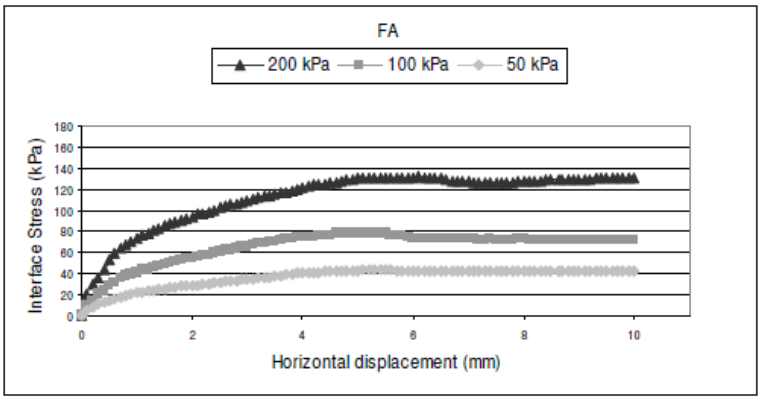

Figure 2.19. The shear stress-horizontal displacement curves of FA group pellets under 50,100 and 200 kPa normal stresses [5].

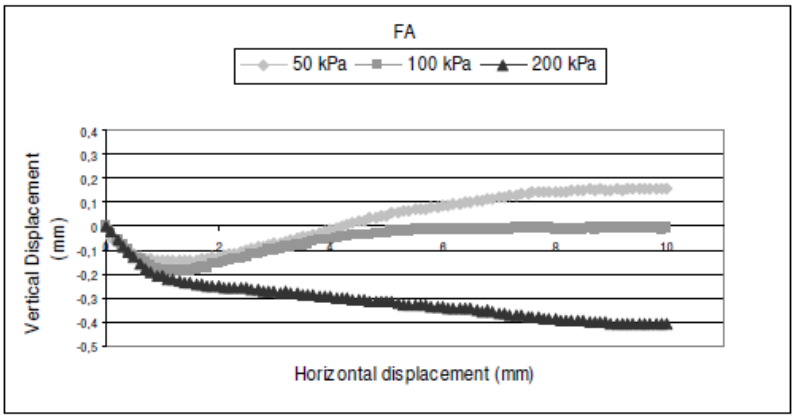

Figure 2.20. The vertical-horizontal displacement curves of FA group pellets under 50,100 and 200 kPa normal stresses [5].

Interface and internal friction tests under 50, 100 and 200 kPa normal stresses for soil to soil and soil to concrete were performed. Results of direct shear tests are similar to Döven and Arslan. Results from Danyıldız show that pellets dilate up to 100 kPa shear stress, but contract at 200 kPa shear stress as seen in Figure 2.19 and Figure 2.20. According to Danyıldız, the internal friction angle of fly ash pellets at peak shear stress is 30.09° [5], [45].

Granulometry of the pellets is similar to that of the studies from Döven and Arslan. Degradation is increasing as the normal stress increases from 50 kPa to 100 kPa as seen in Figure 2.21. According to Danyıldız, The FAC10 and FAC20 group pellets were relatively more resistant to crushing in comparison with FA group pellets [5].

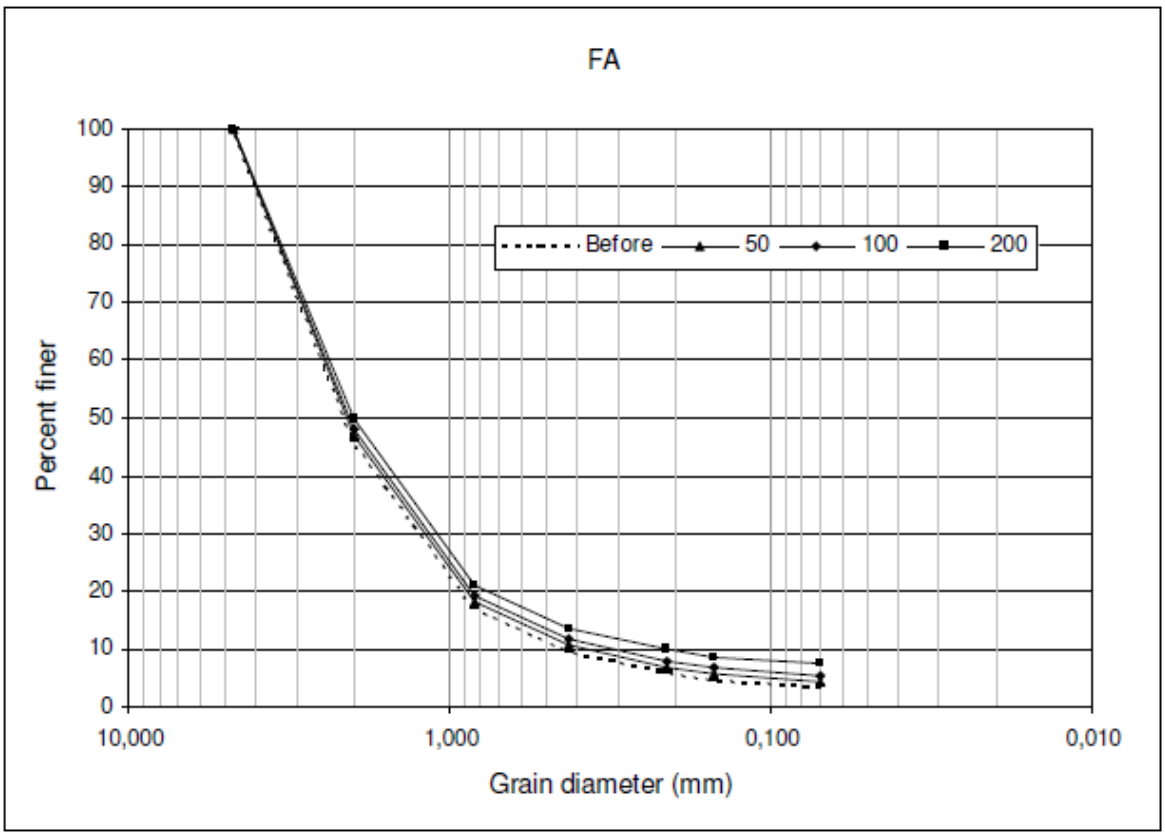

Figure 2.21. The sieve analysis test results of FA group pellets before and after direct shear tests, under 50 kPa, 100 kPa and 200 kPa normal stresses [5].

	FA		FAC10		FAC20	
	ϕ	δ	ϕ	δ	ϕ	δ
	30.09°	27.57°	36.55°	33.15°	37.98°	33.89°
Normal Stress (kPa)	Max Shear Stress (kPa)	Max Interface Stress (kPa)	Max Shear Stress (kPa)	Max Interface Stress (kPa)	Max Shear Stress (kPa)	Max Interface Stress (kPa)
50kPa	42.94	30.45	39.08	28.42	37.86	27.87
100kPa	78.23	58.30	79.98	58.67	81.31	60.82
200kPa	131.13	109.11	151.02	125.90	155.83	128.50

Figure 2.22. The overall performance of pellets in shear and interface stress tests [5].

Figure 2.22 shows the overall performance of all pellet groups in shear and interface stress tests. Results of interface tests performed by Danyıldız showed that the interface performance is highly related to crushing strength, shape and surface characteristics of granular materials, and also the surface roughness of concrete blocks. The effects of grain crushing, particle shape and the surface roughness of both pellets and concrete are important in the interface behavior between pellets and concrete as stated by Danyıldız [5].

A new technology was developed at Boğazici University by Saygılı and Baykal, to add more water into fly ash samples to enhance the pozzolanic reactions, leading to the cementitious mineral formation. Fly ash at optimum water content and fly ash with additional 10% by weight of snow were compacted, sealed and cured for one, seven, 14, 28, and 90 days at 21°C. Snow addition had a remarkable effect on improving the freeze-thaw and thermal conductivity properties of the compacted fly ash specimens. After snow addition, snow causes 30% increase in the void ratio of samples. Snow increased the total water content of samples by 48%. Dry unit weight of samples decreased by 30% as seen in the Figure 2.23. The higher void ratio of snow-added fly ash is important in terms of insulation capability and freeze-thaw resistance. The amount of fly ash to compact the same volume of the embankment will decrease, causing significant cost savings.

For embankments constructed on soft soils, the 12% lower unit weight of snow-added embankment will decrease the settlement of the embankment while increasing the factor of safety against the bearing capacity failure [1].

	Fly Ash (FA)	Fly Ash + Snow (FI)	% Change
Dry Unit Weight (kN/m^3)	13.41	11.78	12% decrease
Water Content w%	19.54	28.89	48% increase
Void Ratio e	0.90	1.17	30% increase

Figure 2.23. Comparison of the properties of compacted fly ash and compacted fly ash and snow [1]

Results showed that; in embankments, the snow added fly ash would show higher performance than that of the compacted control fly ash samples, because it possesses better drainage characteristics and no tension cracks would develop, therefore embankments constructed with snow added fly ash samples will be more resistant to frost action [1], [46], [47], [48].

	Weight (grams)	Unit Weight ($grams/cm^3$)	K (W/m°C)	Change (%)
FA	411.14	13.29	0.301	-
FI10	379.02	12.62	0.342	13.6
FI20	340.01	11.26	0.369	22.5
FI30	264.97	9.15	0.359	19.2

Figure 2.24. Properties of fly ash and snow-added compacted fly ash samples used for thermal insulation (cured for 90 days) [1]

By comparing three types of snow-added fly ash specimens for thermal insulation, it was found that 20% snow-added fly ash specimen was a better mixture for making blocks having better thermal properties.

20% snow-added fly ash block was found to be superior to 10% , 30% snow-added and control fly ash block in terms of thermal conductivity, K ranging from 0.369 to 0.301 W/m^0C as shown in Figure 2.24. 30% snow-added fly ash block was found to be superior to 20%, 10 % snow-added and control fly ash block in terms of weight. The surface temperatures of the specimens recorded at different time periods on the surface of the hotbox apparatus are represented in Figure 2.25 [1].

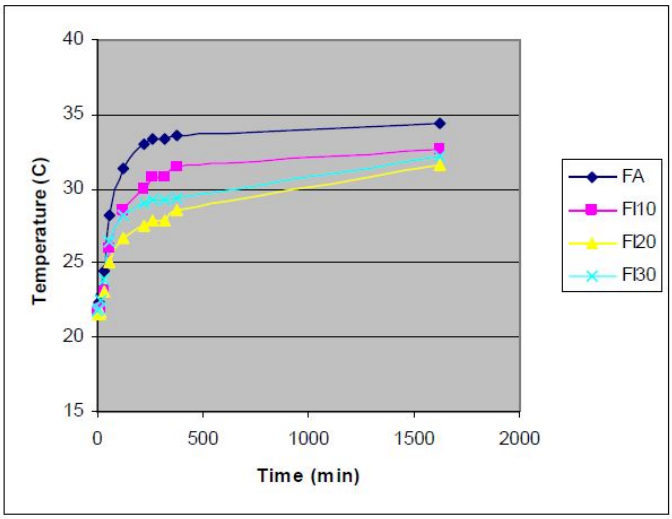

Figure 2.25. The surface temperatures of the specimens recorded at different time periods on the surface of the hotbox apparatus [1].

Erdurak studied on the artificial sand production for laboratory uses. Erdurak evaluated the performance of artificial sand and prepared natural sand samples, crushed sand samples and artificial sand samples produced from cement and fly ash, alternatively. Specific gravity, water absorption, crushing strength, direct shear, cyclic triaxial, roundness and sphericity and constrained modulus experiments were performed. The results of direct shear tests performed on uniformly graded (between 20–30 sieve sizes) fly ash pellets are presented in Figure 2.26 and Figure 2.27. Although the peak shear strength values in dense state are almost same with the shear strength values of the uniformly graded samples produced from fly ash, the shear strength values of well-graded samples produced from fly ash in the loose state are clearly higher than the uniformly graded samples in the same relative density and under same normal stresses.

The vertical displacement versus horizontal displacement curves for pellets produced from fly ash with the grain size distribution of Standard sand well graded is represented. Unlikely, all samples in loose state show a dilation behavior as seen in Figure 2.27 [6].

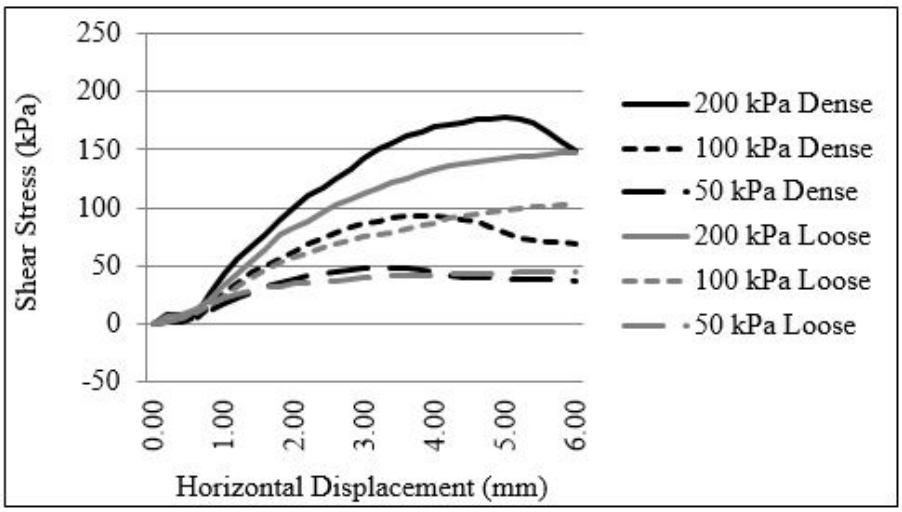

Figure 2.26. Shear stress vs. horizontal displacement curve for pellet produced with fly ash with grain size distribution of Standard sand well graded. [6]

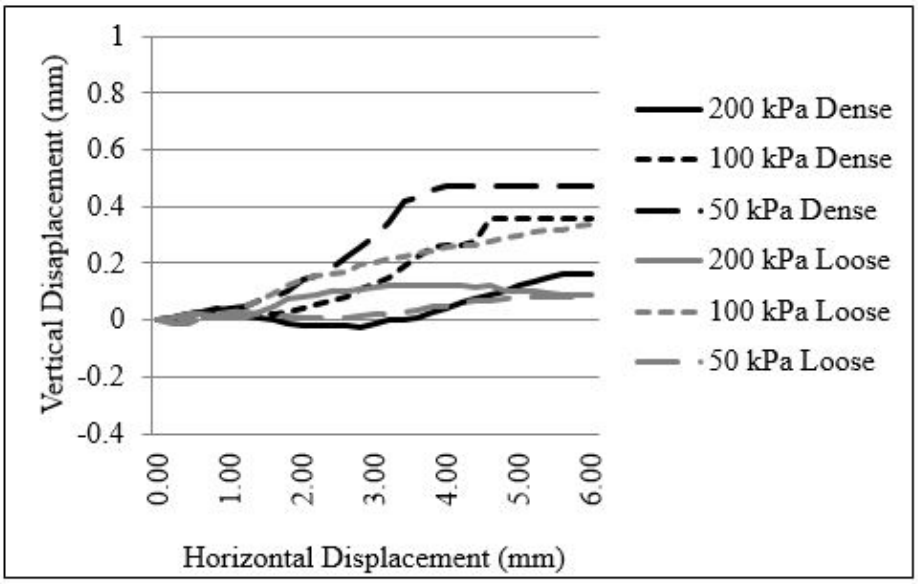

Figure 2.27. Vertical displacement vs. horizontal displacement curve for pellet produced with fly ash with grain size distribution of Standard sand well graded. [6]

In further review of literature; Takmaz investigated the behavior of manufactured sand under cyclic loading. The main objective of the research is to understand how the cyclic behavior of fly ash pellets differs from the same grain size sands. Takmaz evaluated the cyclic behavior of fly ash pellets and compared these results with trends of Sile and Kilyos sands at similar relative densities and loading conditions. Takmaz determined the index properties of sands and fly ash pellets as seen in Figure 2.28 and Figure 2.29 [7].

Sand Type	Specific Gravity	Maximum Void Ratio	Minimum Void Ratio	D_{50}
Sile	2.61	0.78	0.52	0,26
Kilyos	2.66	0.77	0.44	0,65

Figure 2.28. Index properties of Sile and Kilyos sands [7].

Fly Ash Pellet Type	Maximum Void Ratio	Minimum Void Ratio
Well graded	1.08	0.57
Poorly graded	1.13	0.66

Figure 2.29. Index properties of fly ash pellets [7].

Crushing value test is performed on individual pellets to find an average strength value for each grain size. Crushing strength results are similar to those studies of Döven, Danyıldız. Crushing load increases as the diameter size of the pellets increase. Although the crushing load increase with the diameter size, the crushing strength decreases if the diameter of the pellets increases as seen in Figure 2.30 [7].

sieve size (mm)	Particle number	$d_{average}$ (mm)	crushing strength (N)	average values for crushing strength	σ (N/cm2)	$\sigma_{average}$ (N/cm2)	$\sigma_{average}$ (kPa)
19	1	20,0	297,13	301,18	0,74	0,75	7,53
	2	20,0	301,15		0,75		
	3	20,0	305,18		0,76		
	4	20,0	289,21		0,72		
	5	20,0	313,24		0,78		
16	1	17,5	212,40	216,50	0,69	0,71	7,07
	2	17,5	214,45		0,70		
	3	17,5	216,50		0,71		
	4	17,5	218,55		0,71		
	5	17,5	220,60		0,72		
12,5	1	14,3	202,65	204,05	1,00	1,00	10,05
	2	14,3	204,46		1,01		
	3	14,3	204,16		1,01		
	4	14,3	205,42		1,01		
	5	14,3	203,56		1,00		
10	1	11,3	99,65	98,61	0,79	0,78	7,79
	2	11,3	97,46		0,77		
	3	11,3	99,46		0,79		
	4	11,3	100,01		0,79		
	5	11,3	96,48		0,76		
8	1	9,0	64,57	64,22	0,80	0,79	7,93
	2	9,0	66,49		0,82		
	3	9,0	63,13		0,78		
	4	9,0	61,48		0,76		
	5	9,0	65,46		0,81		
6	1	7,2	41,87	41,00	0,82	0,80	8,02
	2	7,2	40,99		0,80		
	3	7,2	42,48		0,83		
	4	7,2	39,92		0,78		
	5	7,2	39,76		0,78		
5	1	5,5	38,48	38,40	1,26	1,26	12,58
	2	5,5	37,49		1,23		
	3	5,5	39,02		1,28		
	4	5,5	39,87		1,31		
	5	5,5	37,15		1,22		

Figure 2.30. Crushing strength test results of fly ash pellets [7].

Direct simple shear tests are performed on Sile, Kilyos sands and fly ash pellets. The specimens were consolidated under 50 kPa and 100 kPa vertical stresses and then sheared with cyclic simple shear loading. Results are given in Figure 2.31 to Figure 2.32. The damping ratio values are increasing non-linearly as the shear strain is increasing. As seen in the Figure 2.31, after 1% of strain the damping ratio values for fly ash pellets tend to be higher than the Sile sand. For higher CSR values, it is seen that the damping ratio values are remarkably higher. Under cyclic loading, fly ash pellets behave in the same trend as Kilyos and Sile sands. Their secant shear modulus values degraded with shear strain following the same trend under same loading conditions. The same trends observed also for damping ratio values [7].

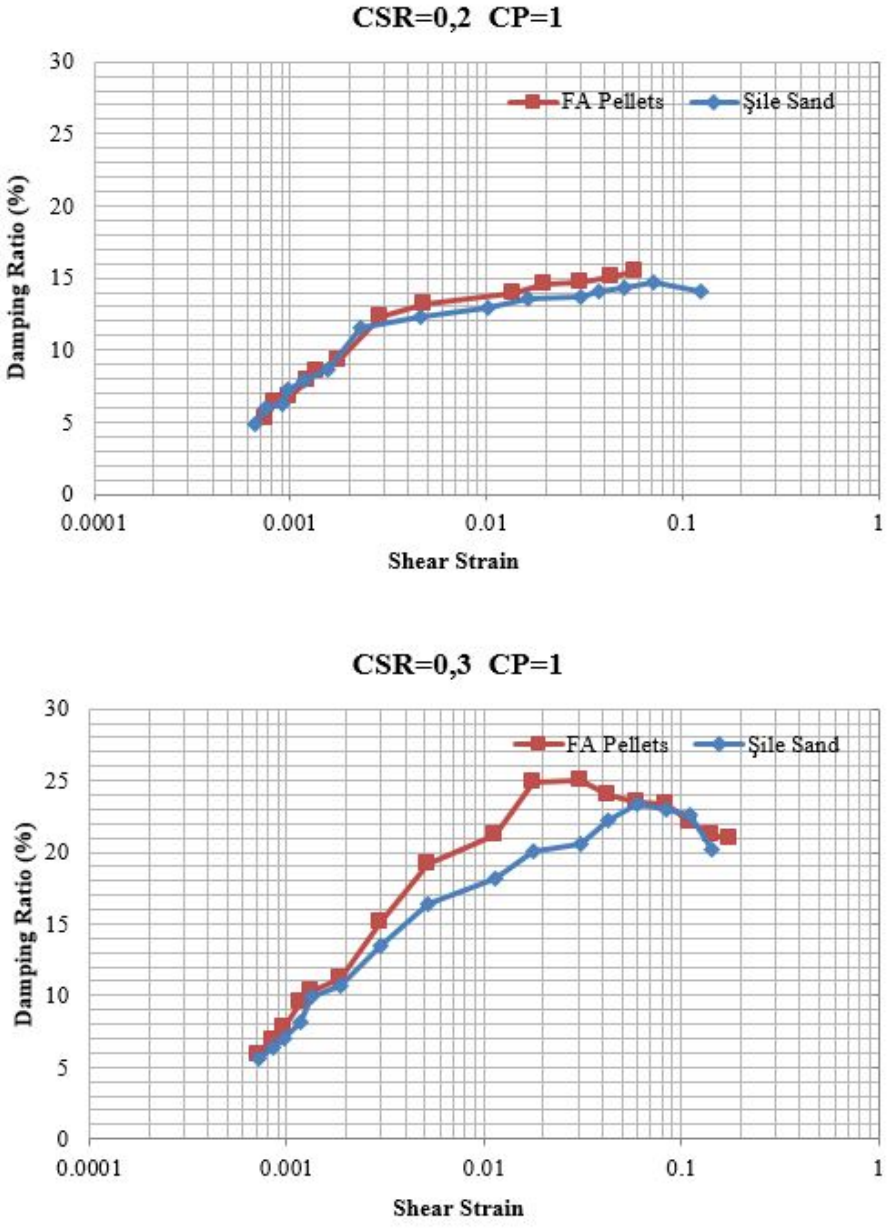

Figure 2.31. Damping curves of Sile sand and the well graded pellets at given loading conditions [7].

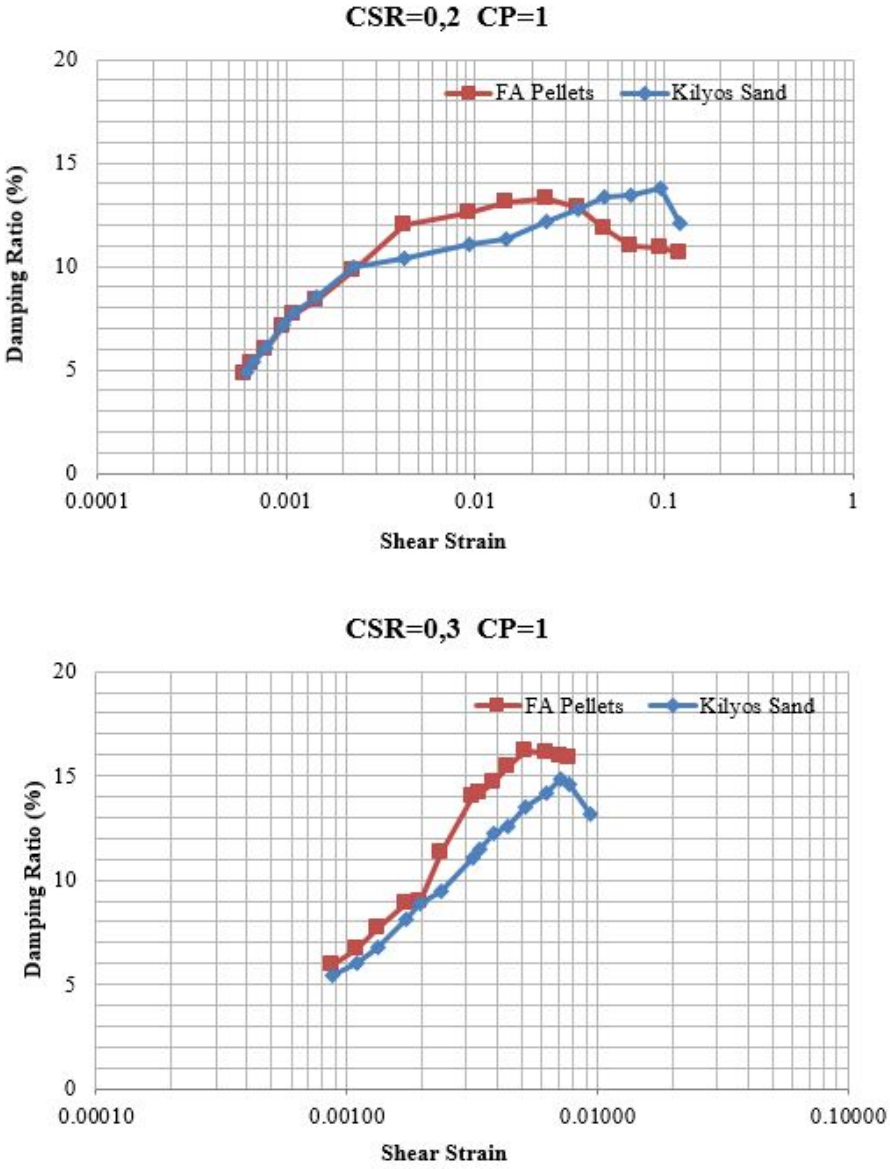

Figure 2.32. Damping curves of Kilyos sand and the poor graded pellets at given loading conditions [7]

3. METHODOLOGY

The aim of the present study is to evaluate the performance of fly ash pellets subjected to freeze thaw cycles. Pellets formed with only fly ash are produced by cold bonding pelletization process. Fresh pellets were cured in the curing room at 25°C with eighty percent relative humidity for 28 days. The pellets were kept in plastic bags to preserve their moisture content. The pellets were covered with snow to simulate the frozen soil. A freeze-thaw cycle in this experiment is intended to correspond to one year duration in the cold regions. The effectiveness of freeze-thaw procedure is assessed by the help of thermal imaging. Furthermore, specific gravity, water absorption, California Bearing Ratio (CBR), thin section, cyclic simple shear, direct shear and crushing value tests were conducted. Ten CBR tests were conducted to see the effect of freeze-thaw cycles. Average California bearing ratio values were calculated for both control and freeze-thawed group. Grain size distributions before and after the direct shear test have been conducted to examine the amount of crushing of pellets. Internal friction angle was determined after freeze-thaw test. The pellets were examined by optical microscope in order to investigate physical deformations as a result of the freeze-thawing test such as peeling on the surface of the pellets. Thermal images of pellets were obtained during freeze-thaw cycles with the thermal imager. Also, ESEM analysis were performed to examine microfabric of pellets.

In the design of embankments, slope stability is an important issue. In this concept, internal friction angle of fly ash pellets must be determined. Direct shear test device was used to perform direct shear test. Tests were performed under 25, 50 and 100 kPa normal stresses. In total, 12 direct shear tests were performed on the pellets.

In CBR Test, the purpose is to determine the bearing capacity and the mechanical strength of pellets. CBR tests were performed on the samples since the primary purpose of this study is to evaluate the performance of fly ash pellets that are intended to be uses for embankment construction in cold regions. The tests were performed on pellets for both control and freeze-thawed groups to observe the change in bearing capacity.

Crushing value tests are the mechanical tests which measures the maximum compressive load a pellet can handle before fail. In this study, crushing value tests were performed on 40 pellets for every pellet size.

3.1. Materials

3.1.1. Fly Ash

In this study fly ash is used for the production of pellets without any additives. Type of the fly ash was C and it is obtained from Soma Thermal Plant located 2 km out of Soma, Manisa. The plant has six units with 1034 MW energy capacity. At the Soma thermal power plant, 30,000 tons of coal is burnt and 12.000 tons of fly ash is produced per day. The lignite coal is burned in all units. The minimum calorific value of coal is specified to be 2200 kcal/N. The fly ash is collected by electrostatic precipitators and handled both by dry and wet methods. The residues collected from units one to six are hauled to the lagoons commissioned in Yırca and Ayıtlı villages with 9 x 10 m^3 and 70 x 10^6 m^3 volumetric capacities respectively. The residues obtained from units seven and eight are deposited to the site next to the power plant. The related statistical data are given in Figure 3.1 [3].

Units	Coal Consumption (tons/day)	Calorific Value (kcal/N)	Fly Ash Production (%)	Precipitator Efficiency (%)
1-2-3-4	4000	2200	37-43	98-99
5-6	6000	1550	52-64	99
7-8	500	3325	25	97

Figure 3.1. The statistical figures related with the coal combustion, calorific value and fly ash production of the Soma thermal power plant [3]

3.1.2. Snow

Ice or snow which was used in this study has been collected from Bogazici University in the winter season and stored in special bags in a deep freezer at -17°C through the test period. The main reason behind the use of the snow was to expose fly ash pellets to realistic conditions.

Particles of snow commonly range in size from about 0.1 mm to several millimetres. Freshly deposited snow has a bulk density less than 0.1 gr/cm^3. On the contrary, it can be as high as 0.4 gr/cm^3 if dry snow is deposited after being carried by strong winds. According to Dorsey, the bulk density of ice at 0°C and atmospheric pressure varies from 0.92 to 0.918 gr/cm^3 [19].

Barnes indicated that ice density decreases slightly with age [19]. Nichols reported densities at 0°C of 0.91 and 0.92 gr/cm^3 for newly formed natural ice, one year-old natural ice frozen at low temperatures, respectively [20]. However, Barnes found much smaller variation in the ice samples taken from the St.Lawrence River; densities at 0°C of new, one-year-old and two-year-old ice were 0.92 gr/cm^3. There are many other factors affecting the variation of the bulk density of ice. These include the number and nature of the cracks, the degree of air entrapment, ice purity, dislocation, and stacking fault vacancy. The true value of it, reported to be 0.92 $\pm$ 0.00005 gr/cm^3, was determined by Ginnings and Corruccini [49].

3.2. Experimental Study

3.2.1. Pelletization Process

The pelletization disc consists of five main units and these are; a pelletizing disc with a diameter of 90 cm, a motor reduction unit, water spraying system consist of 3 spraying tunnels, a carrying frame and a speed controller unit which is capable of changing revolution speed of the disc between 0 to 11 with 10 revolution per minute sensitivity.

The function of the blades are [43], [42]:

- ensuring different grain size of rolled material move in different path for ease in controlling the grain size distribution. In this way, coarse size material moves in interior path and fine size material stay in outer path.
- creating a barrier before radial rotating rolled material to compact them more by bumping to the blades and,
- sustaining the pellet production process smoothly and to remove any material that sticks to the bottom and walls of the pelletizer disc.

Only fly ash was used in pelletization process for the purpose of the project. Firstly, trial pellet production was done by observing the stages of pellet formation, the size and apparent strength of pellets with changing number of water spray tunnels, changing water spraying intervals, amount of sprayed water and the revolution speed of the pelletizing disc. The angle and revolution speed parameters were determined for the desired grain size around 2 mm to 10 mm. The grain size distribution of produced fly ash pellets for this study as given in Figure 3.2. According to the same graph, mean particle size (D_{5_0}) is approximately 4 mm. In order to check the suitability of the fresh pellets for various conditions such as hauling and stockpiling, the pellets were dropped from a height of 115 cm [3].

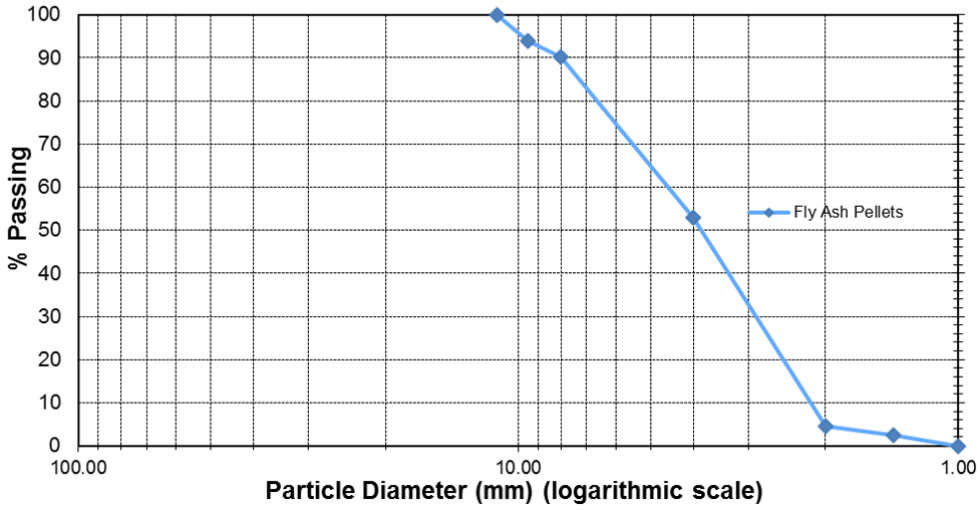

Figure 3.2. Grain Size Distribution of Fly Ash Pellets

The application of the theoretical equations with the defined parameters and observations on the formation displayed that the working angle should be changed between 35 and 50° and the rotation speed should be changed between 35 and 55 revolutions per minute [3]. Angle of pelletizer disc and revolution speed were 45° and 43 rpm, in this project, respectively.

Since the capacity of the pelletizer disc was considerably larger than those in the previous studies, the formation of first fresh pellets occurred between 15-20 minutes. The total pelletization time was determined as around 60 minutes with 10 kilogram fly ash capacity. It was concluded that in this capacity, 50 minutes duration for pelletization process was sufficient.

3.2.2. Freeze-Thaw Test

Main purpose of the test is to determine resistance of fly ash pellets which are exposed to freezing and thawing cycles. In this test, 10 cycles were performed on 8 different samples. Every cycle represents one year for cold regions. Freeze-thaw testing is conducted by exposing the product to freezing temperatures approximately -17° for 18 hours, and then allowing it to thaw at 40° temperature for 2 hours. This process completes one cycle of the test.

Figure 3.3. Fly ash samples with snow addition at the beginning of freezing cycle

In this study, to represent conditions of cold regions, standard freeze-thaw method was not used. Thermal imaging was used to verify the implemented method. Weather conditions are not rapid in cold regions. However, ASTM C666 standard consist of lowering the temperature of the specimens from 4 to -18 °C and raising it from -18 to 4°C in not less than 2 nor more than 5 hours.

A freezer capable of maintaining a temperature of -18°C was used. The temperature of the freezer was monitored by a thermometer within the freezer. The tray dimensions were 30x45x8 cm. For the beginning of the cycle, based on the weight of pellets, snow was added to the trays 25 percent by weight. After that, at the end of each cycle, this procedure was repeated until pellets are totally submerged in water at freezing stage as seen in Figure 3.3. The purpose of adding snow is to simulate climate conditions of cold regions by direct contact of pellet and snow.

Thermal images were taken by thermal imager as seen in Figure 3.4. In general, the concept of thermal cameras can basically be explained to sense the change of temperature in the environment. Every object emits infrared energy related to their temperature. This energy is called as heat signature. Electronic images are created based on the information about the temperature differences which are collected by the device through the radiation that emits from objects. Most of the times the objects are not the same temperature as other objects surrounding them; thus in a thermal image this temperature difference will be very distinct. An automatic calibration for the ambient and camera temperature is provided. In this study, thermal imager consists of FPA type detector with 120x120 pixel resolution was used to see the changes in temperature of fly ash pellets during the freeze-thaw cycles.

Figure 3.4. Thermal Imager

Change of temperatures on fly ash pellets at the time of freeze-thaw experiment are observed with an infrared camera. Results are given in the Figure 3.8 to Figure 3.6. Thermal imager which is used in this study has auto-calibrate property. Thus, maximum and minimum temperatures adjusted based on momentary image to approach ideal contrast. These temperatures demonstrated in degrees centigrade on the bottom of the each image. In order to better observe the heat changes at extreme temperatures, it has been heated and frozen for slightly longer periods than the normal cycle in some images.

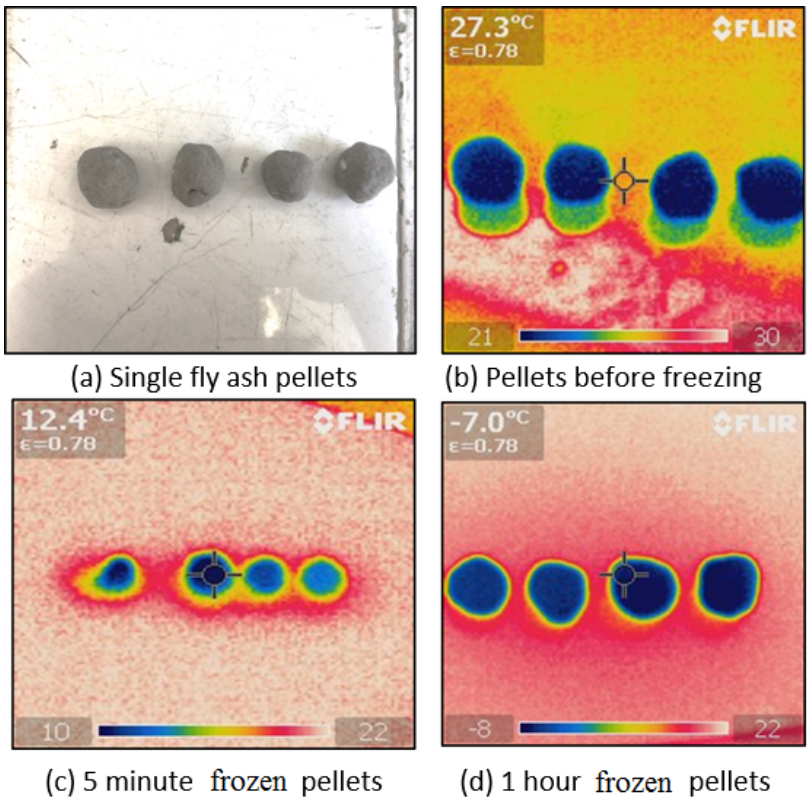

(a) Single fly ash pellets (b) Pellets before freezing

(c) 5 minute frozen pellets (d) 1 hour frozen pellets

Figure 3.5. Thermal images of single pellets during freezing

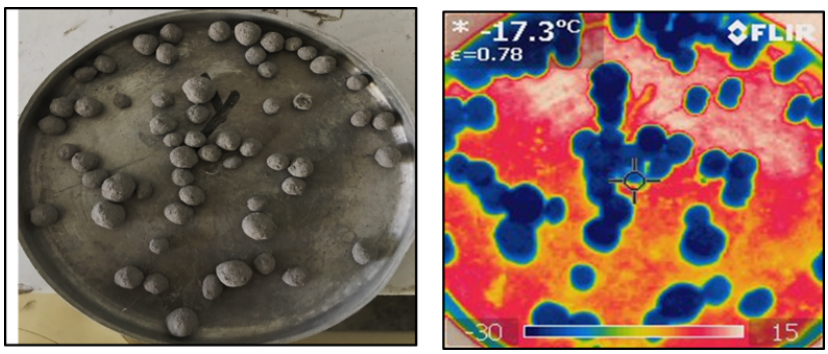

(a) Fly ash pellet sample before freezing (b) 3 hours frozen pellets

Figure 3.6. Thermal images of pellet samples during freezing

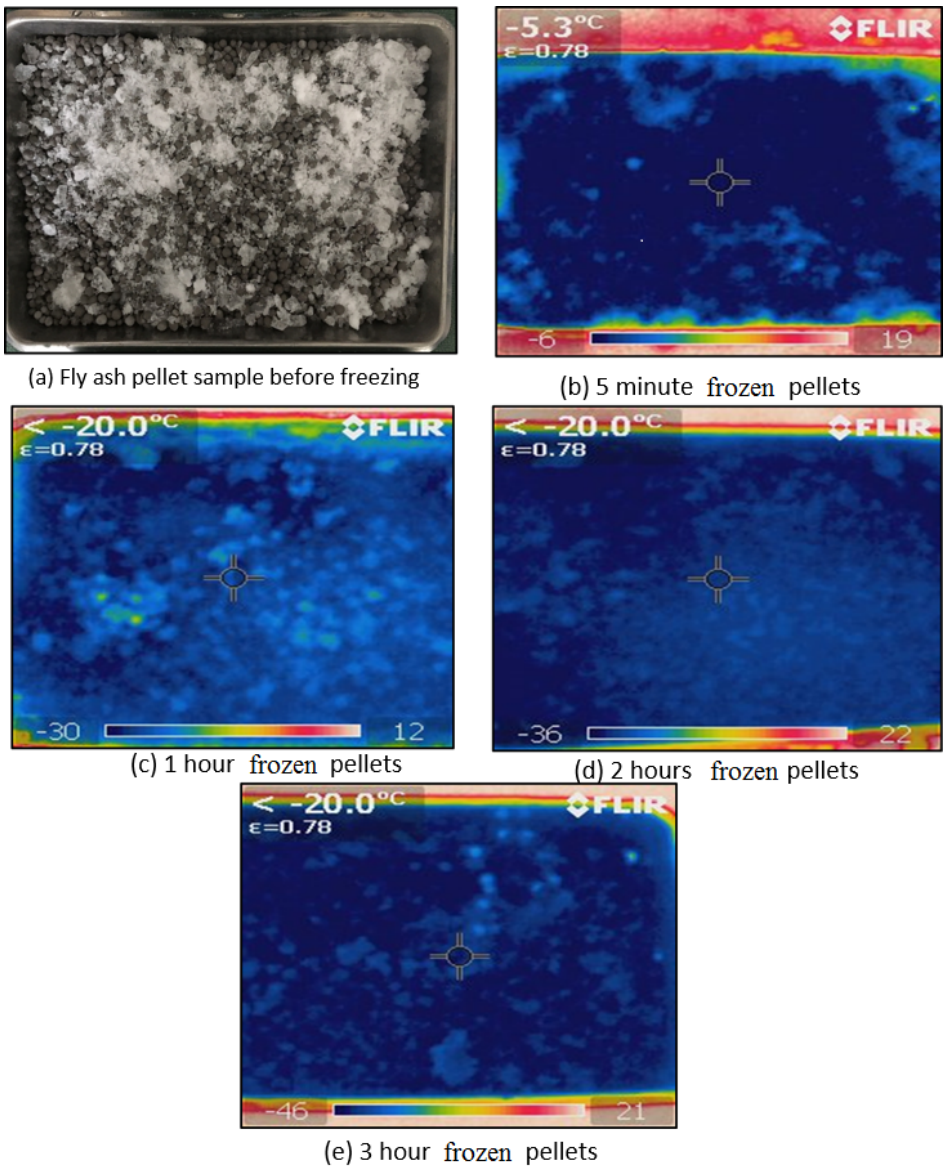

(a) Fly ash pellet sample before freezing

(b) 5 minute frozen pellets

(c) 1 hour frozen pellets

(d) 2 hours frozen pellets

(e) 3 hour frozen pellets

Figure 3.7. Thermal images of pellets in tray during freezing

Pellets were covered with the snow and they were exposed to freezing. 2 hours later, it can be seen in the Figure 3.5 and Figure 3.7 that pellets have reached the sufficient freezing temperature. Suggested freeze-thaw procedure was evaluated by thermal imaging during freeze-thaw cycles. Based on the thermal observations of fly ash pellets, required time for uniform temperature distribution for freezing-thawing stages verified as minimum 2 hours.

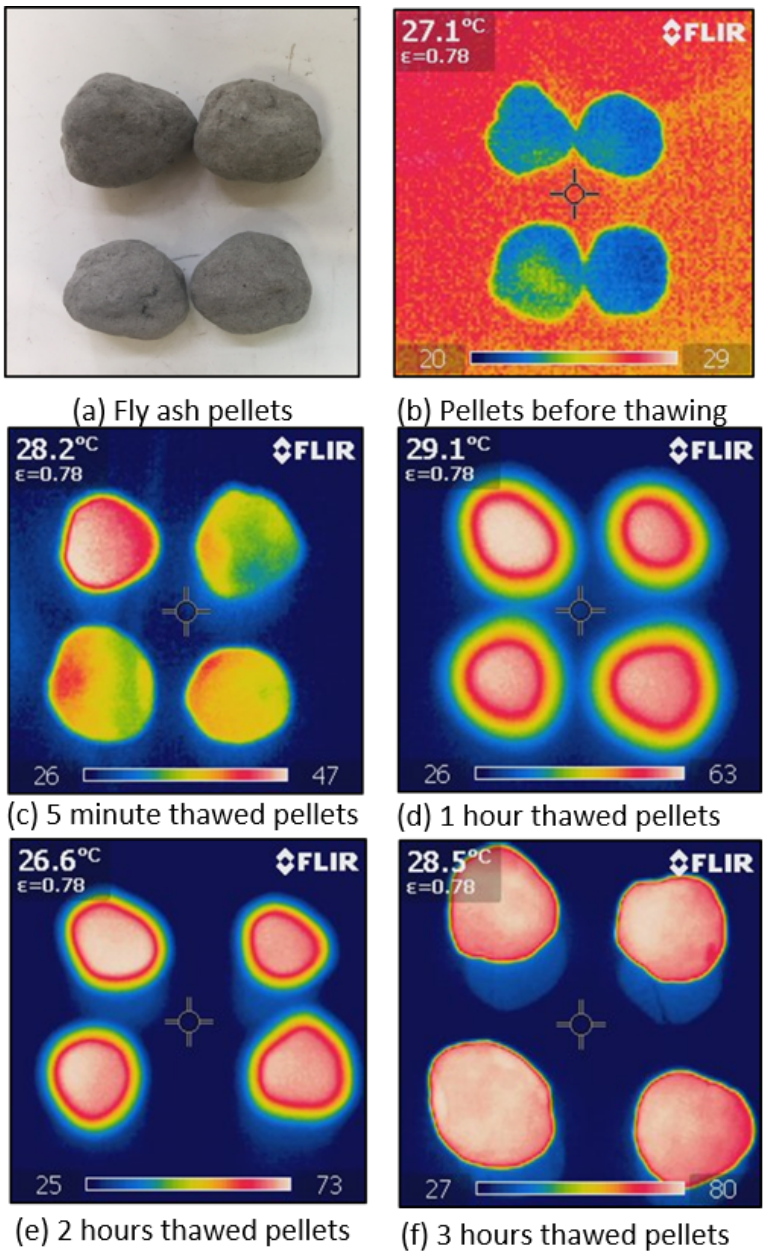

(a) Fly ash pellets

(b) Pellets before thawing

(c) 5 minute thawed pellets

(d) 1 hour thawed pellets

(e) 2 hours thawed pellets

(f) 3 hours thawed pellets

Figure 3.8. Thermal images of single pellets during thawing

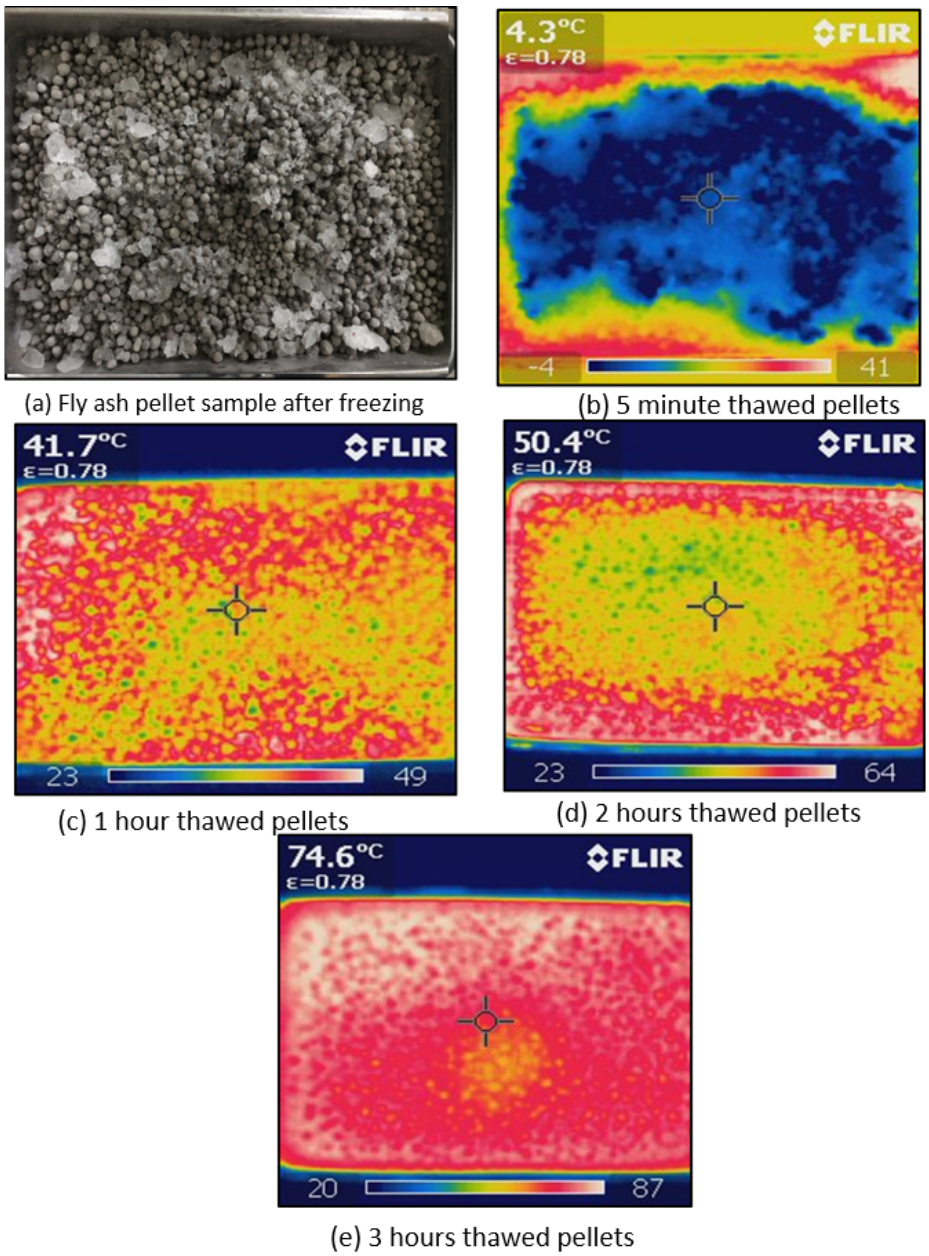

(a) Fly ash pellet sample after freezing

(b) 5 minute thawed pellets

(c) 1 hour thawed pellets

(d) 2 hours thawed pellets

(e) 3 hours thawed pellets

Figure 3.9. Thermal images of container with pellets during thawing

From the figures, it can be evaluated that, pellets start to warm up from the inner parts. After 2 hours thawing, pellets have reached sufficient temperature for thawing stage as displayed in Figure 3.8 and Figure 3.9. Close view of thawing stage are given in Figure 3.10. In order to better observe the heat changes at extreme temperatures, it has been heated and frozen for slightly longer periods than the normal cycle in some images.

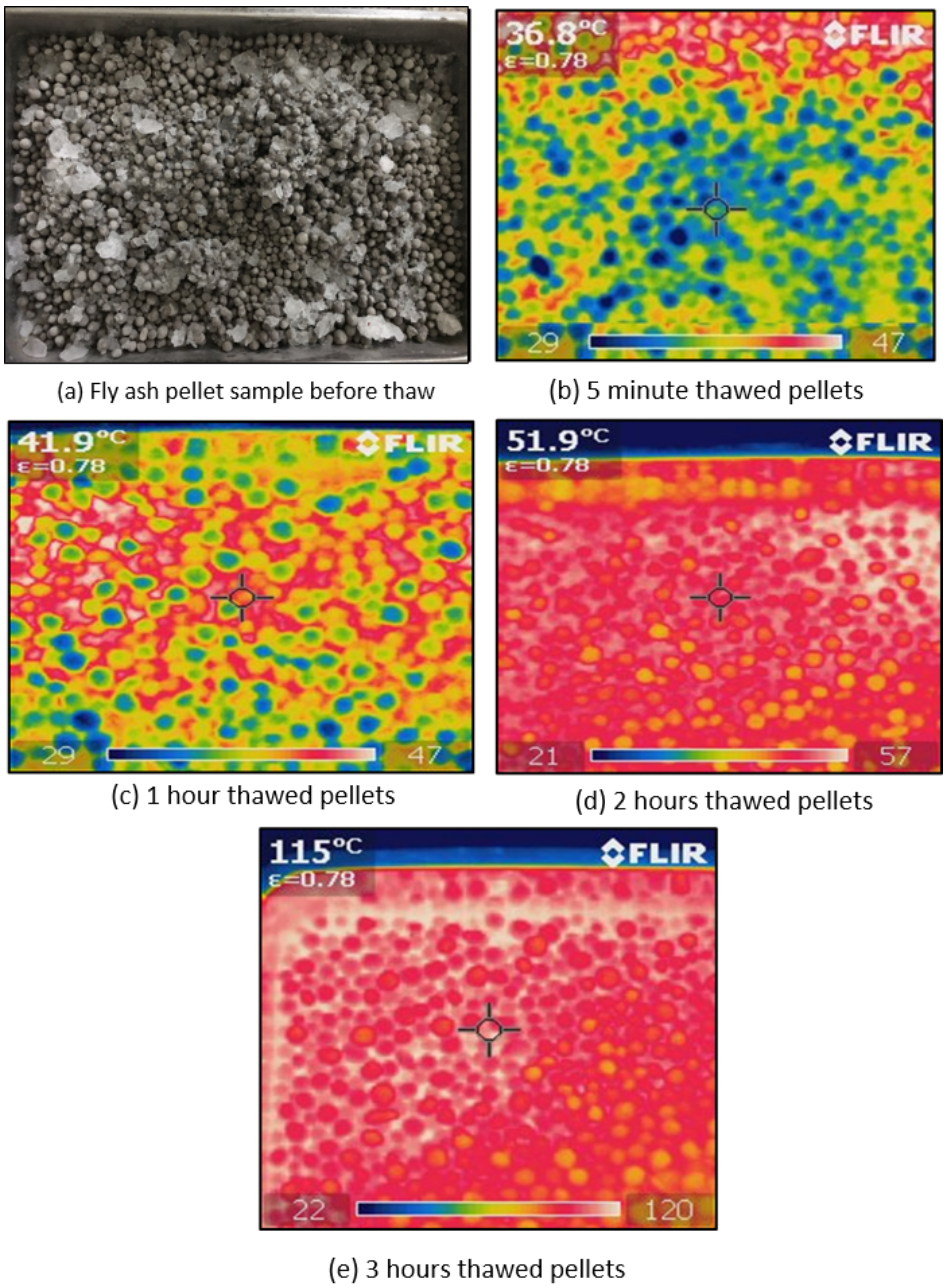

(a) Fly ash pellet sample before thaw

(b) 5 minute thawed pellets

(c) 1 hour thawed pellets

(d) 2 hours thawed pellets

(e) 3 hours thawed pellets

Figure 3.10. Thermal images of container with pellets during thawing, (close view)

Part b and c of Figure 3.10 demonstrates that pellets does not look like a whole and they do not have the same temperature until one hour. However, after 2 hours, temperature difference between each pellet disappears based on the d and c parts of the same figure and all pellets have reached the thawing temperature.

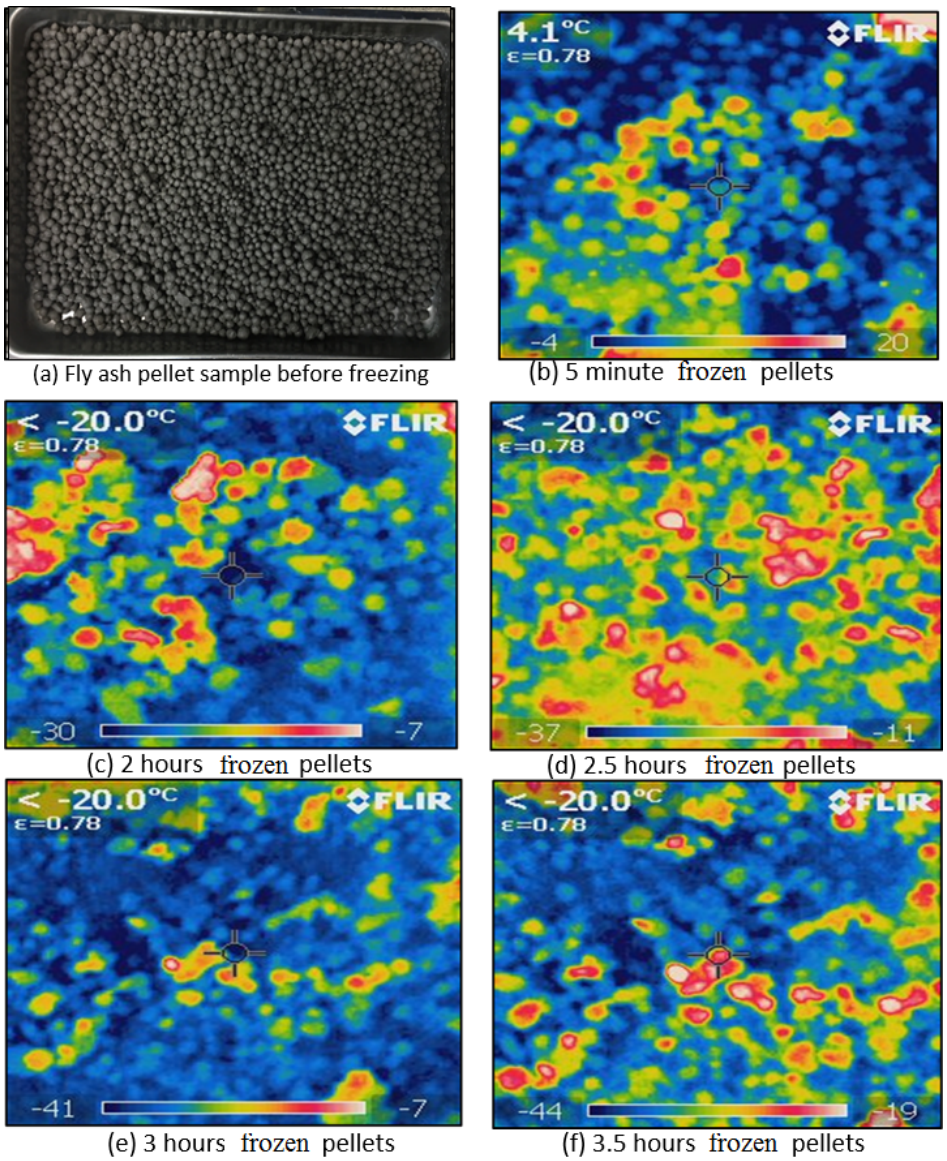

(a) Fly ash pellet sample before freezing

(b) 5 minute frozen pellets

(c) 2 hours frozen pellets

(d) 2.5 hours frozen pellets

(e) 3 hours frozen pellets

(f) 3.5 hours frozen pellets

Figure 3.11. Thermal images of container with pellets during freezing, (close view)

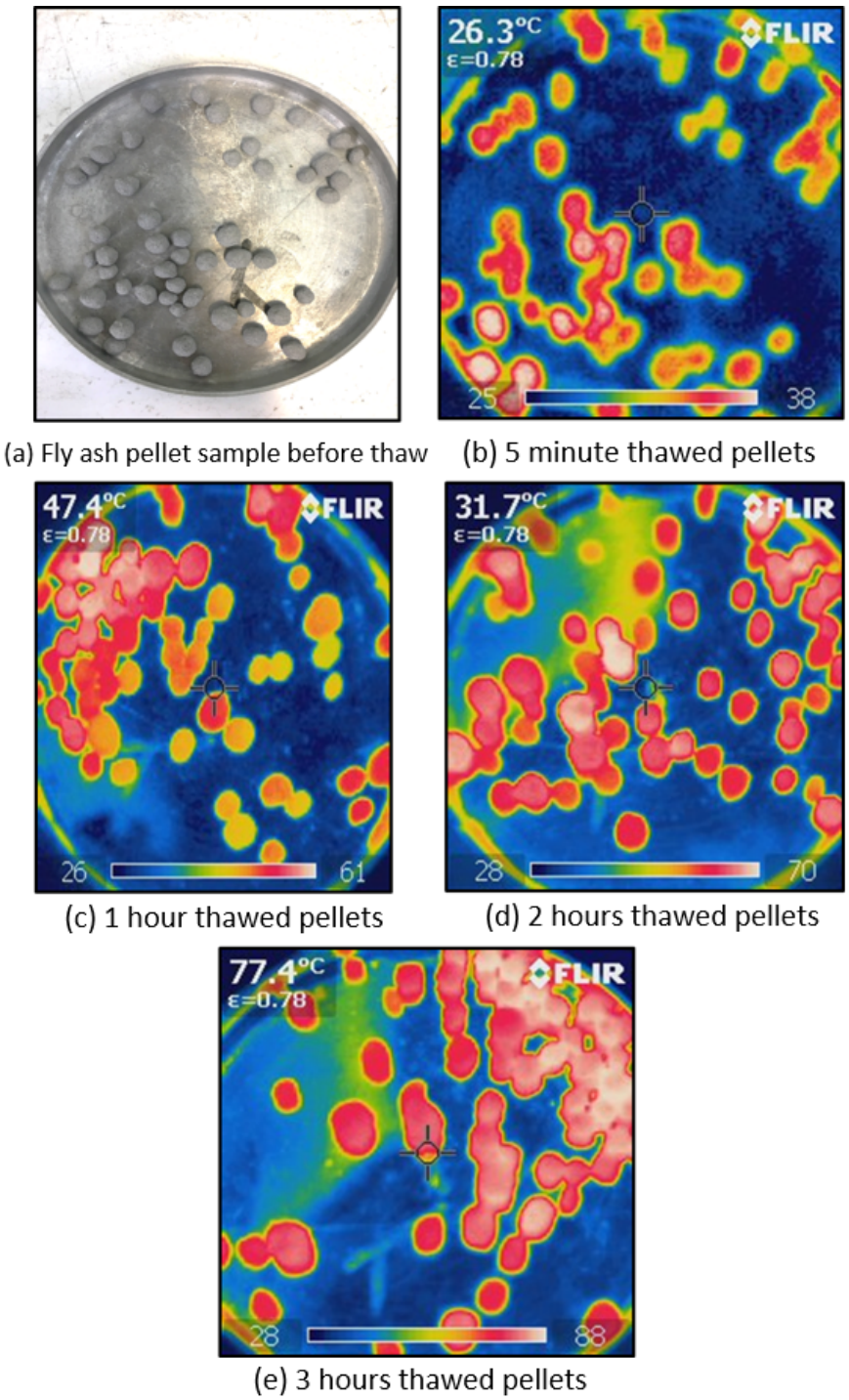

(a) Fly ash pellet sample before thaw (b) 5 minute thawed pellets

(c) 1 hour thawed pellets (d) 2 hours thawed pellets

(e) 3 hours thawed pellets

Figure 3.12. Thermal images of pellet samples during thawing

3.2.3. Specific Gravity and Water Absorption

For all eight groups of pellets, bulk specific gravity, bulk specific gravity at saturated surface, apparent specific gravity, and water absorption values were obtained with respect to ASTM C127-04, after freeze-thaw experiment.

Specific gravity, is the ratio of the density of any substance to the density of a sample substance such as gas-free distilled water at the same temperature.It is the property generally used for calculation of the volume holded by the aggregate in various mixtures. In addition, specific gravity is used in the computation of voids in aggregate. Specific gravity in saturated surface dry state is used if the aggregate is wet. If its absorption has been satisfied, then materials are called as wet. Adversely, the specific gravity in oven dry state is used for computations when the aggregate is dry or assumed to be dry. Apparent specific gravity is used for the the condition in which the permeable pores of particle are filled with water to the extent achieved by submerging in water for the appropriate amount of time, but without free water on the surface of the particles. Water absorption values are used to calculate the change in the mass of an aggregate due to water absorbed in the pore spaces within the component of particles, based on the dry condition. The related definitions are given in Table 3.1.

Table 3.1. Definitions of Specific Gravity and Water Absorption

Saturated Surface Dry State Bulk Specific Gravity	=	A/(B-C)
Oven Dry State Bulk Specific Gravity	=	B/(B-C)
Apparent Specific Gravity	=	A/(A-C)
Water Absorption (%)	=	[(B-A)/A]*100

In Table 3.1,

- A is the weight of the oven-dry specimen in air, gr,
- B is saturated surface dry specimen weight in air, gr,
- C is saturated specimen weight in water, gr.

3.2.4. Crushing Strengths of Pellets

Crushing value test is a practical and straightforward experiment that a single pellet is placed between parallel support plates and the center of bottom plate. Then, the load was applied with a constant rate of 0.01 mm/sec over the entire test period till failure occurs. Test setup is given in Figure 3.13.

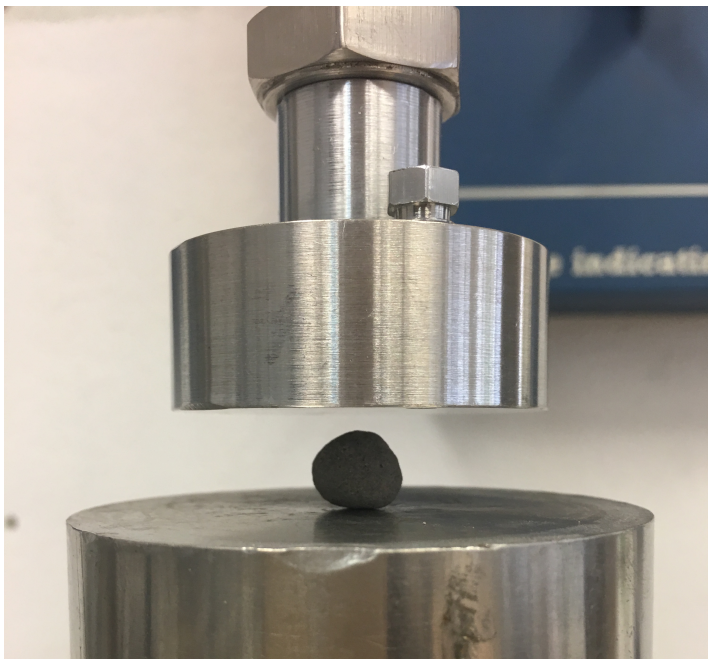

Figure 3.13. Crushing Value Test Setup

Single pellet crushing tests were performed on eight groups of pellets to obtain crushing strengths of pellets after the freeze-thaw cycles. Before the freeze- thaw test, pellets were cured for 28 days in the curing room. The pellets used in crushing tests were selected randomly from each grain size. 40 random pellets from each grain size have been crushed until failure. A triaxial compression test frame was used. Tests were performed on total number of 200 single pellet to achieve more accurate and consistent results. The sizes of the pellets were changing between 2 mm to 9.5 mm. A spacer was used on the bottom plate of compression frame for implementing the load.

3.2.5. California Bearing Ratio (CBR)

The California Bearing Ratio (CBR) test is a strength test that compares the bearing capacity of the crushed well-graded aggregate with the test sample. That is why, a high quality crushed stone should have a CBR 100 percent and also CBR value can be above 100 percent. It is primarily intended for assessing the strength of cohesive materials having maximum particle sizes less than 19 mm according to AASHTO. However, it can be used for various purposes.

The CBR test involves applying load to a small penetration piston at a rate of 1.25 mm per minute and recording the total load at penetrations ranging from 0.5 mm up to 12.5 mm. Demonstration of a CBR test are given in Figure 3.14.

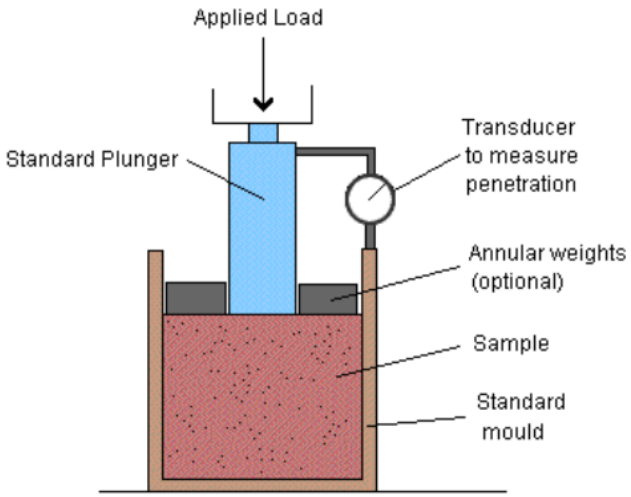

Figure 3.14. Sketch of Typical CBR Setup

The CBR value at 2.5 mm penetration is taken as the CBR value. If the CBR value corresponding to a penetration of 5 mm exceeds that for 2.5 mm, the test should be repeated. If identical results follow, the CBR corresponding to 5 mm penetration should be taken for design. In this study, 5 mm penetration is chosen as the CBR value. The maximum aggregate sizes used in the experiments for each group were 9.5 mm.

3.2.6. Direct Shear Test

The direct shear test was performed on direct shear test device. 100x100x42 mm direct shear box were used to evaluate the shear strength parameters of fly ash pellet aggregates as seen in Figure 3.15. The device was capable of applying various speeds ranging between 0 to 10 mm/min. In this study, the speed of horizontal displacement was chosen as 1 mm/min. The experiments were run for 25 kPa, 50 kPa and 100 kPa normal pressures for each eight group of fly ash pellets.

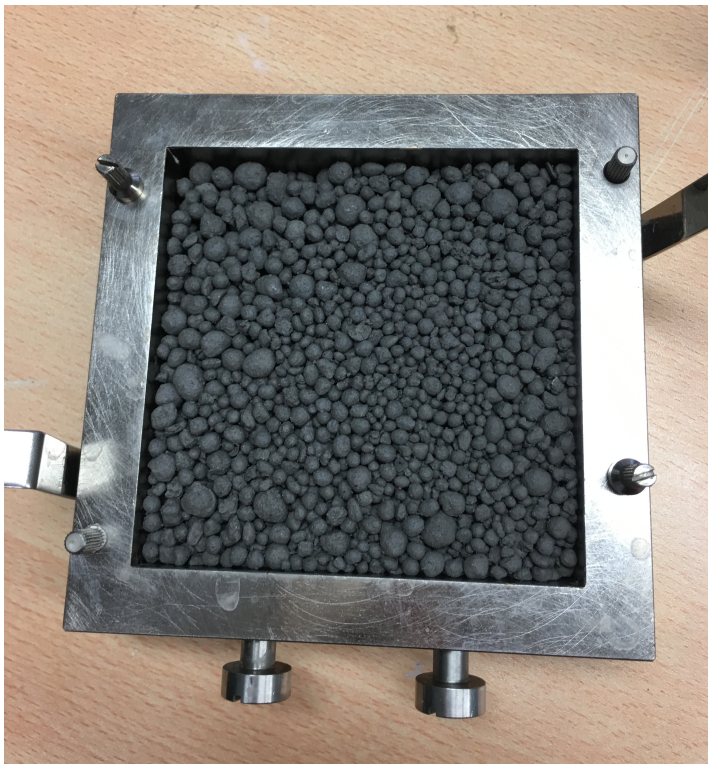

Figure 3.15. Figure of 100x100x42 cm direct shear box

The grain size distribution has a significant effect on shear strength of soils. Therefore, the crushed amount of aggregates were obtained by comparing the grain size distributions before and after the tests to see the effect of shear test.

According to ASTM D 3080, the minimum specimen width for square specimen shall be 50 mm or not less than ten times the maximum particle size diameter, the minimum initial specimen thickness shall be 12 mm, but not less than six times the maximum particle diameter, and minimum specimen width to thickness ratio shall be 2:1. Therefore, according to ASTM D 3080, 100x100 mm square box was used in the test because the maximum diameter of the aggregates is 3.35 mm, and the height of the box is 42 mm that is bigger than six times of the maximum particle size. Height of the fly ash pellets was changing between 22 to 27 mm.

During the test, horizontal displacements, horizontal forces and vertical displacements were recorded. A maximum displacement was chosen as 10 mm due to the limitations of the direct shear test device. All samples were prepared in pre-determined granulometry and mixed again to ensure homogeneity. The target normal pressure was achieved by applying vertical loads on the beam hanger that transfer loads to the load cap by 1:10 ratio.

3.2.7. Surface Scaling Analysis

Peeling is a surface defect appeared after the freezing-thawing experiment. After 10 freeze-thaw sequence it has been noticed that majority of fly ash pellets displayed some kind of peeling on their surfaces. Generally, surface peeling is an effect resulted from the expansion of water upon freezing. During the cycles it has been noticed that number of freeze-thaw cycle is an important issue in terms of surface defect. If the amount of cycles increases, severity of peeling on surface of pellets increases too.

The surface of the pellets were analyzed by an optical microscope, the findings were photographed with respect to only 28 days cured pellets. Moreover, fly ash pellets from control group and freeze-thawed group compared side by side to evaluate the effect of freeze-thaw. The analysis was performed on the sieve sizes such as 9.5 mm and 8 mm, where the peeling effect is visible on the surface of pellets.

3.2.8. Thin Section Analysis

In optical mineralogy, a thin section is a laboratory preparation of a rock, mineral or soil, for use with a polarizing petrographic microscope, electron microscope and electron microprobe. Prior to sectioning, all samples are covered with epoxy in order to obtain optimum sawing quality as seen in Figure 3.16. A thin sliver of pellet is cut from the sample with a diamond saw. It is then mounted on a glass slide and smoother using progressively finer abrasive grit until the sample is only 30 μm thick. Two samples were obtained from both control and freeze-thawed group. Control group samples are labeled as 1A and 1B. Freeze-thawed group samples are labeled as 2A and 2B.

Figure 3.16. Sample preparation for thin section analysis

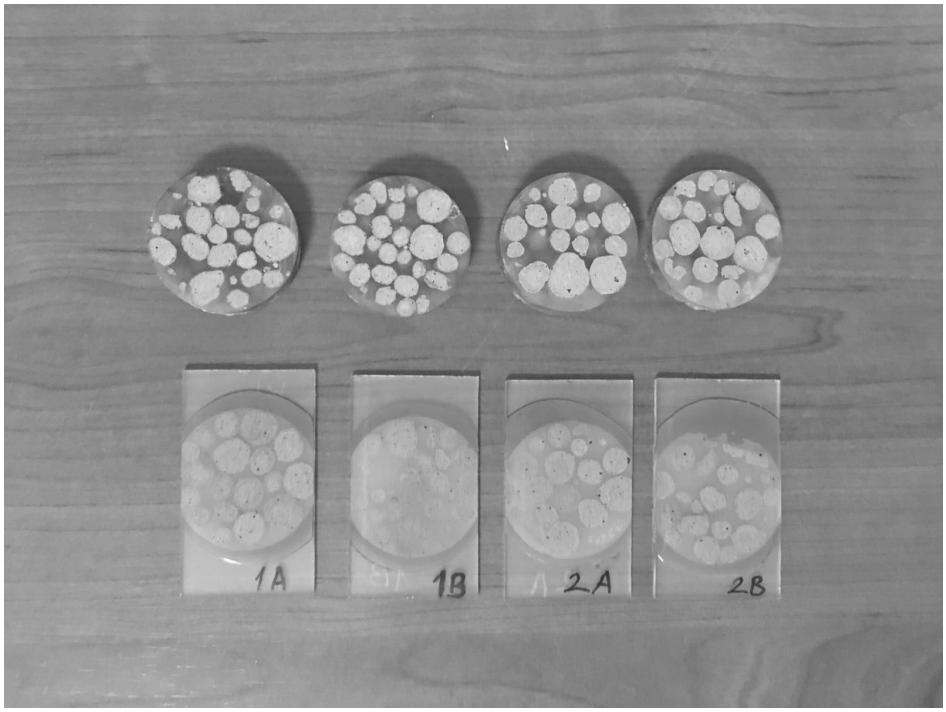

Figure 3.17. Thin section samples

4. RESULTS AND DISCUSSION

4.1. Unit Weight

The results of unit weight experiments are given in Table 4.1. The unit weights of fly ash pellets are ranging between 9.3 to 10.1 kN/m^3 and the average unit weight is 9.6 kN/m^3.

Table 4.1. Unit weights of fly ash pellets

	Control Group		Freeze-Thawed Group	
Sample Number	Unit Weight (kN/m^3)	Average Unit Weight (kN/m^3)	Unit Weight (kN/m^3)	Average Unit Weight (kN/m^3)
1	9.8	9.7	9.3	9.6
2	9.4		10.1	
3	9.8		9.5	
4	9.6		9.7	

4.2. Specific Gravity and Water Absorption

Oven dried bulk specific gravity, saturated surface dry bulk specific gravity, apparent relative density and water absorption values of fly ash pellets are given in Table 4.2.

Table 4.2. Specific gravity and water absorption values of fly ash pellets

	A(gr)	B(gr)	C(gr)	Oven Dry SG	Saturated Surface SG	Apparent SG	Water Absorption (%)
Control Group	106	137	52.5	1.25	1.62	1.98	30
Freeze-Thawed Group	107	140	52.3	1.22	1.6	1.96	30.84

4.3. Maximum and Minimum Index Density

Maximum and minimum index density tests are given in Table 4.3. The unit weights determined in section 4.1 were used in determination of relative density. Soils can be considered as dense above relative density of 65 %.

Below 65%, they are considered as medium dense and below 35% soils are generally accepted as loose. Maximum and minimum index density of fly ash pellets are given in Table 4.3.

Table 4.3. Maximum and Minimum Index Density of Fly Ash Pellets

e_{min}	e_{max}	γ_{min} (kN/m^3)	γ_{max} (kN/m^3)
0.55	0.71	7.5	11.24

4.4. Crushing Strength of Pellets

The crushing strength test was performed on all samples of control group pellets by applying load on 28 days cured individual pellets. 40 pellets were tested for each grain size and the results are expressed in terms of strength that pellets were failed. The average of 40 values were taken to represent the crushing strength of these samples. All values are given in Appendix A.

Table 4.4. Average crushing strength of pellets for control and freeze-thawed groups

	Control Group	
Sieve Size (mm)	**Average Crushing Load (N)**	**Average Crushing Strength (σ,N/mm^2)**
9.5	540.00	7.18
8	409.00	7.70
4	190.00	10.97
3.35	164.00	15.43
2	67.00	16.10
	Freeze-Thawed Group	
Sieve Size (mm)	**Average Crushing Load (N)**	**Average Crushing Strength (σ,N/mm^2)**
9.5	440.00	5.87
8	330.00	6.22
4	140.00	8.13
3.35	123.00	11.50
2	59.00	13.90

The results of the experiments are given in Table 4.4, and Figure 4.1. As shown in Figure 4.1, as the grain size of pellets decreases, average strength of fly ash pellets increases.

For both groups, maximum strength was achieved by pellets with 2 mm grain size. Although the failing loads on pellets increases with larger sieve sizes, in terms of strength, it is revealed that 2 mm pellets are the strongest ones.

According to Table 4.4, average crushing strength of the control group decreases as the diameter of the pellets increases. The crushing strength increases by 7% when the grain size decreases from 9.5 mm to 8 mm, crushing strength increases by 37% when the grain size decreases from 8 mm to 4 mm, 36% when the grain size decreases from 4 mm to 3.35 mm and crushing strength increases by 6% when the grain size decreases from 3.35 mm to 2 mm.

For freeze-thawed group, the crushing strength increases by 17% when the grain size decreases from 9.5 mm to 8 mm, crushing strength increases by 33% when the grain size decreases from 8 mm to 4 mm, 50% when the grain size decreases from 4 mm to 3.35 mm and crushing strength increases by 17% when the grain size decreases from 3.35 mm to 2 mm.

Average crushing strength of freeze-thawed group for minimum 2 mm pellets decreased by 14 % from 16 to 14 kN/mm^2. For minimum of 3.35 mm pellets, it decreased by 20%, from 15 to 12 kN/mm^2. For minimum of 4 mm pellets, it decreased by 28%, from 11 to 8 kN/mm^2. 8 and 9.5 mm pellets also lose strength in percentage of 25% and 15%.

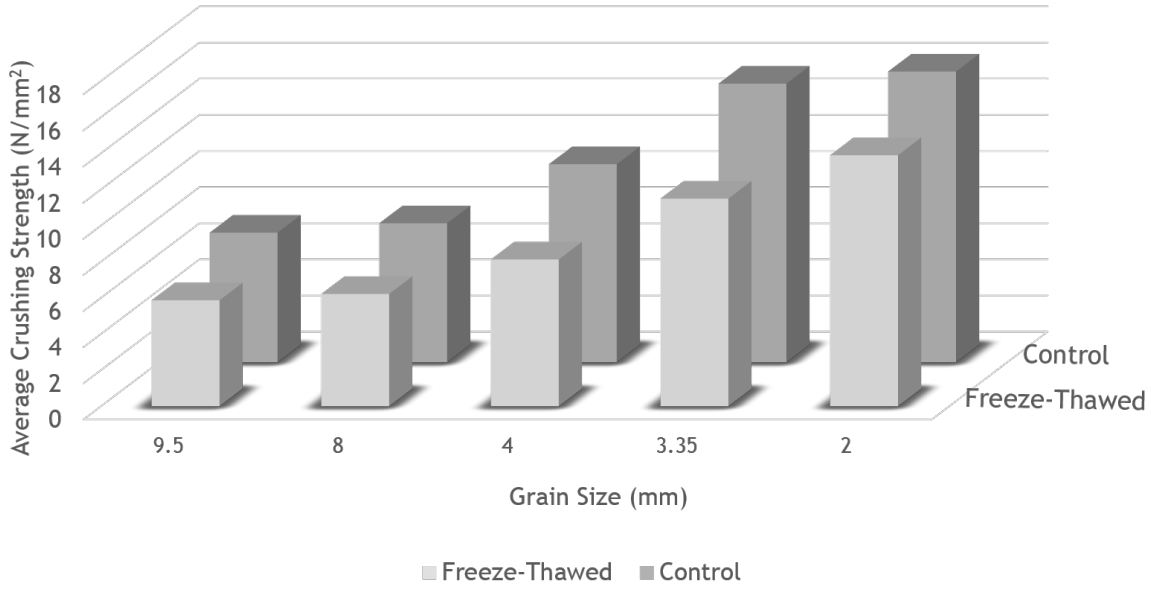

Figure 4.1. Average strength of fly ash pellets with respect to grain size

4.5. Direct Shear Test

Horizontal displacement, vertical displacement and shear stresses of samples were recorded for all samples of fly ash pellets under 25, 50 and 100 kPa normal stresses. A maximum displacement was chosen as 10 mm due to the limitations of the direct shear test device. Result are given in Figure E.1 to Figure E.8. Since the grain size distribution has a significant impact on shear strength of granular soil, all samples were prepared in predetermined granulometry. All samples were prepared at 38-45% relative density with 0.63-0.65 void ratio. Internal friction angle of fly ash pellets was calculated by using the maximum shear stress and taking arc-tangent values of the normal versus shear stress lines. Average internal friction angle found in this study is given in Table 4.5. Comparative results from every sample are given in Figure 4.2. In this figure, CG and FZT represents control and freeze-thawed group, respectively.

Table 4.5. Average angle of internal friction of fly ash pellets

	Control Group		Freeze-Thawed Group	
Test Number	Angle of Internal Friction (ϕ)	Average (φ)	Angle of Internal Friction (ϕ)	Average (φ)
1	36	35	36	36
2	34		35	

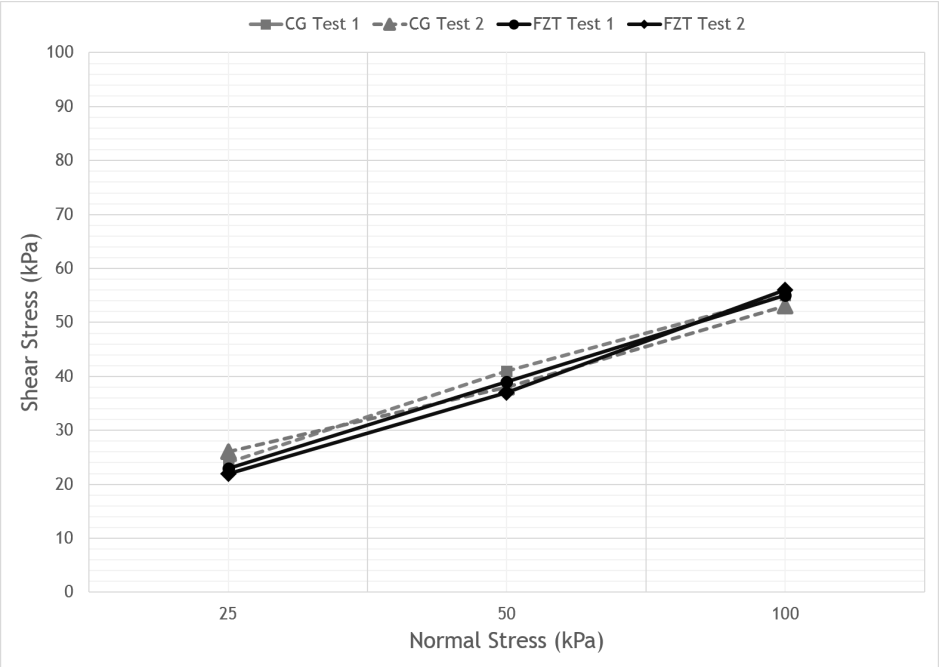

Figure 4.2. Comparative angle of friction results for freeze-thawed group

As shown in Figure 4.3, dashed lines in the graph display sieve analysis under normal loads of 25, 50 and 100 kPa before the direct shear test. For three normal loads of direct shear, as the load increases, deterioration of the particles increases as expected. Comparative results of all 8 samples of grain size distributions of pellets before and after direct shear tests are given in Appendix B.

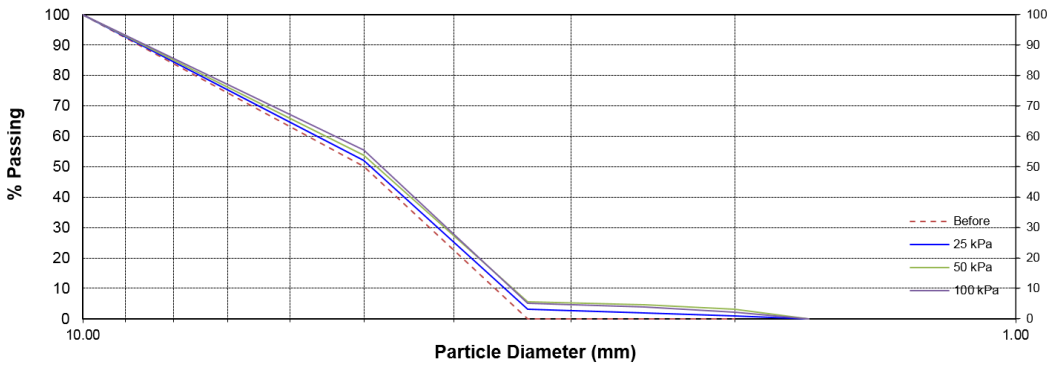

Figure 4.3. Sieve analysis results before and after the direct shear test

Horizontal displacement versus shear stress and vertical displacement graphs of control group are given in Figure 4.4 and Figure 4.5. For all samples, according to shear stress versus horizontal displacement graphs, they demonstrates plastic behavior of pellets under changing normal stresses. The plastic behavior means that although deformation occurs as a result of yielding stress, the structure constructed from fly ash pellets have the ability of mobilizing the maximum strength. The reason of displaying plastic behavior come from lower crushing strength compared to that of the natural aggregates.

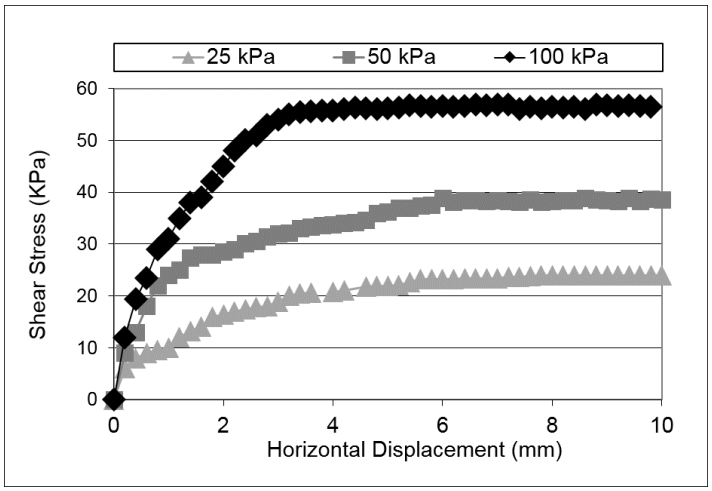

Figure 4.4. Horizontal displacement versus shear stress curves of fly ash pellets under 25, 50 and 100 kPa normal stresses for freeze-thawed group

For the first test of freeze-thawed group, shear stress was 21.44 kPa under 25 kPa normal stress. After that, with 50 kPa normal stress, shear stress increased to 39.15 kPa. Also, fly ash pellets tested under 100 kPa normal stress has the peak shear stress with 55.1 kPa where horizontal displacement was 3 mm. In vertical versus horizontal displacement graph, fly ash pellets initially shows a contractive behaviour. Then, dilation occurred. Dilation decreases as the normal load increases. Maximum dilation is obtained at 25 kPa normal stress.

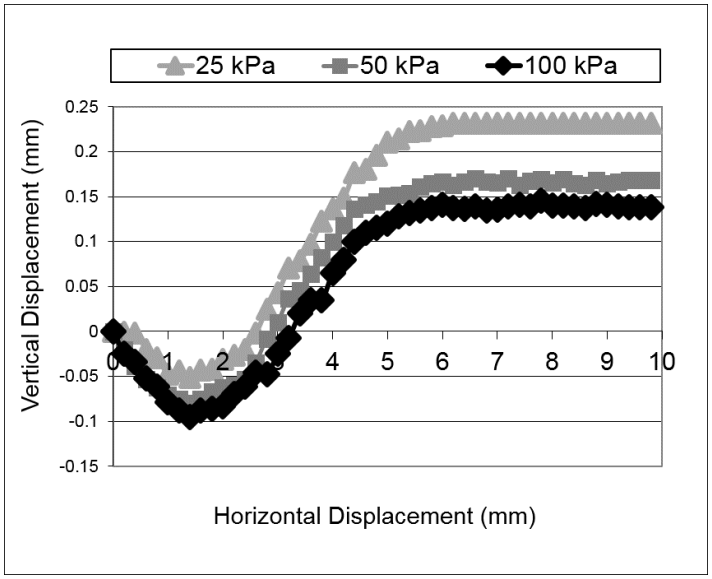

Figure 4.5. Horizontal displacement versus vertical displacement curves of fly ash pellets under 25, 50 and 100 kPa normal stresses for freeze-thawed group

4.6. California Bearing Ratio (CBR)

California bearing test is conducted on all samples of pellets. In conjunction with the aim of this project which is to evaluate the performance of pellets with no water addition in cold regions, experiments were performed on dry fly ash pellets. However, AASHTO T193 standard was still followed during the test. The surcharge weights which are placed on the samples was 4 split metal weights and each of them were 25 N. The total surcharge load placed on the samples was 98 N. The CBR test performed by applying load with a piston at a rate of 1.25 mm per minute and recording the total load at penetrations ranging from 0.5 mm to 12.5 mm. The CBR tests resulted with higher force for 5 mm penetration compared to 2.5 mm penetration, hence 5 mm penetration is chosen as the CBR value. Cylindrical moulds were used with 152 mm internal diameter and height of 178 mm. CBR test compares reference material with well-graded crushed stone, bearing ratio of the pellets can be found using standard unit loads. Standard unit loads are given in Table 4.6.

$$CBR \quad (\%) = \frac{x}{y} \tag{4.1}$$

In this equation, x is the material resistance or the unit load on the piston for 2.5 mm or 5 mm penetration, y is the standard unit load for well-graded crushed stone.

Table 4.6. Total standard load values for CBR test

Penetration depth (mm)	Unit Standard load Kgf/ cm^2	Total Standard load (Kgf)
2.50	70	1370
5.00	105	2055
7.50	134	2630
10.00	162	3180
12.50	183	3600

Table 4.7. Average CBR results for control and freeze-thawed group of fly ash pellets

Number of Test	CBR (%, Control)	CBR (%, Freeze-thawed)	Average CBR (%, Control)	Average CBR (%, Freeze-thawed)
1	16	5	16	10
2	17	8		
3	15	10		
4	15	10		
5	16	10		

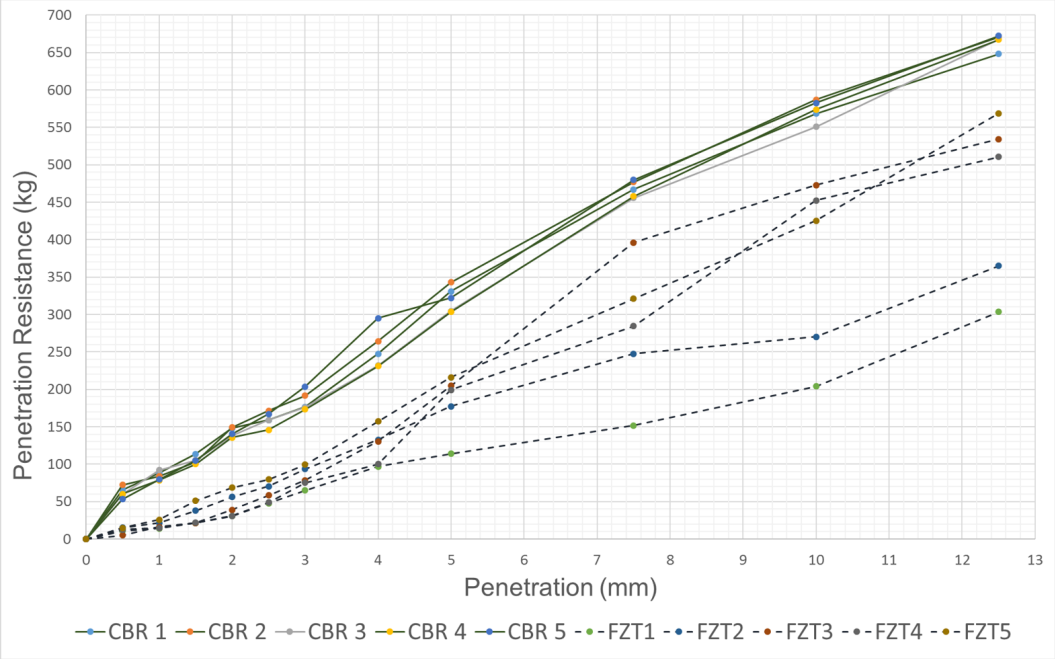

Figure 4.6. Comparative CBR results for control and freeze-thawed group of fly ash pellets

FZT represents freeze-thawed group and CBR represents control group in Figure 4.6. It can be concluded that penetration resistances of control groups for all penetration levels are higher than those for the freeze-thawed group. According to same table, CBR test results for freeze-thawed groups change more than values of control samples. While values for freeze-thawed group vary between 10% to 5%, values of control group vary between 15%-17%. Average CBR of fly ash pellets decreased by 36% as an effect of freeze-thaw. Decrease in CBR value validates the results of crushing value tests. In crushing value test, decrease of average crushing strength of 4 mm pellets was 28%, while the decrease in CBR value was 36% for the same grain size.

According to first CBR test on control group, fly ash pellets reached 2.5 mm penetration with 159 kilogram resistance. When piston penetrated 5 mm into the pellet sample, penetration resistance was 331 kilogram. In the second CBR test while 2.5 mm penetration has been reached at 175 kilogram load, 5 mm penetration refers to approximately 350 kilogram load.

These values are higher than the first trial of CBR test. In addition, highest CBR value achieved with test 2. Also, increase rate is higher than first test. Based on the third test, 2.5 mm penetration reached at 160 kilogram and 5 mm penetration achieved at approximately 300 kilogram.

The same increase pattern is observed in previous tests followed by third test too. Test 4 and 5 followed the same load range which 2.5 mm reached at approximately 150 and 160 kilogram, respectively. In terms of 5 mm penetration, sequentially, penetration level resulted with 300 and 325 kilogram. In case of fifth test, maximum resistance value of the test was 675 kilogram in accordance with 12.5 mm penetration. In the same test, 5 mm penetration which used in the calculation of CBR value for this test, have reached to roughly 325 kilogram penetration resistance.

After freeze-thaw, both maximum resistance and resistance value corresponding to the 2.5 and 5 mm penetration decreased compared to the CBR results before freeze-thaw test. Detailed results of all CBR tests and penetration resistance values are given in Appendix C.

4.7. Environmental Scanning Electron Microscope Analysis

Environmental scanning electron microscope (ESEM), is a type of electron microscope. ESEM can examine a specimen at various temperatures and under vacuum. ESEM provides an image of the microstructural development of the tested specimens.

Figure 4.7. Environmental Scanning Electron Microscope

Figure 4.8. Vacuum preparation for ESEM

For micro-structural analysis,environmental scanning electron microscope analysis were performed on control and freeze-thawed specimen. 350x and 2000x magnifications were used for both condition.

ESEM analysis were carried on at Boğaziçi University Advanced Technologies Research and Development Center and Philips XL30 ESEM-FEG/EDAX machine were used as seen in Figure 4.7. ESEM validates the results from previous sections. For sample preparation, fly ash pellets were kept in vacuum to eliminate moisture to a certain level as seen in Figure 4.8.

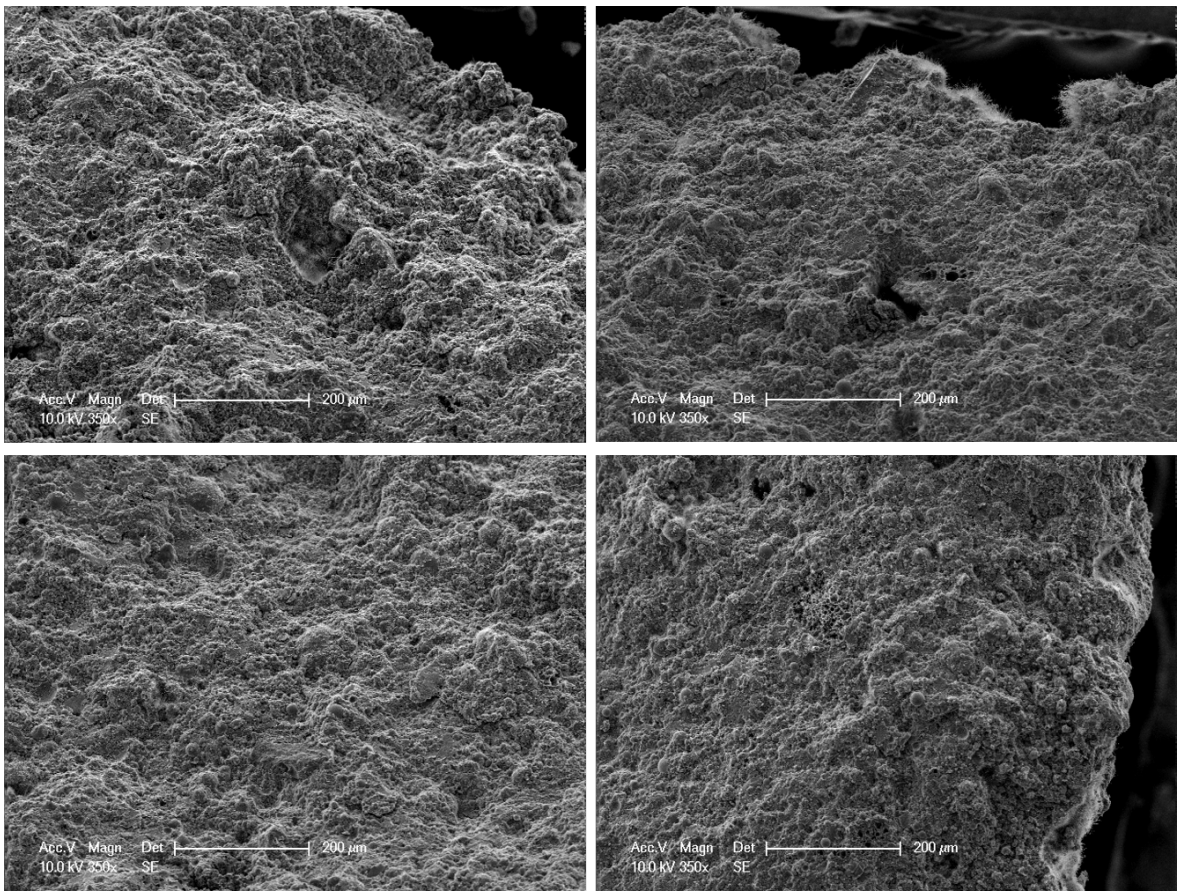

Figure 4.9. ESEM micrographs for control group (350x)

Figure 4.9 and 4.10 demonstrates the microfabric of the control group. Fly ash pellets are covered by hydration products like CSH. There are numerous voids visible in the structure of the control group, however, they decreased in freeze-thawed one. In addition, voids are not visible in control group which indicates the presence of ettringite ($Ca_6Al_2(SO_4)_3(OH)_{12}.26H_2O$). In the b part of the Figure 4.9, needle-like formation of ettringite are seen. Also, significant intensification of ettringites are observed in Figure 4.10. Magnification of 2000x shows these structures in more detail.

They are present in voids and corners of the pellet as seen in a and b parts of the Figure 4.10. The significant presence of ettringite, explains the strength of control group of pellets.

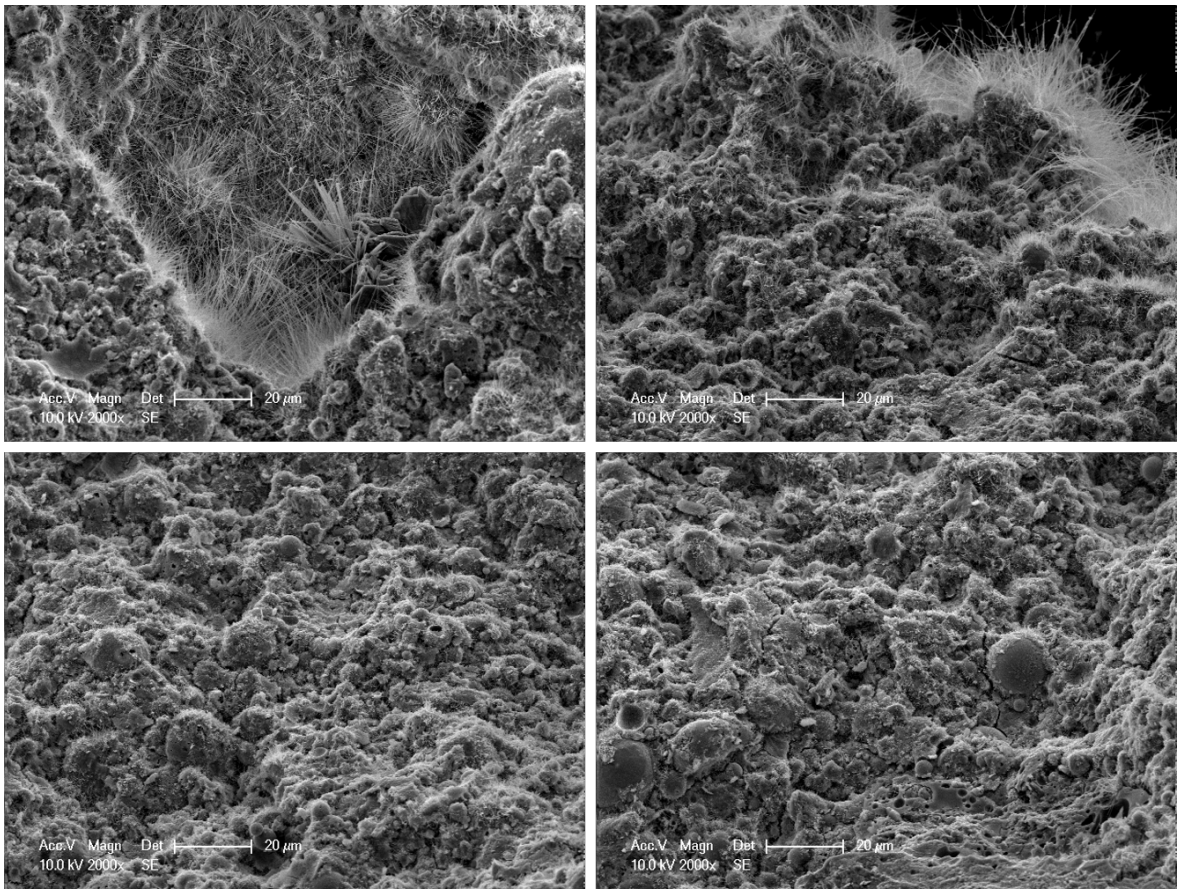

Figure 4.10. ESEM micrographs for control group (2000x)

Freeze-thawed specimens have more dense matrix than control group shown in Figure 4.11 and 4.12. Although, it shows more compact morphology than control group, tiny presence of needle-like ettringite formation leads in lower strength of freeze-thawed pellets. Also, formation of voids express the lack of ettringite formation [1]. As seen in Figure 4.12, smooth and particular shape of control group, disappears in freeze-thawed samples. Distorted shape may be the result of expansion of water in pores of pellets during sequent freeze-thaw cycles. The availability of calcium ions in solution is critical in determining the ettringite formation. Decrease in calcium ions in freeze-thaw group in accordance with the amount of ettringite supports the idea.

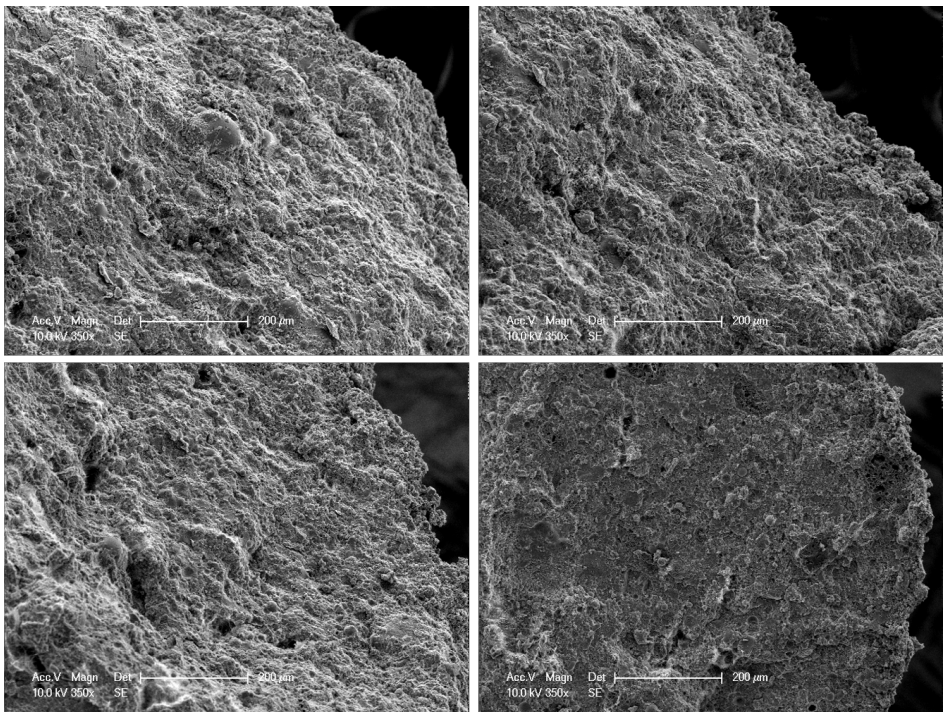

Figure 4.11. ESEM micrographs for freeze-thawed group (350x)

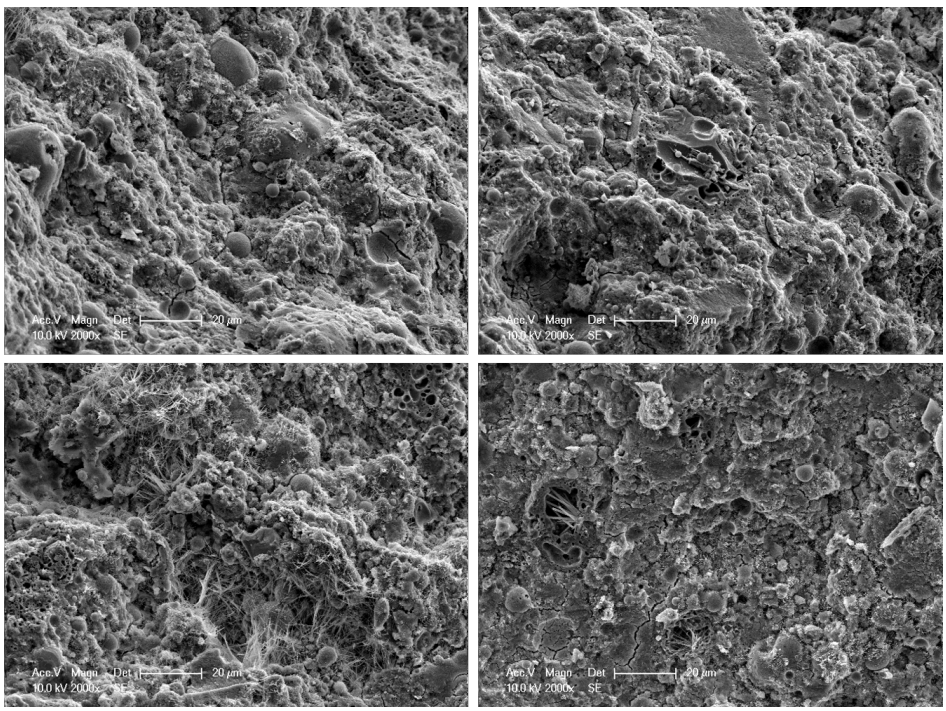

Figure 4.12. ESEM micrographs for freeze-thawed group (2000x)

X-Ray diffraction patterns of control and freeze-thawed group are given in Figure 4.13 and Figure 4.14.

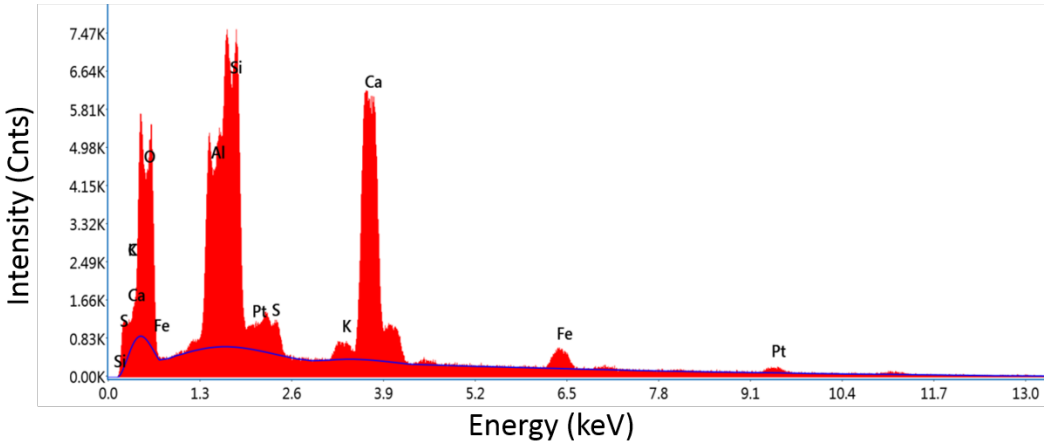

Figure 4.13. X-Ray diffraction patterns of control group

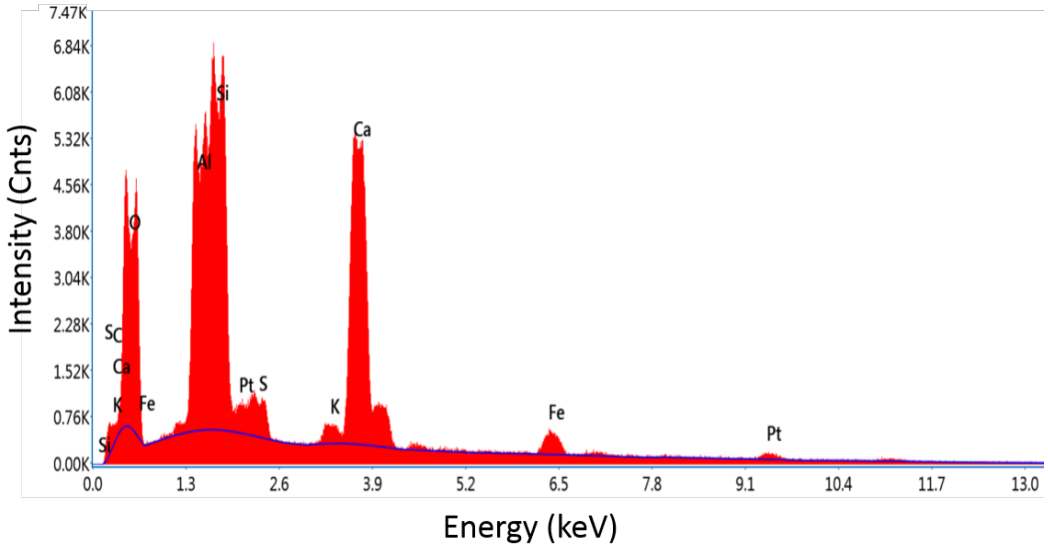

Figure 4.14. X-Ray diffraction patterns of freeze-thawed group

XRD analysis shows which elements fly ash has and the quantity of those elements. Figure 4.13 and Figure 4.14 shows that fly ash has Si, Al, O and Ca mostly, which makes sense; because Saygılı found out that fly ash had quartz(SiO_2), mullite($Al_6Si_2O_{13}$), calcite($CaCO_3$). No difference in mineral structure is observed for freeze-thawed group.

4.8. Surface Scaling Analysis

After the freeze thawing experiment, various surface defects were detected on the surface of the pellets, as mentioned earlier. As demonstrated in Appendix D pellets shows peeling and local flaking on their surfaces. The surface defects caused by the freeze thaw are tried to be determined numerically and they are given in percent. Pellet sizes that surface defect is more evident are examined under an optical microscope. These pellet sizes were identified as 9.5 mm and 8 mm. 30 fly ash pellets from both cases, before and after freeze-thaw test, were chosen randomly from each grain size. Each image has its legend on the bottom right which shows 1 mm for the scaling.

According to observation, pellets has 9.5 mm grain size approximately display % 80 and pellets with 8 mm grain size has % 70 surface detect or peeling rate. As a result, increasing pellet size has negative affect on pellets in terms of freeze-thaw. When water turns into ice,it expands by roughly % 9. During the freeze-thaw test, in thawing phase, added snow turns into water and freezes at freezing stage. As the water in moist fly ash pellet freezes it produces pressure in the pores of the pellet. That is why, it is appropriate to say that this result has been achieved because of the volume of voids are greater as grain size increases. Overall, it can be concluded that, fly ash pellets exhibits % 75 peeling detect on their surfaces after exposing to freeze-thaw. Detailed results of all observations are given in Appendix D.

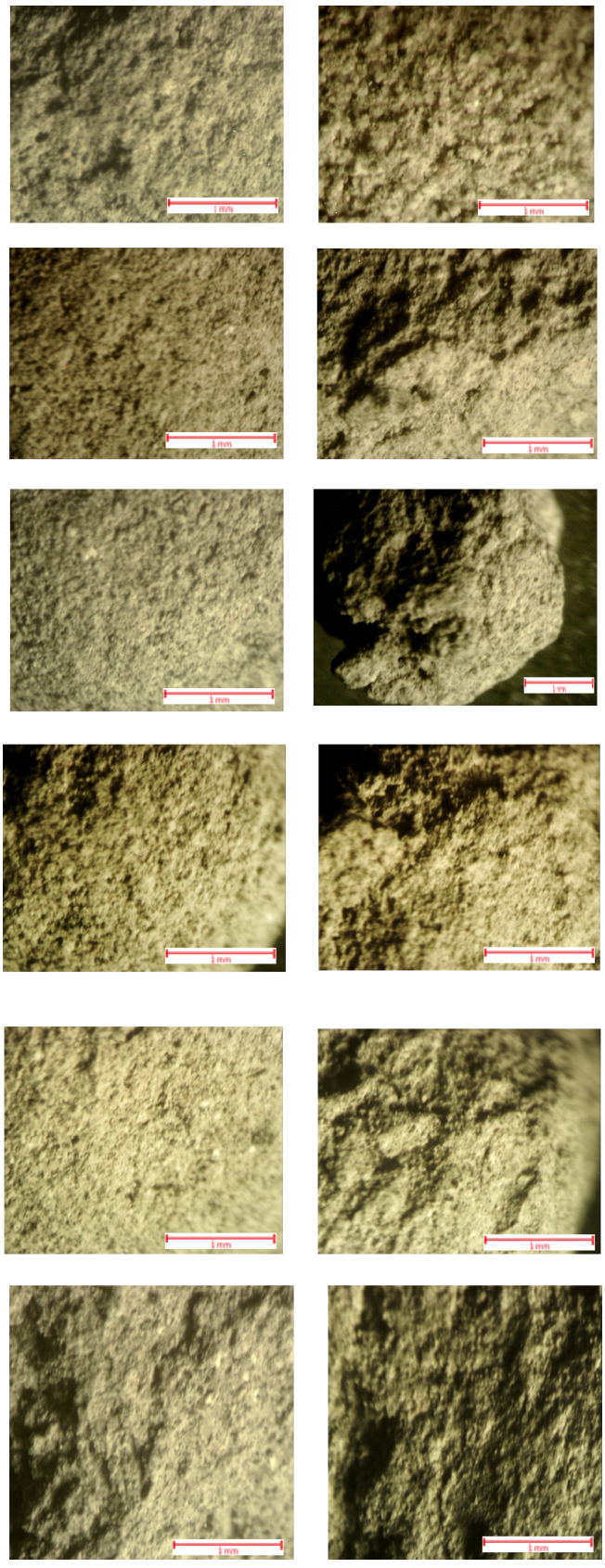

Figure 4.15. The microscopic image of pellets for control and freeze-thawed group

4.9. Thin Section Analysis

Thin section images are validating the surface defects of freeze-thawed group of fly ash pellets. As seen in Figure 4.16, pellets from control group have clean surface without any peeling or flaking. For freeze-thawed group, freeze-thaw effect can be seen on the perimeter of the fly ash pellets as demonstrated in Figure 4.17.

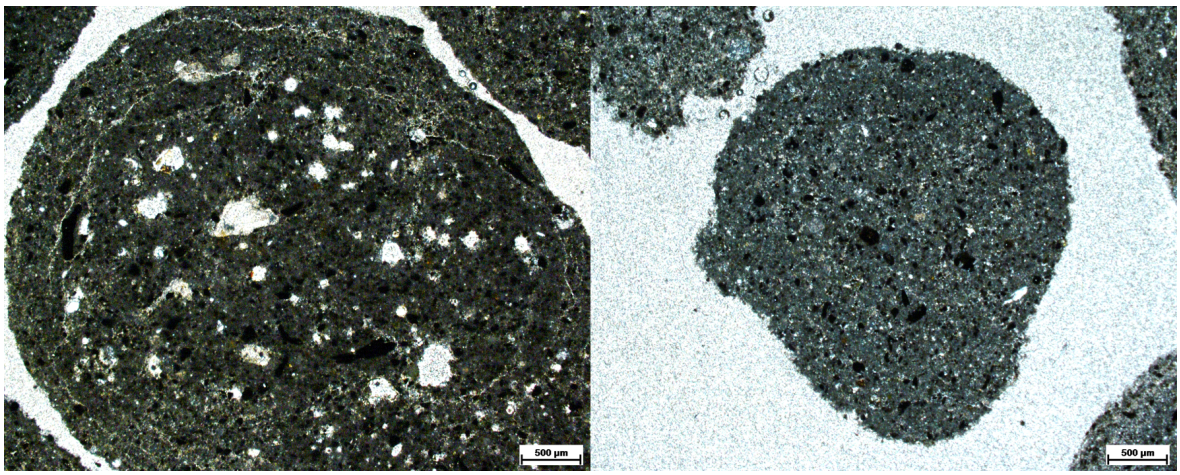

Figure 4.16. The microscopic image of control group

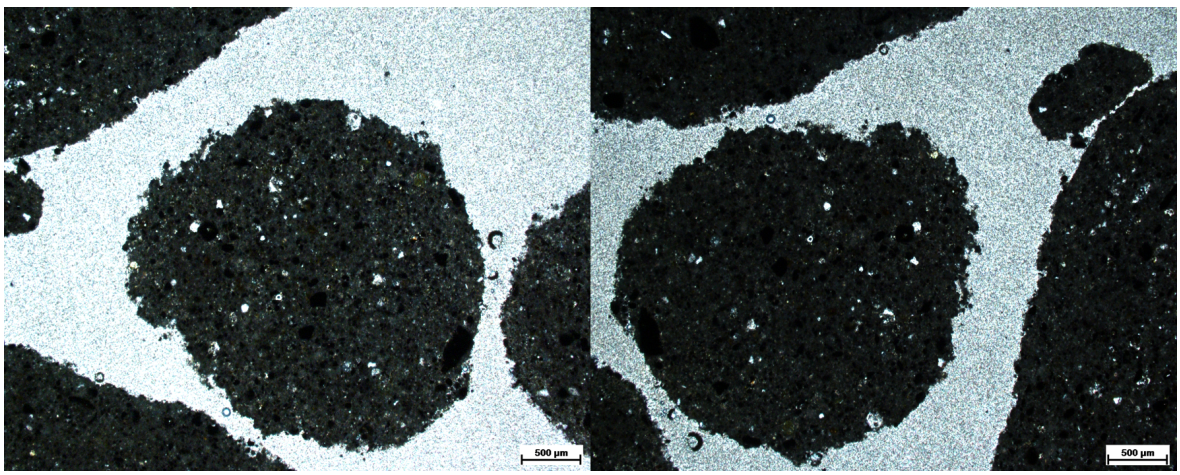

Figure 4.17. The microscopic image of freeze-thawed group

5. CONCLUSIONS

In cold regions, embankments are demanded by many highway projects to achieve design needs in frozen ground. However, proper compaction and transportation of water is a challenging work. Compaction of fly ash pellets is possible without use of water which makes this material advantageous for cold climates. Manufactured pellets can be used in case of any repair, maintenance or urgent situations which needs immediate intervention mainly in highways in cold period. The objective of the present study is to evaluate the performance of pellets subjected to a maximum of 10 freeze-thawing cycles. Suitable usage of fly ash decreases the need for large landfill areas by means of both economic and environmental reasons. It also presents an alternative resource for highway construction applications which requires mass quantity of construction material. Better understanding of the cold weather performance of fly ash pellets will lead to enhanced utilization in cold climates.

- Suggested freeze-thaw procedure was evaluated by thermal imaging during freeze-thaw cycles. Based on the thermal observations of fly ash pellets, the required time for uniform temperature distribution for freezing-thawing stages was verified as minimum 2 hours.

- Control and freeze-thawed groups reached peak shear stress at average 55 kPa. The internal friction angle of both group were 35 degrees. For freeze-thawed group, internal friction angle does not change.

- Based on the prepared samples, the following results are obtained. Average crushing strength for minimum 2 mm pellets decreased by 14 % from 16 to 14 kN/mm^2. For minimum of 3.35 mm pellets, it decreased by 20%, from 15 to 12 kN/mm^2. For minimum of 4 mm pellets, it decreased by 28%, from 11 to 8 kN/mm^2. 8 and 9.5 mm pellets also lose strength in percentage of 25% and 15 %.

- It can be concluded from CBR results that before freeze-thaw experiment overall penetration resistances for all penetration levels are higher than samples tested after freeze-thaw test. While values for freeze-thawed group vary between 10% to 5% , values of control group vary between 15%-17%. Average CBR of fly ash pellets decreased by 36% as an effect of freeze-thaw. Decrease in CBR value validates the results of crushing value tests. In crushing value test, decrease of average crushing strength of 4 mm pellets was 28%, while the decrease in CBR value was 36% for the same grain size.

- According to observation performed on fly ash pellets after freeze-thaw, pellets which have 9.5 mm grain size approximately displays 80 % and pellets with 8 mm grain size shows 70% surface defect or peeling rate. As a result, increasing pellet size has negative effect on pellets in terms of freeze-thaw. That is why, it is appropriate to say that this result has been achieved because of the volume of voids are greater as grain size increases. Overall, it can be concluded that, fly ash pellets exhibits 75% peeling defect on their surfaces after exposing to freeze-thaw. In addition, thin section images are validating the grain perimeter defects of freeze-thawed group of fly ash pellets.

It may be considered that the high water absorption property of fly ash is a disadvantage in terms of freeze-thaw. However, experiments show that, although water expands its volume when it is in a frozen state, the fly ash pellets preserve their shape after ten freeze-thaw cycles. Thus, a disadvantage of fly ash pellets may be turned into an advantage. The water absorption of fly ash pellets will be advantageous during thawing season. Pellets hold a considerable amount of water inside which is 30 % by weight, before releasing it to the environment.

For further studies, model embankment made of fly ash pellets are planned to constructed in cold areas to validate the results of laboratory as case study. This type of study can prove the usability of structures made of solely fly ash pellets in cold regions.

REFERENCES

1. Saygılı, A., *Highway embankment construction using fly ash and snow in cold region*, Ph.D. Thesis, Bogazici University, 1998.

2. B. Andersland, O. and B. Ladanyi, *An Introduction to Frozen Ground Engineering*, 01 1994.

3. Döven, A. G., *Lightweight Fly Ash Aggregate Production Using Cold Bonding Agglomeration Process*, Ph.D. Thesis, Bogazici University, 1998.

4. Arslan, H. and G. Baykal, "Utilization of fly ash as engineering pellet aggregates", *Environmental Geology*, Vol. 50, pp. 761–770, 07 2006.

5. Danyıldız, E., *The Interface Behavior Between Granular Soils and Concrete*, Master's Thesis, Bogazici University, 2007.

6. Erdurak, M. C., *Artificial Sand Production for Laboratory Uses*, Master's Thesis, Bogazici University, 2011.

7. Takmaz, U., *Behavior of Manufactured Sand Under Cyclic Loading*, Master's Thesis, Bogazici University, 2016.

8. Monahan, E. J., *Construction of and on Compacted Fills*, John Wiley & Sons Inc, New York, USA, 1986.

9. Rice, E., "Annual PFA utilization statistics", *The Northern Engineer*, Vol. 4, 1972.

10. Karakuş, D., M. V. Özdoğan, G. Turan, G. Konak and A. H. Onur, "Termik Santral Katı Atık Depolama Sahası Kapasitesinin Arttırılması Olanaklarının Araştırılması: Yatağan Termik Santrali Örneği", *Yerbilimleri Dergisi*, Vol. 39, pp. 103–116, 2018.

11. Wang, J., H. Ban, X. Teng, H. Wang and K. Ladwig, "Impacts of pH and ammonia

on the leaching of Cu(II) and Cd(II) from coal fly ash", *Chemosphere*, Vol. 64, No. 11, pp. 1892 – 1898, 2006.

12. UKAQAA, "Annual PFA utilization statistics", *UK Quality Ash Association*, 2014.

13. Holtz, R., *Foundation Engineering Handbook*, pp. 166–222, 01 1991.

14. Harris, S., H. French, J. A. Heginbottom, G. H. Johnston, B. Ladanyi, D. Sego and R. O. Van Everdingen, "Glossary of Permafrost and Related Ground-Ice Terms", *National Research Council of Canada*, 01 1988.

15. P Huntington, H., M. Boyle, G. Flowers, J. W Weatherly, L. Hamilton, L. Hinzman, C. Gerlach, R. Zulueta, C. Nicolson and J. Overpeck, "The Influence of Human Activity in the Arctic on Climate and Climate Impacts", *Climatic Change*, Vol. 82, 03 2007.

16. Pewe, T., "Quaternary Geology of Alaska", *Geological Survey Professional Paper 835. U.S. Gov.Print. Ofc.*, p. 145, 1975.

17. Satoshi, M., *Laboratory and in-situ studies on mechanical properties of volcanic soil embankment in cold region*, Ph.D. Thesis, Hokkaido University, 2014.

18. Hansbo, S., *Jordmateriallara*, Almqvist Wiksell Forlag AB, Stokholm, 1975.

19. Barnes, H., "On the Density of Ice", *Physical Review*, Vol. 13, pp. 55–59, 1901.

20. Nichols, E., "On the Density of Ice", *Physical Review*, Vol. 8, pp. 21–37, 1899.

21. McManis, K., *Laboratory Evaluation of Fly Ash Treated Embankment and Base Materials: Final Report*, Tech. rep., 1988.

22. Mehta, P. K., *Pozzolanic and Cementitious By-products as Mineral Admixtures for Concrete - A Critical Review*, Vol. 1, American Concrete Institute Publication, 1983.

23. Rosenberg, A., "Using Fly Ash in Concrete", *Precast Inc. Magazine*, 2010.

24. Ristinen R., K. J., *Energy and the Environment*, Vol. 2, John Wiley & Sons Inc, Hoboken, NJ, USA, 2015.

25. L. Smoot, P. S., *Coal Combustion and Gasification*, Hoboken, NJ, USA, 1985.

26. Tom Robl, R. J., Anne Oberlink, *Coal Combustion Products (CCPs)*, Vol. 1, pp. 21–65, Woodhead Publishing, 2017.

27. ACAA, "Fly Ash Facts for Highway Engineers", *American Coal Ash Association*, Vol. FHWA–IF–03–019, p. 81, 2003.

28. Görhan, G., E. Kahraman, M. S. Baspinar and I. Demir, "Uçucu Kül Bölüm II: Kimyasal, Mineralojik ve Morfolojik Özellikler", *Electronic Journal of Construction Technologies / Yapi Teknolojileri Elektronik Dergisi*, Vol. 5, No. 2, pp. 33 – 42, 2009.

29. Güler, G., E. Güler and U. I. H. Mordoğan, "Uçucu Küllerin Özellikleri ve Kullanım Alanları", Türkiye 19. Uluslararası Madencilik Kongresi ve Fuarı, IMCET2005, Dokuz Eylül Üniversitesi, Izmir, Türkiye, 2005.

30. ACI, "Use of Fly Ash in Concrete", *ACI Materials Journal*, , No. 5, pp. 381–409, 1987.

31. Meyers, James, Pichumani, Kapples and Bernadette, "Fly Ash-A Highway Construction Material", *Transportation Research Board*, Vol. FHW A-IP-76-16, 1976.

32. Alonso, J.L. and W. K, *Characterization of Fly Ash*, Tech. rep., Report of Technical Committee 67-FAB, RILEM, London, 1991.

33. Frohnsdorf, C. J. R., G., "Fly Ashes in Cements and Concrete: Technical Needs and Opportunities", *Transportation Research Board*, 1981.

34. Murphy, C. H., "Handbook of Particle Sampling and Analysis Methods", *Analytical Chemistry*, Vol. 56, No. 2, pp. 118A–118A, 1984.

35. Raask, B. N., E., "Pozzolanic Activity of Pulverized Fuel Ash", *Cement and Concrete Research*, Vol. 5, No. 4, pp. 373–376, 1975.

36. J. Collins, R., S. K. Ciesielski and L. S. Mason, "Recycling and use of waste materials and by-products in highway construction: A synthesis of highway practice: Final report", *Transportation Research Board*, 2019.

37. ACAA, "Soil and Pavement Base Stabilization with Self-Cementing Coal Fly Ash", *American Coal Ash Association*, 1999.

38. ASCE, "Fly Ash for Soil Improvement", *Geotechnical Special Publication*, Vol. 13, No. 36, 1993.

39. Edinçliler, A., G. Baykal and A. Saygılı, "Highway embankment construction using fly ash in cold regions", *Resources, Conservation and Recycling*, Vol. 42, pp. 209–222, 2004.

40. Ramme, B., T. Nechvatal and R. T. Naik, "Lightweight Aggregates from Fly Ash", Proceedings of Workshop on Flowable Slurry Containing Fly Ash and Other Mineral By-Products, Fifth International Conference on Fly Ash, Silica Fume, Slag and Natural Pozzolans in Concrete, Milwaukee, Wisconsin, 1995.

41. Yamaguchi, S., T. Fujii, N. Yamamato and T. Nomura, "Kobelco Pelletizing Process", *Kobelco Technology Review*, Vol. 29, pp. 58–59, 2010.

42. Srb, J. and Z. Ruzickova, *Pelletization of Fines*, Elsevier; Distribution for the U.S.A. and Canada, Elsevier Science Pub. Co Amsterdam; New York: New York, N.Y, 1988.

43. Schmidt, P. C., "Size Enlargement by Agglomeration", *New York: John Wiley and*

Sons, Vol. 21, No. 5, pp. 237–237, 1992.

44. Baykal, G. and A. Gürhan Döven, "Utilization of fly ash by pelletization process; theory, application areas and research results", *Resources, Conservation and Recycling*, Vol. 30, pp. 59–77, 07 2000.

45. Edinçliler, A., G. Baykal and K. Dengili, "Determination of static and dynamic behavior of recycled materials for highways", *Resources Conservation and Recycling*, Vol. 42, pp. 223–237, 10 2004.

46. Edinçliler, A., G. Baykal and A. Saygılı, "Influence of different processing techniques on the mechanical properties of used tires in embankment construction", *Waste management (New York, N.Y.)*, Vol. 30, pp. 1073–80, 06 2010.

47. Baykal, G. and A. Saygılı, "A new technique to reduce the radioactivity of fly ash utilized in the construction industry", *Fuel*, Vol. 90, pp. 1612–1617, 04 2011.

48. Saygılı, A. and G. Baykal, "A new method for improving the thermal insulation properties of fly ash", *Lancet*, Vol. 43, pp. 3236–3242, 11 2011.

49. Ginnings, D. C. and R. Corruccini, "An Improved Ice Calorimeter-The Determination of its Calibration Factor and the Density of Ice at 0°C", *NBS Journal of Research*, Vol. 38, 1947.

APPENDIX A: CRUSHING STRENGTHS OF INDIVIDUAL PELLETS

Fly ash pellets are 28 day cured and exposed to 10 cycle of freeze-thaw test. Average crushing strength of fly ash pellets according to grain size are 7.18, 7.70, 10.97, 15.43 and 16.10 N/mm^2 respectively. Crushing values of pellets determined based on their grain size. Every grain size has 40 different and randomly chosen pellets to achieve consistent and more accurate results. Pellets with minimum 2 mm grain size were stronger relative to other sizes. The individual crushing strengths of fly ash pellets are given in Figure A.1 to Table A.5.

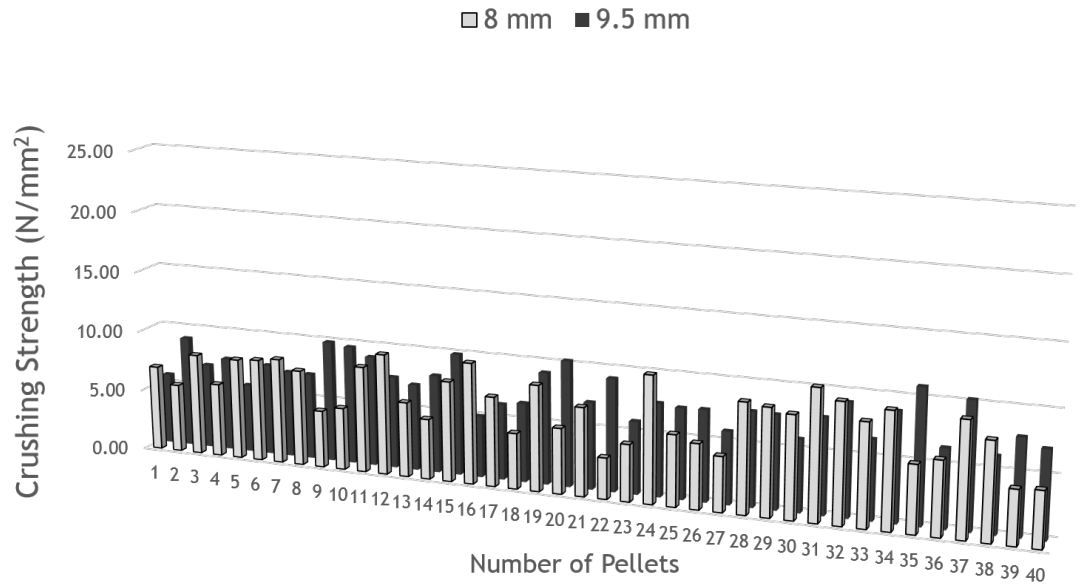

Figure A.1. Crushing strengths of 8 and 9.5 mm pellets for freeze-thawed group

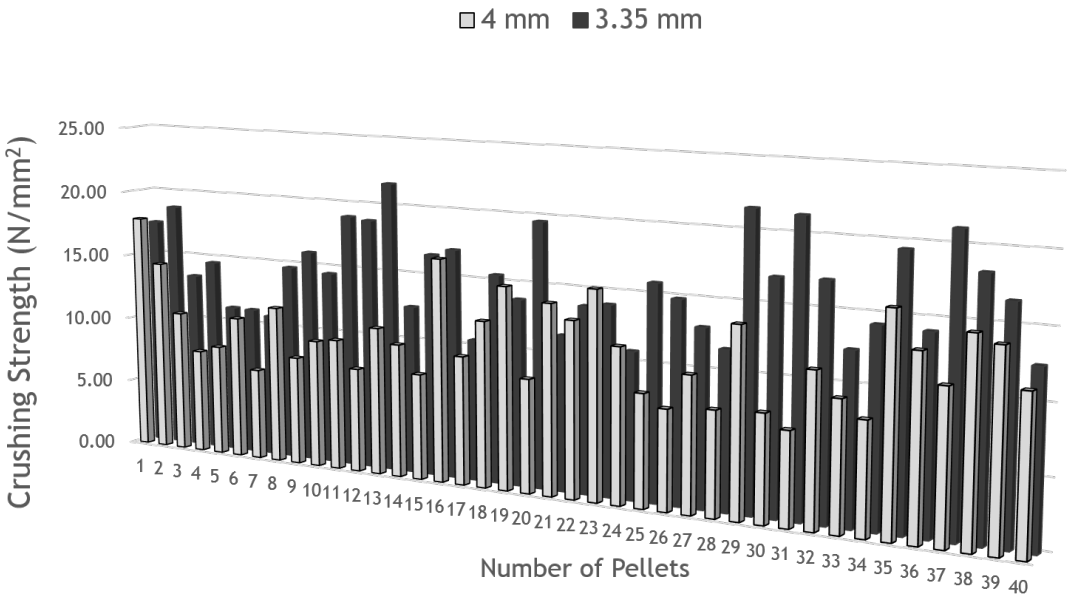

Figure A.2. Crushing strengths of 3.35 and 4 mm pellets for freeze-thawed group

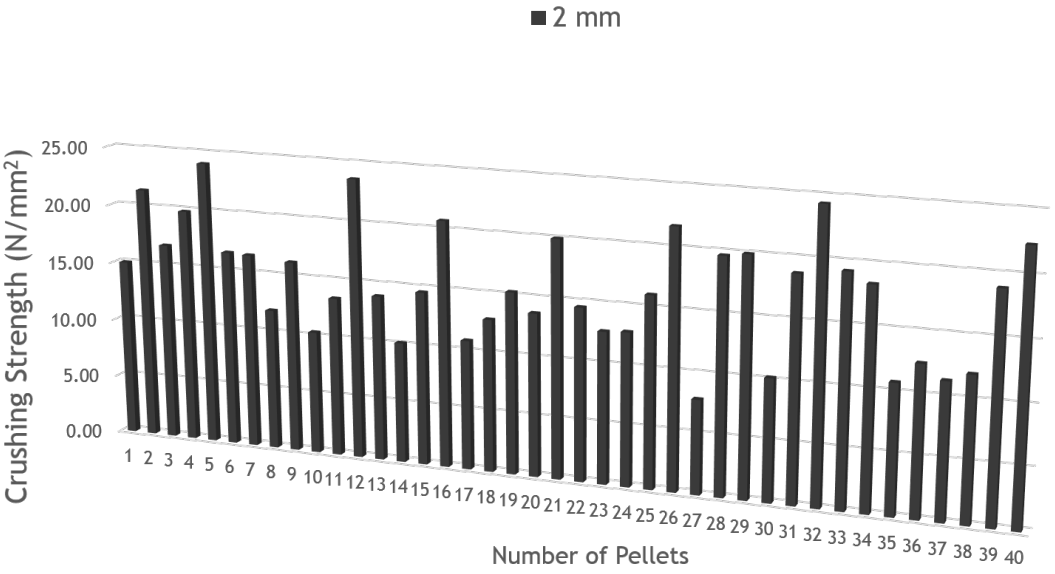

Figure A.3. Crushing strength of 2 mm pellets for freeze-thawed group

Table A.1. Crushing strengths of 9.5 mm fly ash pellets for freeze-thawed group

No	d1	d2	d3	d Average (mm)	Area(mm^2)	Crushing Force (N)	Crushing Strength (σ,N/mm^2)
1	9.57	10.20	9.74	9.84	75.98	529	6.96
2	9.98	9.56	9.78	9.78	75.06	419	5.58
3	9.81	9.55	9.91	9.76	74.80	621	8.30
4	9.54	9.73	9.66	9.64	73.00	438	6.00
5	9.90	9.64	10.00	9.85	76.15	629	8.26
6	9.92	9.90	9.56	9.79	75.32	633	8.40
7	9.73	9.51	9.89	9.71	74.08	640	8.64
8	9.73	9.78	10.30	9.94	77.55	609	7.85
9	9.75	9.54	9.74	9.68	73.54	344	4.68
10	10.30	9.61	9.75	9.89	76.75	391	5.09
11	9.94	9.81	9.85	9.87	76.48	665	8.70
12	9.94	9.83	9.69	9.82	75.72	750	9.90
13	9.68	9.63	9.98	9.76	74.86	459	6.13
14	9.65	9.63	9.54	9.61	72.47	358	4.94
15	9.66	9.79	9.67	9.71	74.00	608	8.22
16	9.74	9.90	9.81	9.82	75.70	750	9.91
17	10.20	9.67	9.67	9.84	76.12	558	7.33
18	9.79	9.65	9.63	9.69	73.73	336	4.56
19	9.76	9.80	9.57	9.71	74.01	641	8.66
20	9.55	9.64	9.59	9.59	72.30	388	5.37
21	9.70	9.83	9.78	9.77	74.96	543	7.24
22	9.60	9.62	9.72	9.65	73.10	246	3.37
23	9.99	9.62	9.91	9.84	76.05	354	4.65
24	9.88	9.93	10.00	9.94	77.54	805	10.38
25	9.73	9.72	9.61	9.69	73.68	430	5.84
26	9.52	9.52	9.75	9.60	72.35	385	5.32
27	9.72	9.70	9.57	9.66	73.31	330	4.50
28	9.86	9.52	9.93	9.77	74.97	674	8.99
29	9.88	9.84	9.84	9.85	76.23	668	8.76
30	10.50	9.84	9.58	9.97	78.12	655	8.38
31	9.70	9.86	9.80	9.79	75.22	803	10.67
32	9.73	9.87	9.54	9.71	74.11	725	9.78
33	10.20	9.71	9.70	9.87	76.53	643	8.40
34	9.90	9.55	9.75	9.73	74.39	705	9.48
35	10.00	9.55	9.86	9.80	75.46	416	5.51
36	9.90	9.88	9.59	9.79	75.26	455	6.05
37	9.92	9.79	9.84	9.85	76.19	712	9.34
38	9.87	9.75	9.82	9.82	75.66	602	7.96
39	9.69	9.84	10.30	9.94	77.65	344	4.43
40	9.52	9.66	9.72	9.63	72.89	332	4.55

Table A.2. Crushing strengths of 8 mm fly ash pellets for freeze-thawed group

No	d1	d2	d3	d Average (mm)	Area(mm^2)	Crushing Force (N)	Crushing Strength (σ,N/mm^2)
1	9.57	10.20	9.74	9.84	75.98	529	6.96
2	9.98	9.56	9.78	9.78	75.06	419	5.58
3	9.81	9.55	9.91	9.76	74.80	621	8.30
4	9.54	9.73	9.66	9.64	73.00	438	6.00
5	9.90	9.64	10.00	9.85	76.15	629	8.26
6	9.92	9.90	9.56	9.79	75.32	633	8.40
7	9.73	9.51	9.89	9.71	74.08	640	8.64
8	9.73	9.78	10.30	9.94	77.55	609	7.85
9	9.75	9.54	9.74	9.68	73.54	344	4.68
10	10.30	9.61	9.75	9.89	76.75	391	5.09
11	9.94	9.81	9.85	9.87	76.48	665	8.70
12	9.94	9.83	9.69	9.82	75.72	750	9.90
13	9.68	9.63	9.98	9.76	74.86	459	6.13
14	9.65	9.63	9.54	9.61	72.47	358	4.94
15	9.66	9.79	9.67	9.71	74.00	608	8.22
16	9.74	9.90	9.81	9.82	75.70	750	9.91
17	10.20	9.67	9.67	9.84	76.12	558	7.33
18	9.79	9.65	9.63	9.69	73.73	336	4.56
19	9.76	9.80	9.57	9.71	74.01	641	8.66
20	9.55	9.64	9.59	9.59	72.30	388	5.37
21	9.70	9.83	9.78	9.77	74.96	543	7.24
22	9.60	9.62	9.72	9.65	73.10	246	3.37
23	9.99	9.62	9.91	9.84	76.05	354	4.65
24	9.88	9.93	10.00	9.94	77.54	805	10.38
25	9.73	9.72	9.61	9.69	73.68	430	5.84
26	9.52	9.52	9.75	9.60	72.35	385	5.32
27	9.72	9.70	9.57	9.66	73.31	330	4.50
28	9.86	9.52	9.93	9.77	74.97	674	8.99
29	9.88	9.84	9.84	9.85	76.23	668	8.76
30	10.50	9.84	9.58	9.97	78.12	655	8.38
31	9.70	9.86	9.80	9.79	75.22	803	10.67
32	9.73	9.87	9.54	9.71	74.11	725	9.78
33	10.20	9.71	9.70	9.87	76.53	643	8.40
34	9.90	9.55	9.75	9.73	74.39	705	9.48
35	10.00	9.55	9.86	9.80	75.46	416	5.51
36	9.90	9.88	9.59	9.79	75.26	455	6.05
37	9.92	9.79	9.84	9.85	76.19	712	9.34
38	9.87	9.75	9.82	9.82	75.66	602	7.96
39	9.69	9.84	10.30	9.94	77.65	344	4.43
40	9.52	9.66	9.72	9.63	72.89	332	4.55

Table A.3. Crushing strengths of 4 mm fly ash pellets for freeze-thawed group

No	d1	d2	d3	d Average (mm)	Area(mm^2)	Crushing Force (N)	Crushing Strength (σ,N/mm^2)
1	4.26	4.41	4.02	4.23	14.03	251	17.89
2	4.36	4.12	5.41	4.63	16.84	243	14.43
3	4.35	5.41	4.70	4.82	18.22	194	10.65
4	5.20	5.14	4.30	4.88	18.71	146	7.80
5	4.27	4.18	4.52	4.32	14.68	122	8.31
6	5.01	4.98	4.86	4.95	19.25	206	10.70
7	5.16	4.18	4.85	4.73	17.58	120	6.83
8	4.99	5.29	5.48	5.25	21.68	256	11.81
9	4.86	5.10	5.21	5.06	20.07	163	8.12
10	5.48	4.94	4.52	4.98	19.45	186	9.56
11	5.10	4.40	4.51	4.67	17.14	168	9.80
12	4.53	5.09	4.05	4.56	16.33	127	7.78
13	4.92	4.94	5.36	5.07	20.22	223	11.03
14	4.85	5.30	5.40	5.18	21.11	210	9.95
15	4.60	4.34	4.15	4.37	14.97	118	7.88
16	4.08	4.32	4.36	4.25	14.21	236	16.61
17	5.43	4.50	4.72	4.88	18.72	179	9.56
18	4.32	4.98	4.61	4.64	16.88	208	12.33
19	4.16	4.28	4.78	4.41	15.26	229	15.01
20	5.44	4.37	4.81	4.87	18.64	157	8.42
21	4.08	4.34	4.77	4.40	15.20	214	14.07
22	4.36	5.25	4.40	4.67	17.15	223	13.00
23	5.11	4.69	4.69	4.83	18.34	282	15.38
24	4.14	4.02	4.73	4.30	14.50	166	11.45
25	4.31	5.28	4.51	4.70	17.35	144	8.30
26	5.23	4.06	5.19	4.83	18.30	135	7.38
27	4.84	4.52	4.63	4.66	17.06	170	9.96
28	4.07	5.02	4.88	4.66	17.04	131	7.69
29	4.39	4.20	5.11	4.57	16.38	226	13.80
30	5.31	5.11	4.17	4.86	18.57	146	7.86
31	4.75	5.08	4.75	4.86	18.53	127	6.85
32	4.78	4.16	4.69	4.54	16.19	181	11.18
33	5.25	5.36	5.08	5.23	21.47	202	9.41
34	4.67	4.57	4.22	4.49	15.81	129	8.16
35	5.09	4.12	4.57	4.59	16.57	262	15.81
36	5.00	4.51	4.90	4.80	18.10	238	13.15
37	5.25	5.22	4.74	5.07	20.20	222	10.99
38	4.80	4.06	4.91	4.59	16.54	242	14.63
39	4.15	4.11	5.03	4.43	15.41	216	14.02
40	5.28	4.41	4.48	4.72	17.51	196	11.19

Table A.4. Crushing strengths of 3.35 mm fly ash pellets for freeze-thawed group

No	d1	d2	d3	d Average (mm)	Area(mm^2)	Crushing Force (N)	Crushing Strength (σ,N/mm^2)
1	3.96	3.81	3.83	3.87	11.75	205	17.45
2	3.90	3.74	3.81	3.82	11.43	214	18.72
3	3.65	3.81	3.64	3.70	10.76	144	13.38
4	3.95	3.91	3.88	3.91	12.03	175	14.55
5	3.75	3.76	3.83	3.78	11.22	125	11.14
6	3.77	3.53	3.35	3.55	9.90	110	11.11
7	3.45	3.41	3.61	3.49	9.57	103	10.76
8	3.80	3.83	3.68	3.77	11.17	164	14.68
9	3.70	3.53	3.87	3.70	10.76	172	15.98
10	3.90	3.90	3.35	3.72	10.85	157	14.47
11	3.50	3.89	3.44	3.61	10.24	194	18.95
12	3.51	3.57	3.54	3.54	9.86	185	18.75
13	3.89	3.41	3.82	3.71	10.78	233	21.61
14	3.93	3.49	3.41	3.61	10.23	128	12.51
15	3.60	3.75	3.66	3.67	10.58	175	16.54
16	3.82	3.55	3.90	3.76	11.10	189	17.03
17	3.74	3.79	3.60	3.71	10.80	113	10.46
18	3.59	3.73	3.44	3.59	10.11	156	15.44
19	3.69	3.62	3.41	3.57	10.01	138	13.78
20	3.62	3.40	3.50	3.51	9.65	189	19.58
21	3.75	3.43	3.59	3.59	10.13	116	11.45
22	3.58	3.93	3.61	3.70	10.77	148	13.74
23	3.85	3.43	3.55	3.61	10.22	143	13.99
24	3.62	3.63	3.61	3.62	10.28	111	10.80
25	3.51	3.61	3.61	3.58	10.05	159	15.82
26	3.69	3.58	3.53	3.60	10.18	151	14.83
27	3.99	3.41	3.87	3.76	11.09	144	12.98
28	3.83	3.81	3.48	3.70	10.78	125	11.59
29	3.51	3.38	3.98	3.62	10.31	222	21.52
30	3.74	3.74	3.51	3.66	10.53	178	16.91
31	3.48	3.35	3.91	3.58	10.07	214	21.25
32	3.62	3.81	3.43	3.62	10.30	175	16.99
33	3.50	3.45	3.93	3.63	10.33	128	12.39
34	3.98	3.63	3.59	3.73	10.95	156	14.25
35	3.70	3.67	3.52	3.63	10.35	201	19.43
36	3.70	3.84	3.62	3.72	10.85	153	14.10
37	3.93	3.50	3.54	3.66	10.50	221	21.04
38	3.68	3.84	3.95	3.82	11.49	210	18.28
39	3.98	3.93	3.50	3.80	11.35	188	16.56
40	3.98	3.70	3.82	3.83	11.54	144	12.48

Table A.5. Crushing strengths of 2 mm fly ash pellets for freeze-thawed group

No	d1	d2	d3	d Average (mm)	Area(mm^2)	Crushing Force (N)	Crushing Strength (σ,N/mm^2)
1	2.42	2.47	2.15	2.35	4.33	65.00	15.03
2	2.07	2.48	2.36	2.30	4.16	89.00	21.41
3	2.23	2.16	2.06	2.15	3.64	61.00	16.78
4	2.11	2.54	2.31	2.32	4.23	84.00	19.85
5	2.12	2.00	2.54	2.22	3.87	93.00	24.06
6	2.14	2.07	2.11	2.11	3.49	58.00	16.62
7	2.32	2.65	2.29	2.42	4.59	76.00	16.54
8	2.12	2.40	2.54	2.35	4.35	52.00	11.95
9	2.07	2.54	2.37	2.33	4.25	69.00	16.25
10	2.40	2.05	2.51	2.32	4.23	44.00	10.41
11	2.47	2.33	2.10	2.30	4.15	56.00	13.49
12	2.16	2.08	2.07	2.10	3.46	82.00	23.67
13	2.61	2.56	2.29	2.49	4.85	68.00	14.01
14	2.38	2.25	2.48	2.37	4.41	45.00	10.21
15	2.07	2.59	2.58	2.41	4.57	67.00	14.66
16	2.34	2.33	2.18	2.28	4.09	85.00	20.78
17	2.65	2.41	2.46	2.51	4.93	54.00	10.95
18	2.47	2.43	2.09	2.33	4.27	55.00	12.89
19	2.34	2.25	2.21	2.27	4.04	62.00	15.35
20	2.13	2.08	2.25	2.15	3.63	50.00	13.76
21	2.03	2.52	2.29	2.28	4.09	82.00	20.05
22	2.51	2.51	2.44	2.49	4.87	71.00	14.59
23	2.30	2.34	2.19	2.28	4.07	52.00	12.78
24	2.53	2.54	2.17	2.41	4.57	59.00	12.91
25	2.38	2.36	2.01	2.25	3.97	64.00	16.11
26	2.50	2.07	2.05	2.20	3.81	83.00	21.78
27	2.56	2.43	2.52	2.50	4.92	39.00	7.93
28	2.11	2.23	2.12	2.15	3.65	72.00	19.74
29	2.27	2.31	2.28	2.28	4.10	82.00	20.01
30	2.56	2.43	2.18	2.39	4.48	46.00	10.27
31	2.64	2.60	2.29	2.51	4.95	93.00	18.80
32	2.13	2.30	2.11	2.18	3.73	91.00	24.39
33	2.01	2.06	2.56	2.21	3.84	74.00	19.29
34	2.60	2.50	2.16	2.42	4.61	85.00	18.44
35	2.23	2.44	2.45	2.37	4.42	48.00	10.87
36	2.21	2.18	2.44	2.27	4.06	51.00	12.57
37	2.42	2.59	2.37	2.46	4.74	54.00	11.38
38	2.18	2.46	2.38	2.34	4.30	52.00	12.08
39	2.22	2.02	2.13	2.12	3.54	67.00	18.94
40	2.47	2.14	2.09	2.24	3.93	88.00	22.39

APPENDIX B: SIEVE ANALYSIS RESULTS OF PELLETS

The grain size distributions of pellets before and after direct shear tests for all samples are given in Figure B.1 to Figure B.4. Table B.1. values show that there is a higher decrease in the grain size for freeze thaw-applied pellets which can be related to the lower crushing strength of freeze-thaw applied pellets.

Table B.1. Decrease in Granulometry for fly ash pellets

Control Group		
Test Number	**Normal Stress (kPa)**	**Decrease by Weight (%)**
1	25	5
	50	6
	100	9
2	25	4
	50	6
	100	8
Freeze Thawed Group		
1	25	6
	50	8
	100	10
2	25	5
	50	9
	100	10

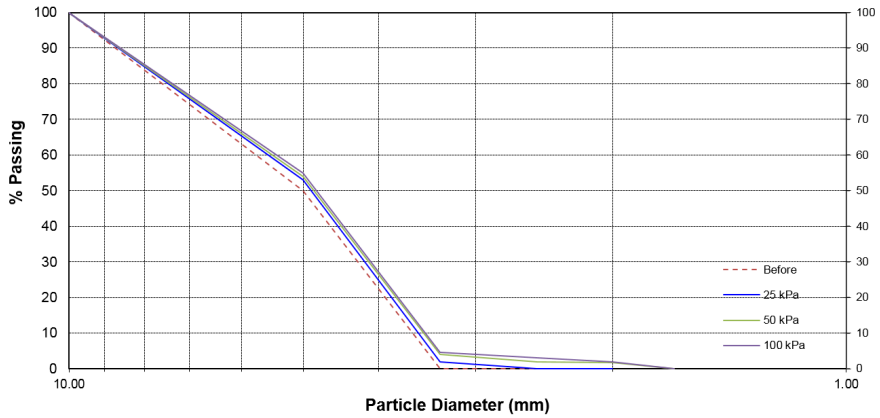

Figure B.1. The sieve analysis test results of fly ash pellets for freeze-thawed group, test 1

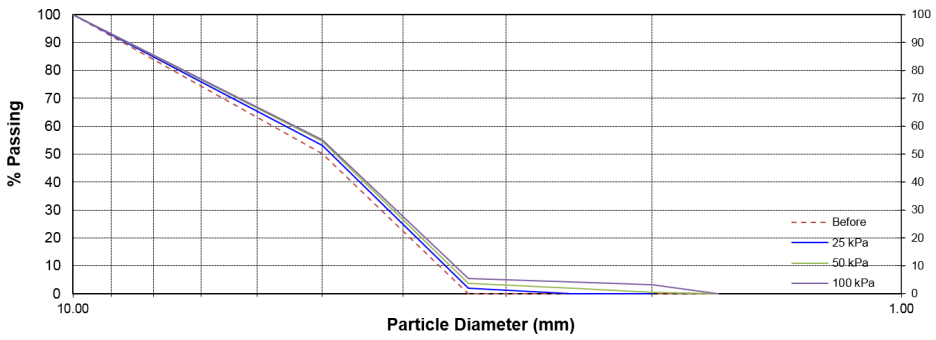

Figure B.2. The sieve analysis test results of fly ash pellets before and after direct shear tests for freeze-thawed group, test 2

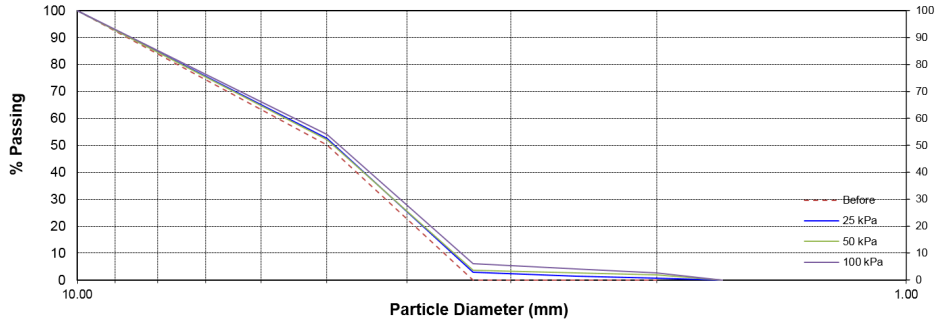

Figure B.3. The sieve analysis test results of fly ash pellets before and after direct shear tests for control group, test 1

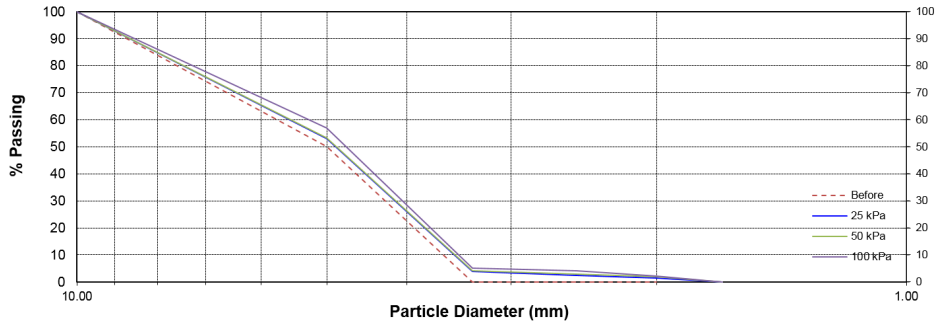

Figure B.4. The sieve analysis test results of fly ash pellets before and after direct shear tests for control group, test 2

APPENDIX C: CALIFORNIA BEARING RATIO TEST RESULTS

California bearing ratio of fly ash pellets for control and freeze-thawed group are given in Table C.1 to Table C.4.

Table C.1. CBR test results for control group

Control CBR-1			Control CBR-2			Control CBR-3		
Penetration (mm)	Load(N)	kg	Penetration (mm)	Load(N)	kg	Penetration (mm)	Load(N)	kg
0	0	0	0	0	0	0	0	0
0.5	644	65.71429	0.5	710	72.44898	0.5	586	59.79592
1	862	87.95918	1	825	84.18367	1	902	92.04082
1.5	1114	113.6735	1.5	1006	102.6531	1.5	1030	105.102
2	1452	148.1633	2	1462	149.1837	2	1350	137.7551
2.5	1557	158.8776	2.5	1681	171.5306	2.5	1557	158.8776
3	1730	176.5306	3	1877	191.5306	3	1722	175.7143
4	2427	247.6531	4	2592	264.4898	4	2271	231.7347
5	3242	330.8163	5	3360	342.8571	5	2984	304.4898
7.5	4578	467.1429	7.5	4674	476.9388	7.5	4465	455.6122
10	5571	568.4694	10	5751	586.8367	10	5398	550.8163
12.5	6353	648.2653	12.5	6573	670.7143	12.5	6544	667.7551

Table C.2. CBR test results for control group

Control CBR-4			Control CBR-5		
Penetration (mm)	Load(N)	kg	Penetration (mm)	Load(N)	kg
0	0	0	0	0	0
0.5	590	60.20408	0.5	521	53.16327
1	770	78.57143	1	781	79.69388
1.5	982	100.2041	1.5	1029	105
2	1328	135.5102	2	1374	140.2041
2.5	1431	146.0204	2.5	1638	167.1429
3	1698	173.2653	3	1995	203.5714
4	2263	230.9184	4	2891	295
5	2975	303.5714	5	3158	322.2449
7.5	4486	457.7551	7.5	4702	479.7959
10	5622	573.6735	10	5710	582.6531
12.5	6536	666.9388	12.5	6589	672.3469

Table C.3. CBR test results for freeze-thawed group

Control CBR-1			Control CBR-2			Control CBR-3		
Penetration (mm)	Load(N)	kg	Penetration (mm)	Load(N)	kg	Penetration (mm)	Load(N)	kg
0	0	0	0	0	0	0	0	0
0.5	644	65.71429	0.5	710	72.44898	0.5	586	59.79592
1	862	87.95918	1	825	84.18367	1	902	92.04082
1.5	1114	113.6735	1.5	1006	102.6531	1.5	1030	105.102
2	1452	148.1633	2	1462	149.1837	2	1350	137.7551
2.5	1557	158.8776	2.5	1681	171.5306	2.5	1557	158.8776
3	1730	176.5306	3	1877	191.5306	3	1722	175.7143
4	2427	247.6531	4	2592	264.4898	4	2271	231.7347
5	3242	330.8163	5	3360	342.8571	5	2984	304.4898
7.5	4578	467.1429	7.5	4674	476.9388	7.5	3965	404.5918
10	5571	568.4694	10	5751	586.8367	10	4778	487.551
12.5	6353	648.2653	12.5	6573	670.7143	12.5	5244	535.102

Table C.4. CBR test results for freeze-thawed group

Control CBR-4			Control CBR-5		
Penetration (mm)	Load(N)	kg	Penetration (mm)	Load(N)	kg
0	0	0	0	0	0
0.5	590	60.20408	0.5	521	53.16327
1	770	78.57143	1	781	79.69388
1.5	982	100.2041	1.5	1029	105
2	1328	135.5102	2	1374	140.2041
2.5	1431	146.0204	2.5	1638	167.1429
3	1698	173.2653	3	1995	203.5714
4	2263	230.9184	4	2891	295
5	2975	303.5714	5	3158	322.2449
7.5	3386	345.5102	7.5	4702	479.7959
10	4822	492.0408	10	5710	582.6531
12.5	5536	564.898	12.5	6589	672.3469

APPENDIX D: MICROSCOPIC IMAGES FOR SURFACE SCALING

Microscopic images for surface scaling analyses of fly ash pellets for control and freeze-thawed groups are given in Figure D.1 to Figure D.5.

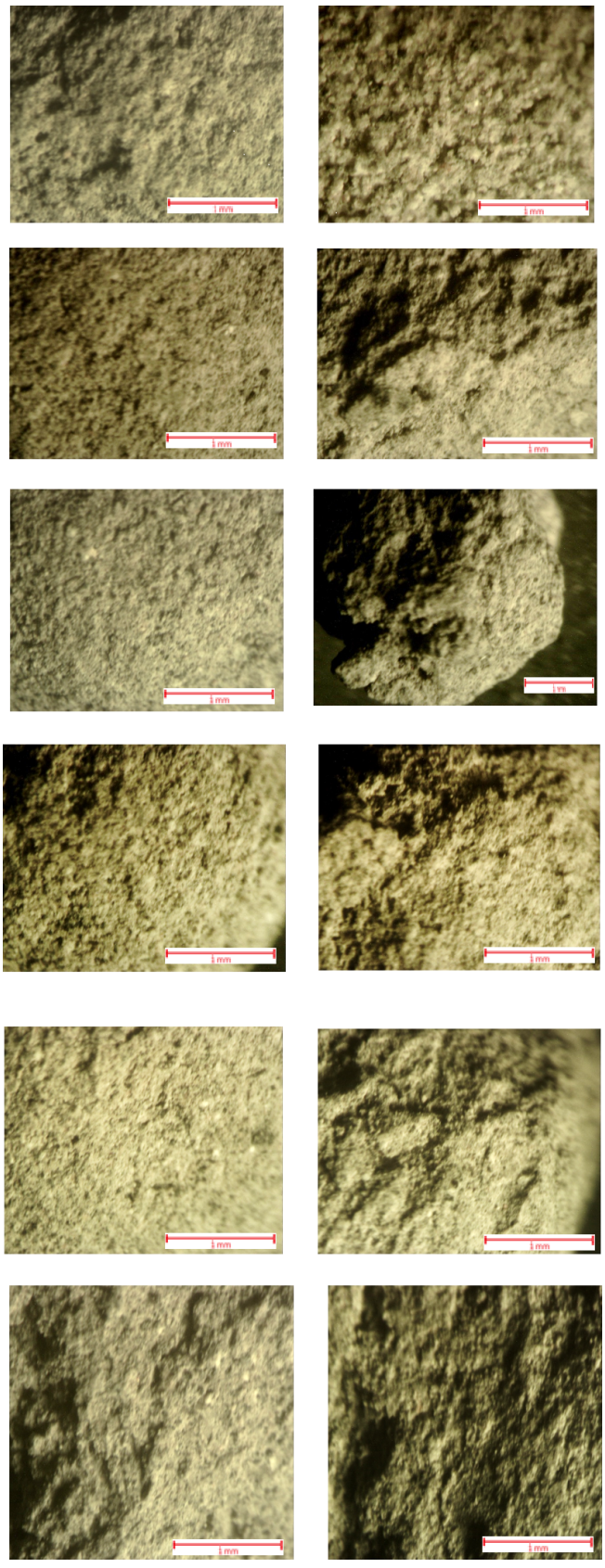

Figure D.1. The microscopic image of pellets before and after freeze-thawing

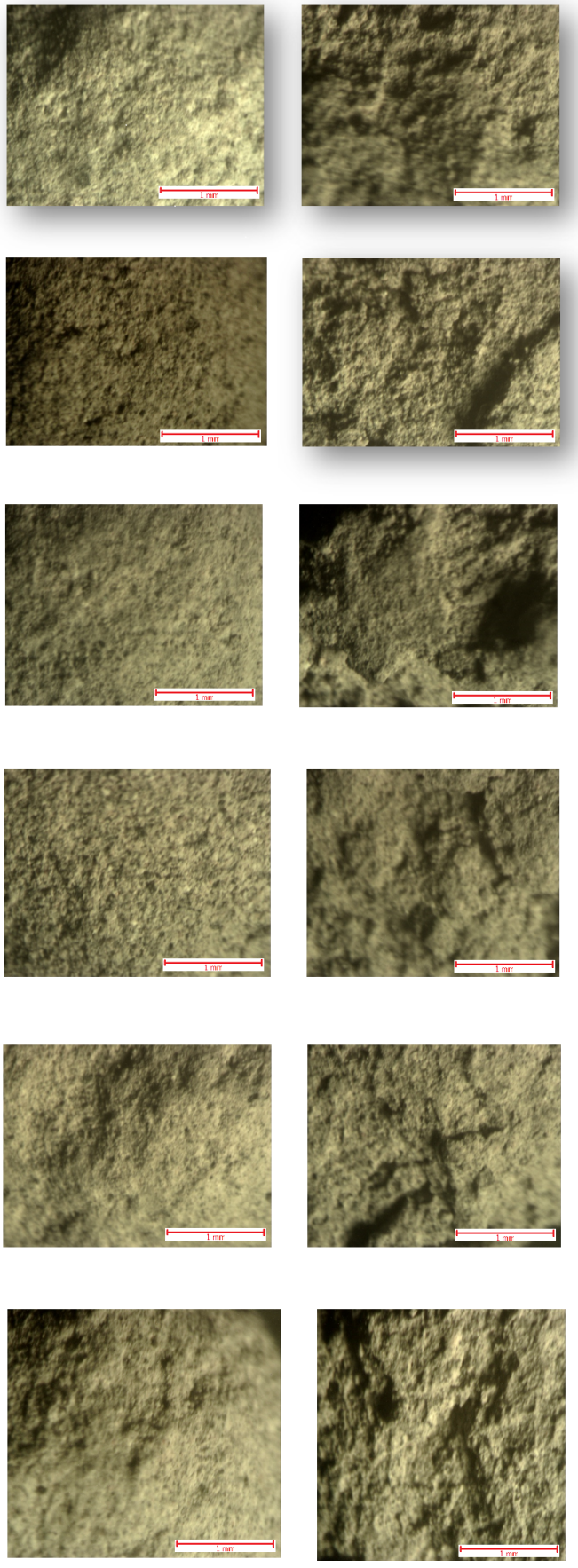

Figure D.2. The microscopic image of pellets before and after freeze-thawing

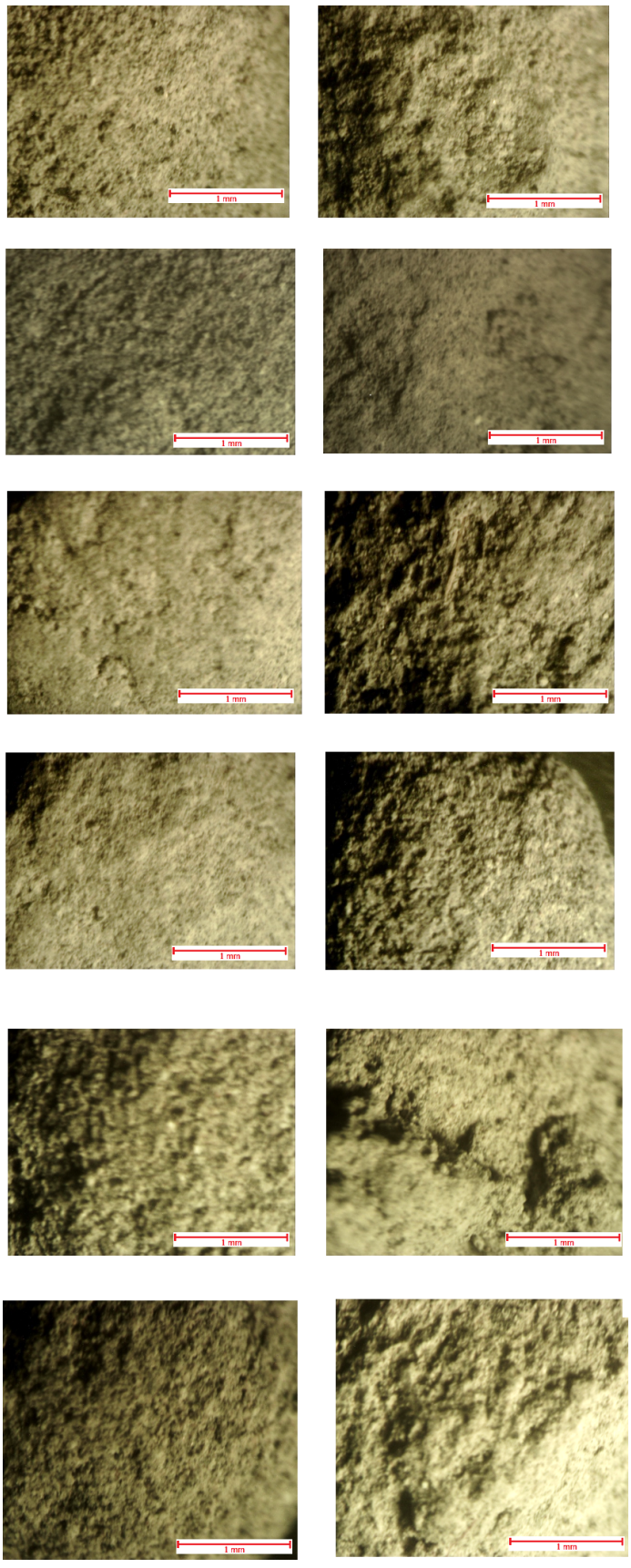

Figure D.3. The microscopic image of pellets before and after freeze-thawing

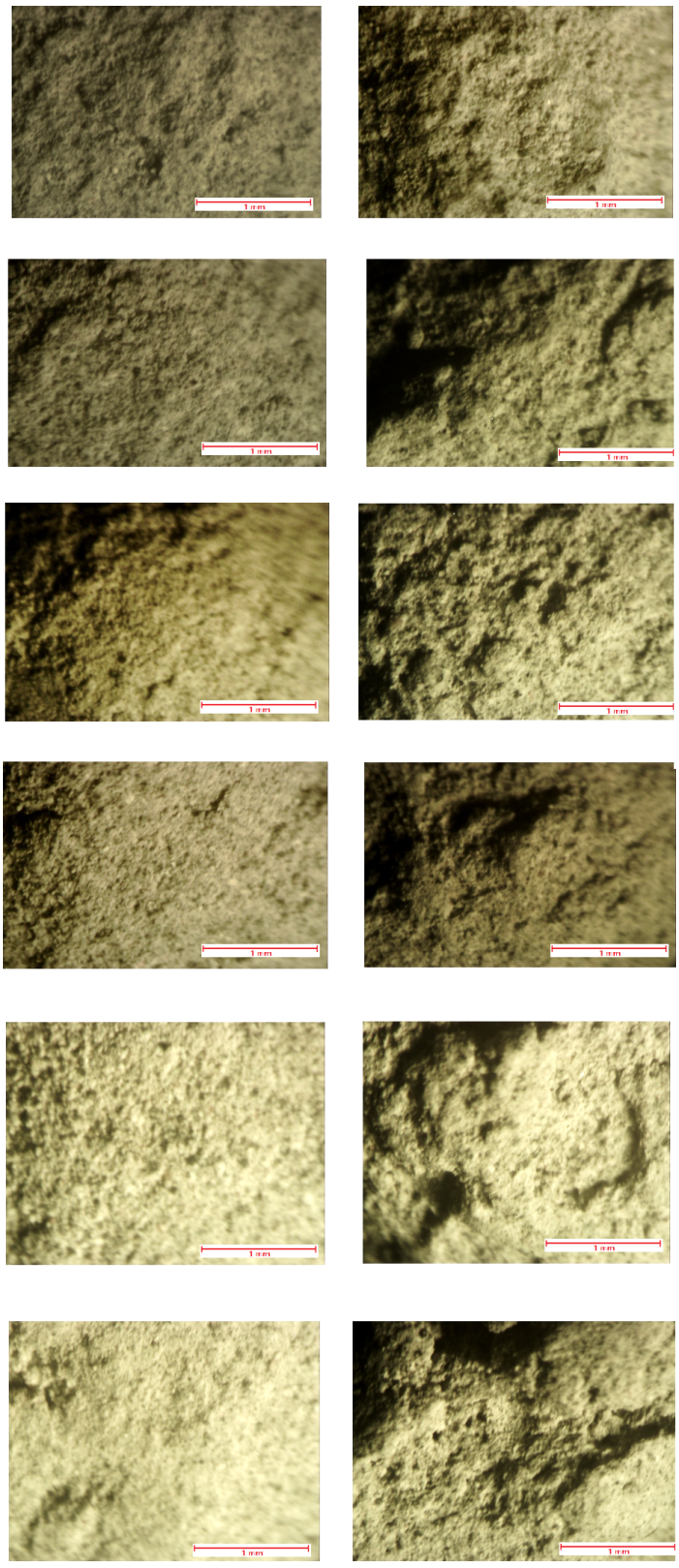

Figure D.4. The microscopic image of pellets before and after freeze-thawing

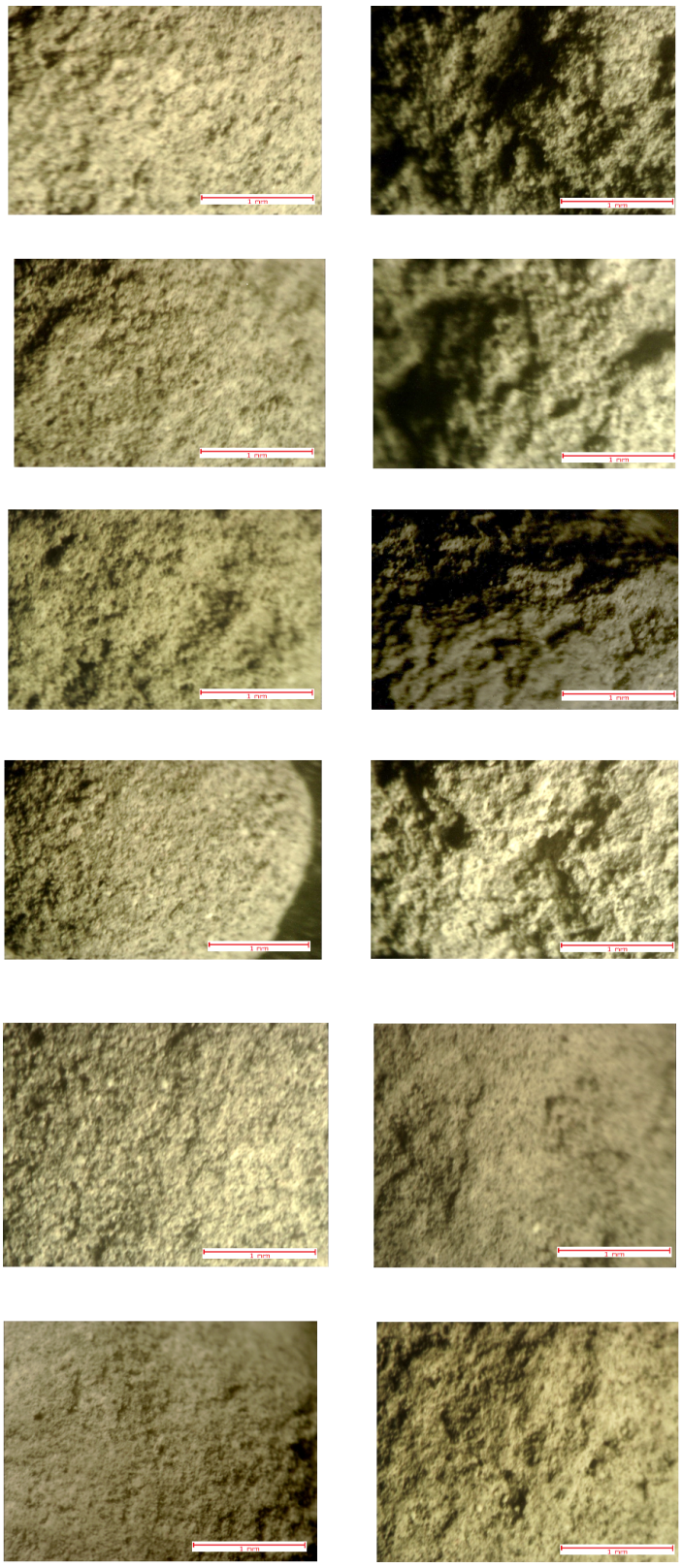

Figure D.5. The microscopic image of pellets before and after freeze-thawing

APPENDIX E: DIRECT SHEAR TEST RESULTS

Horizontal displacement versus shear strength and vertical displacement graphs of fly ash pellets for control and freeze-thawed groups are given in Figure E.1 to Figure E.8. CG and FZT represents control and freeze-thawed group, respectively.

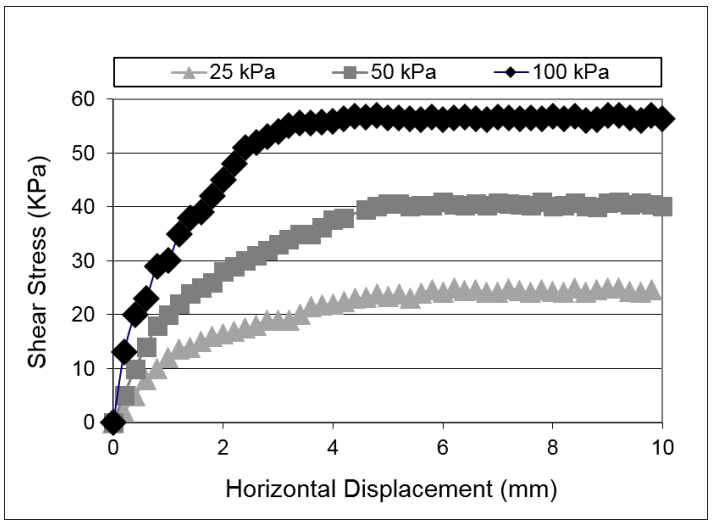

Figure E.1. Horizontal displacement versus shear stress curves of fly ash pellets under 25, 50 and 100 kPa normal stresses for CG-1

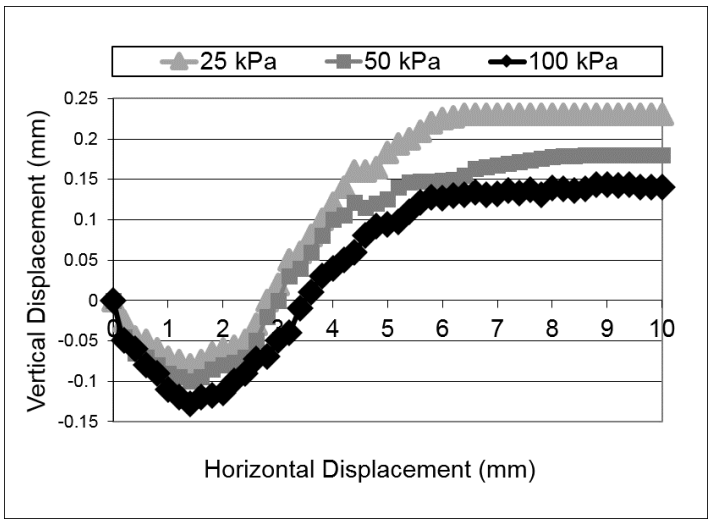

Figure E.2. Horizontal displacement versus vertical displacement curves of fly ash pellets under 25, 50 and 100 kPa normal stresses for CG-1

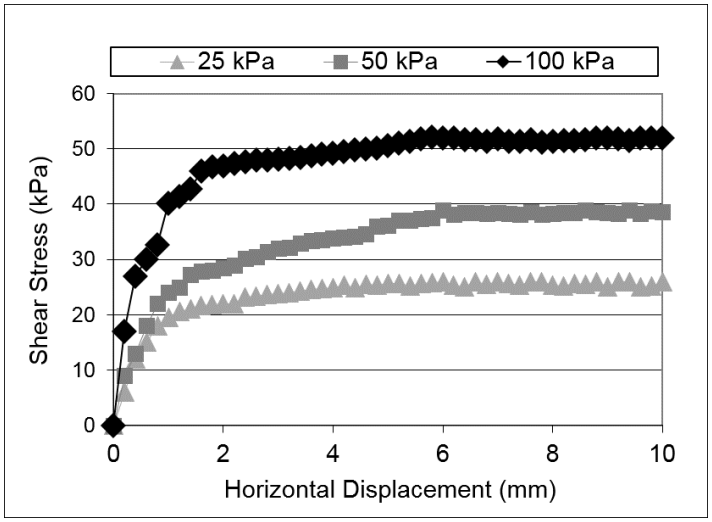

Figure E.3. Horizontal displacement versus shear stress curves of fly ash pellets under 25, 50 and 100 kPa normal stresses CG-2

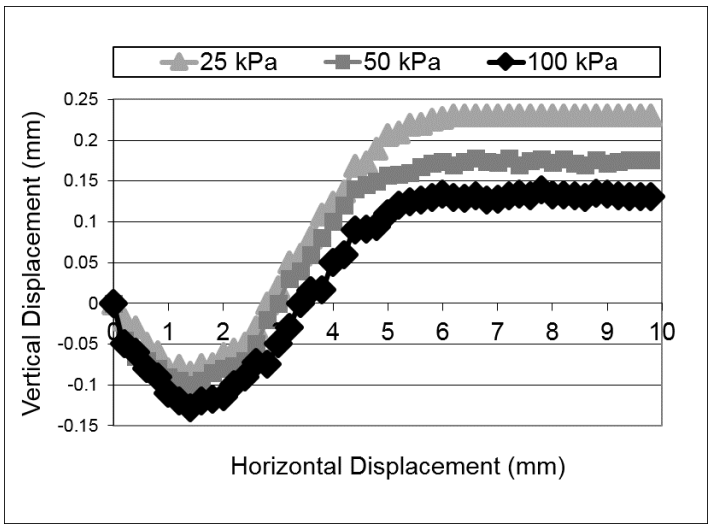

Figure E.4. Horizontal displacement versus vertical displacement curves of fly ash pellets under 25, 50 and 100 kPa normal stresses CG-2

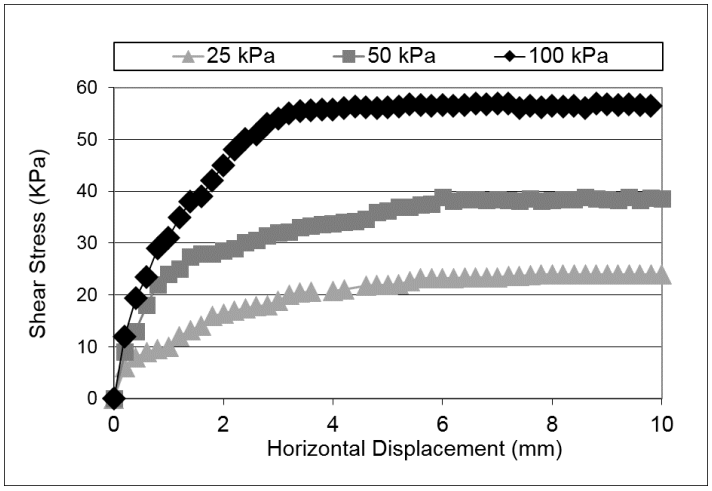

Figure E.5. Horizontal displacement versus shear stress curves of fly ash pellets under 25, 50 and 100 kPa normal stresses for FZT-1

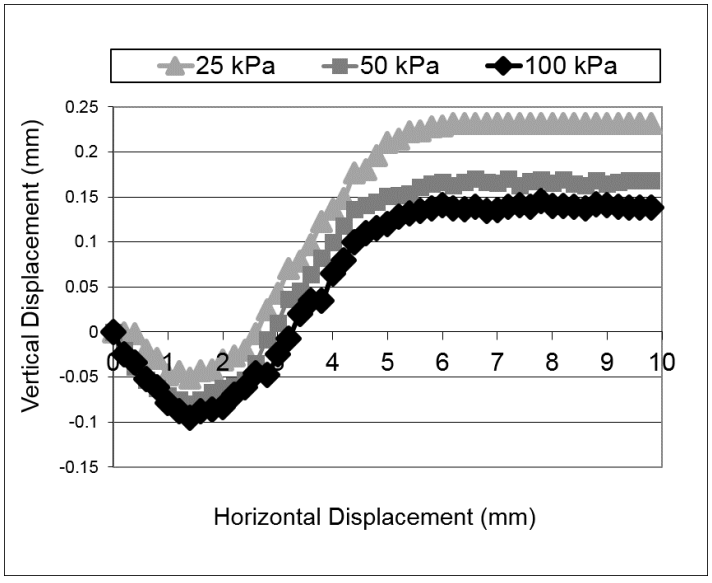

Figure E.6. Horizontal displacement versus vertical displacement curves of fly ash pellets under 25, 50 and 100 kPa normal stresses for FZT-1

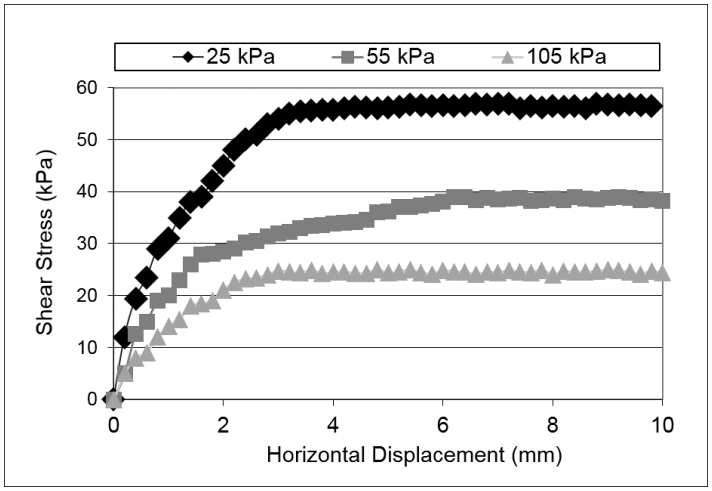

Figure E.7. Horizontal displacement versus shear stress curves of fly ash pellets under 25, 50 and 100 kPa normal stresses for FZT-2

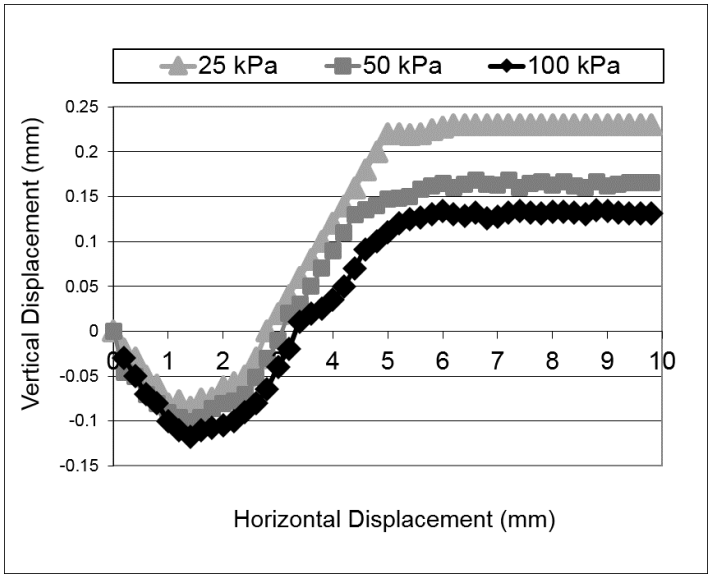

Figure E.8. Horizontal displacement versus vertical displacement curves of fly ash pellets under 25, 50 and 100 kPa normal stresses for FZT-2